UNIVERSITY OF CALIFORNIA SAN DIEGO

Biophysical and Biochemical Applications of Isomorphic Fluorescent Cyclic Dinucleotide Analogs

A dissertation submitted in partial satisfaction of the requirements for the degree Doctor of Philosophy

in

Chemistry

by

Yao Li

Committee in charge:

Professor Yitzhak Tor, Chair
Professor Thomas Hermann
Professor Victor Nizet
Professor Valerie Schmidt
Professor Navtej Toor

2019

The dissertation of Yao Li is approved, and it is acceptable in quality and form for publication on microfilm and electronically:

_____

_____

_____

_____

_____

Chair

University of California San Diego

2019

DEDICATION

I dedicate this thesis to my parents.

EPIGRAPH

In my life, I had come to realize that, when things were going very well, indeed, it was just the time to anticipate trouble. And, conversely, I learned from pleasant experience that at the most despairing crisis, when all looked sour beyond words, some delightful "break" was apt to lurk just around the corner.

Amelia Earhart

TABLE OF CONTENTS

LIST OF FIGURES

LIST OF SCHEMES

LIST OF EQUATIONS

LIST OF TABLES

LIST OF SPECTRA

ACKNOWLEDGEMENTS

I acknowledge, with gratitude, my debt of thanks to Dr. Yitzhak Tor for giving me this opportunity to work in his lab, and for his advice and guidance that supported me throughout my graduate studies.

I would like to thank my thesis committee members for their continuous support and flexibility. I very much appreciate the help and support from Dr. Victor Nizet's, Dr. Jeffrey Esko's and Dr. Michael Burkart's laboratories. I would also like to thank Dr. Yongxuan Su at the MS facilities for his help with Mass spectroscopy and LC-MS analysis.

Many members from the Tor lab have been extremely supportive and helpful. I'm incredibly grateful to have shared part of my life in graduate school with them: Lisa, Andrea, Patrycja, Alex, Paul and Kaivin.

Lastly, I would like to thank my parents for their love and support, and my friends for sharing and cheering for life with me.

In regards to the material in this dissertation, please note the following:

Chapter 3, 4 and 5, in full, are currently being prepared for submission for publication for the material. Li, Y.; Fin, A; Ludford, P. T.; Rovira, A. R.; Tor, Y., Monitoring the formation and degradation of c-di-GMP analogs using fluorescence. The thesis author was the primary author of this material.

Chapter 6, in full, is currently being prepared for submission for publication for the material. Li, Y.; Fin, A; Ludford, P. T.; Rovira, A. R.; Tor, Y., Synthesis and Cellular Activity of Systematically Modified Cyclic Dinucleotides. The thesis author was the primary author of this material.

VITA

2019	Ph.D. in Chemistry University of California San Diego
2016	M.S. in Chemistry University of California San Diego
2013	B. Sc.in Chemistry Minzu University of China

PUBLICATIONS AND PATENT

Li, Y.; Fin, A; Ludford, P. T.; Rovira, A. R.; Tor, Y., Monitoring the formation and degradation of c-di-GMP analogs using fluorescence (In preparation)

Li, Y.; Fin, A; Ludford, P. T.; Rovira, A. R.; Tor, Y., Synthesis and Cellular Activity of Systematically Modified Cyclic Dinucleotides (In preparation)

Feldmann. J.; Li, Y.; Tor, Y., Emissive synthetic cofactors: A highly responsive NAD+ analogue reveals biomolecular recognition features, Chem. Eur. J. 2019 (online)

Li, Y.; Fin, A; McCoy, L. S.; Tor, Y., Polymerase-Mediated Site-Specific Incorporation of a Synthetic Fluorescent Isomorphic G Surrogate into RNA, Angew.Chem. Int.Ed. 2017, 56,1303 –1307.

Chen, H. Y.; Hu, J.; Zhang, J.; Guo, K.; Li, Y.; Lan, B. H., Separation of Particles of Rare Earth Oxides by Dielectrophoresis, Materials Science Forum, 2016 ,852, 542-546.

Yang, W. Z.; Zhang, Y.; Li, Y.; Pu, W. W.; Lan, R., Mask with High Filtering Performance and High Air Permeability Performance, National Patent of China CN202697795 U, Jan. 30, 2013

ABSTRACT OF THE DISSERTATION

Biophysical and Biochemical Applications of Isomorphic Fluorescent Cyclic Dinucleotides Analogs

by

Yao Li

Doctor of Philosophy in Chemistry

University of California San Diego, 2019

Professor Yitzhak Tor, Chair

As cyclic dinucleotides' impact on pathogenic bacteria and eukaryotic cells is gradually being recognized, shedding light on the enzymatic pathways involved in its production, degradation and recognition is of significance. Fluorescence-based techniques have been playing key roles in modern biochemical and biophysical research

due to their high sensitivity and informativeness. In order to take advantage of fluorescence-based techniques, we developed isomorphic emissive cyclic dinucleotide analogs using previously developed fluorescent nucleoside analogs in the Tor lab.

Instead of going through the challenging chemical synthesis of cyclic dinucleotide analogs, we decided to exploit bacterial dinucleotide cyclases, DncV and DisA, to convert emissive nucleoside triphosphates into corresponding cyclic dinucleotides (CDNs). Rewardingly, DncV and DisA were able to synthesize emissive cyclic dinucleotides with thGTP, ^{tz}GTP, thATP and ^{tz}ATP with yields comparable to that of native NTPs. Using DncV and DisA, a library of emissive CDNs were successfully synthesized.

To demonstrate the power and utility of these fluorescent CDN analogs, we sought to use them to monitor the enzyme-mediated conversion of CDNs, which is an important process in CDN signaling in cells. The quantum yields of the emissive CDNs were found to be significantly lower than that of corresponding nucleosides, which is caused by fluorescence quenching by adjacent nucleobases in the CDNs. We thus utilized the quenching effect to monitor DncV-mediated CDN synthesis with steady state fluorescence spectroscopy. By carefully analyzing the emission spectra of the reaction, we were able to derive reaction rate constants comparable to those calculated from HPLC analysis. It is a great advantage to monitor such a process with fluorescence, as traditional methods such as radioisotope labeling or HPLC cannot be used for real-time monitoring, and the experimental procedures are often time-consuming. We speculate that such a fluorescence-based method of monitoring enzymatic processes can

be further optimized for high throughput screening of inhibitors for enzymes involved in CDN signaling.

In order to demonstrate the iso-functionality of the emissive CDNs, their abilities to activate the innate immune response was also studied in RAW 264.7 cells, by monitoring protein dynamics and gene expression of the cells. To our surprise, although the emissive CDNs have very close chemical structures with each other, they demonstrated very different abilities to trigger an innate immune response, which possibly indicated difference binding affinities of the analogs to STING, the cellular receptor. We believe that with careful analysis of these results, along with structural comparison of emissive CDNs, valuable insights into the signaling mechanism of CDN-STING-IFN pathway could be provided. Moreover, our results put forth new approaches for the design, preparation and implementation of new CDN analogues with altered recognition features and tuned potency and duration of the triggered cellular immune response.

1 Introduction to cyclic dinucleotides

1.1 Overview

Cyclic dinucleotides (CDNs) are macrocyclic compounds comprise two ribonucleoside monophosphate residues connected by either canonical 5'-3' phosphodiester bond or non-canonical 5'-2' phosphodiester bond (**Figure 1.1**). The CDNs containing only 5'-3' phosphodiester bonds were often referred to as canonical or bacterial CDNs, and have been only found in prokaryotes.[1] So far there have been 3 types of canonical CDNs discovered, cyclic diguanylate (c-di-GMP), cyclic diadenylate (c-di-AMP) and cyclic GMP-AMP (3',3'-c-GAMP). CDNs have been found essentially in all known bacteria, and play important roles in regulating various central processes in bacteria, including biofilm formation, motility, virulence, etc.[1-3] Recent studies have also revealed that theses bacterial CDNs are recognized as pathogen-associated molecular patterns (PAMPs) and trigger innate immune responses in eukaryotic cells.

More interestingly, a non-canonical CDN (2',3'-c-GAMP) containing one 3'-5' phosphodiester bond and one 2'-5' phosphodiester bond was found to be produced exclusively in eukaryotic cells.[4-5] Unlike the bacterial CDNs that are expressed ubiquitously in bacteria, this endogenous CDN is only produced upon cytosolic double-stranded DNA (dsDNA) detection.[6] Similar to bacterial CDNs, 2',3'-c-GAMP binds to the downstream cellular component and trigger potent innate immune responses. [4]

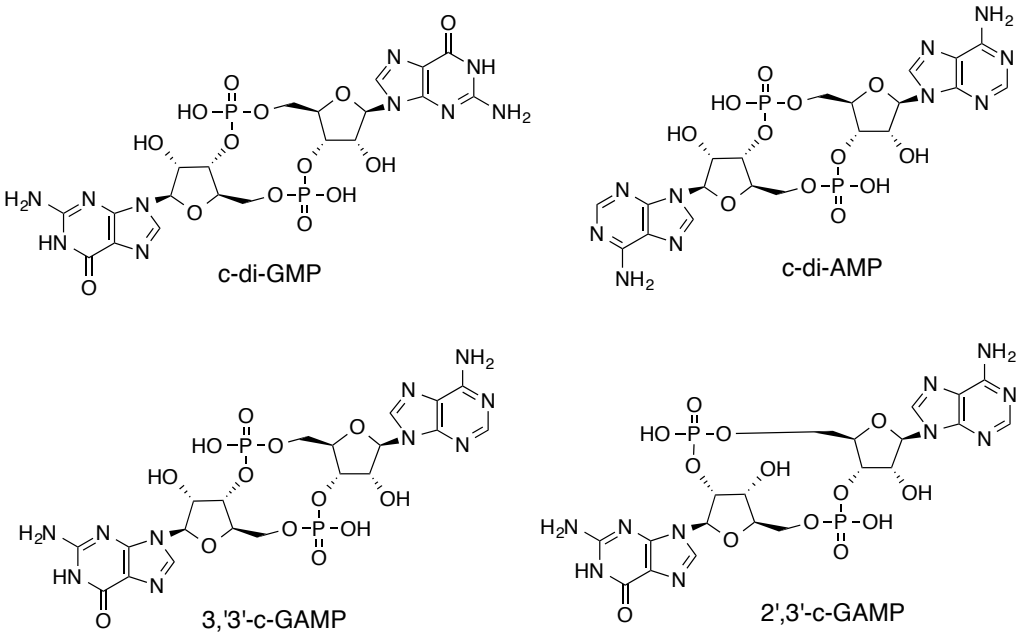

Figure 1.1 Structures of native cyclic dinucleotides.

Intensive studies in recent years have led to remarkable discoveries on the distinctive roles CDNs play as secondary signaling molecules in both pathogenic bacteria and host cells. Novel approaches such as genetic screening, chemical modification and protein engineering have also been taken to further investigate CDN signaling mechanisms and develop therapeutics tools targeting enzymes and receptors involved in CDN signaling pathways.[1, 6-7]

1.2 The biological function of cyclic dinucleotides in bacteria

1.2.1 C-di-GMP as secondary messenger in bacteria

In 1987, Ross and colleges discovered that cyclic diguanylate (c-di-GMP), formed enzymatically form GTP, was able to activate the cellulose synthase in *Acetobacter xylinum*.[8] In recent years, the growing interest in the biological functions of c-di-GMP has led to the discovery of complex regulatory pathways that modulate the

global and local concentration of c-di-GMP, and signaling targets of c-di-GMP. C-di-GMP is now recognized as a nearly universal secondary messenger in bacteria that coordinates various bacterial central processes, including biofilm formation, cell-cell signaling, motility, virulence, stress survival, and differentiation.[2, 9-14]

The global and local concentrations of c-di-GMP are tightly regulated in response to the intracellular and extracellular signals. This is achieved by the coordinated activity of diguanylate cyclases (DGCs) containing GGDEF domains and phosphodiesterases (PDEs) with EAL or HD-GYP domains. [1-2] Various types of c-di-GMP-binding effectors translate the c-di-GMP signal inputs into activities of enzyme complexes or transcription factors by binding to downstream cellular components.[2] In addition to some DGCs and PDEs that could trigger regulatory effects and demonstrate catalytic activities[15-16], several families of c-di-GMP effectors have been identified and characterized, which include proteins that contain PilZ domains,[17-19] transcriptional regulators,[20-22] mRNA riboswitches,[23] and degenerate GGDEF/EAL domain proteins.[24,2]

C-di-GMP is universally recognized as a key factor in controlling the switch between planktonic and sessile lifestyles of bacteria by regulating their biofilm formation.[25] Generally speaking, low concentration of c-di-GMP in the cells is often associated with motility, whereas high level of c-di-GMP has been demonstrated in various types of bacteria to promote the attachment to surfaces and formation of microcolonies, which lead to biofilm formation.[25] C-di-GMP was also observed asymmetrically distributed during cell division of several bacteria strains, including *P. aeruginosa* and *C. crescentus*.[26-27] During the cell cycles of those bacteria, c-di-GMP

concentration decreases in one of the daughter cells for a short period after cell division, which is mediated by the asymmetric distribution of PDEs during divisions.[27] The low c-di-GMP concentration at this stage of the cell cycle was proposed to promote motility and help the bacteria to adapt to new environments after division.[2] It has been revealed that c-di-GMP signaling pathways affect the virulence of numerous pathogenic bacteria.[14] C-di-GMP signaling has been associated with several processes, including the expression and secretion of virulence factors, adherence to host cells, host cell invasion, resistance to oxidative stress, and modulating immune responses of host.[14, 28-30] However, weather c-di-GMP inhibits or promotes pathogen virulence is dependent on the type of pathogen, infection route, and the stage of infection, etc.[14]

1.2.2 C-di-AMP in gram-positive bacteria

A newer member of the cyclic dinucleotide signal molecules produced by bacteria is c-di-AMP, which was discovered only 10 years ago in the structural study of DisA, a protein involved in DNA damage repair in *T. maritima* and *B. subtilis*.[31] So far it has been studied mostly in gram-positive bacteria, including *B. subtilis*, *L. monocytogenes*, *S. aureus* and *Streptococcus* spp., though it was also discovered in a few gram-negative bacteria such as *C. trachomatis* and *B. burgdorferi*.[3] Similar to c-di-GMP pathways, the cellular level of c-di-AMP is also modulated by deadenylate cyclases (DACs) and phosphodiesterases (PDEs), and the signal is further transmitted to effector molecules through c-di-AMP receptors. However, the sources of stimuli and detailed signaling mechanisms are still far from being understood. Unlike c-di-GMP signaling pathways, where numerous amount of receptor proteins or RNA riboswitches have been identified, only a limited number of receptor proteins and one type of RNA

riboswitch (ydaO) have been discovered for c-di-AMP, which leaves plenty of room to investigate c-di-AMP signaling mechanisms.[3]

C-di-AMP has been associated with cell-wall homeostasis in *B. subtilis, L. monocytogenes* and *S. aureus*, as lowering c-di-AMP level either by overexpress PDEs or deplete DACs caused cell wall defects and increased susceptibility to peptidoglycan-targeting antibiotics.[32-34] Corrigan and colleagues discovered that potassium transporter protein KtrA was a c-di-AMP-binding protein using affinity chromatography.[35] It was demonstrated in several studies that the binding of c-di-AMP to KtrA inhibits potassium transportation.[36-38] Furthermore, it was recently illustrated that the only known c-di-AMP binding riboswitch *ydaO* was located at the upstream of the transcript of a high-affinity potassium transporter (KimA) in *B. subtilis.*[39] The conformational change of *ydaO* riboswitch triggered by c-di-AMP binding blocks translation of the KimA and downregulates intracellular potassium concentration.[39] This is consistent with the observation that c-di-AMP accumulates in bacteria grown in high extracellular potassium concentration, but not in low potassium concentration.[39] These studies indicated that the control of potassium homeostasis is an important function of c-di-AMP. Observations suggest that c-di-AMP regulates DNA damage repair, sporulation as well as citric acid cycle.[3, 40-41] However, as mentioned above, only a limited number of c-di-AMP associated enzymes and receptors have been identified, thus thorough molecular analysis needs to be done in order to better understand the mechanisms of how c-di-AMP regulates certain physiological and pathogenic processes.

1.2.3 C-GAMP in *V. cholerae*

3',5'-cyclic-GAMP (c-GAMP) was the most recently discovered member of bacterial cyclic dinucleotides.[42] First discovered in 2012, this unique hybrid molecule was found to be produced by the dinucleotide cyclase DncV in the human pathogen El Tor *V. cholerae* from GTP and ATP.[42] The expression of DncV is positively associated with the virulence factor of El Tor *V. cholerae,* ToxT.[42] c-GAMP was involved in the regulation of virulence, motility and colonization in mammalian host of *V. cholerae,* alhough very few receptors of c-GAMP have been identified so far.[1, 42-44] Breaker and Hammond group have demonstrated that c-GAMP controls the expression of genes involved in exoelectrogenesis, a process that in important for bacteria colonization on surfaces, through c-GAMP binding riboswitches in *Geobacter* spp.[43, 45] Waters and Ng group recently identified the first bacterial protein receptor of c-GAMP, CapV, in *V. cholerae*. c-GAMP directly binds to CapV and activates its serine hydrolase/phospholipase activity, which leads to the degradation of cell membrane.[44] Further investigation needs to be done to analyze the outcome of such regulatory system.

1.3 Cyclic dinucleotides and the innate immune system

The innate immune system of eukaryotes has various ways of detecting invading pathogens, and one of the most fundamental mechanisms is to recognize molecules that are exclusively synthesized by pathogenic microorganisms. The pattern recognition receptors (PRRs) of the innate immune system are able to distinguish pathogen-associated molecular patterns (PAMPs) from molecules produced by the host and trigger corresponding innate immune responses, which could further modulate adaptive immune response.[46]

The canonical CDNs (c-di-GMP, c-di-AMP and 3',3'-c-GAMP) have been found essentially in all know bacteria but not any eukaryotes. Their widespread distribution and versatile roles they play in numerous bacterial signaling pathways made them perfect PAMPs for bacterial infection detection. The endoplasmic reticulum (ER)-located transmembrane protein STING (stimulator of interferon genes) has been identified as the direct sensor of bacterial CDNs.[47] Structural analysis of STING has revealed that the ligand binds to STING C-terminal domain (CTD) through hydrophobic affinity and hydrogen bonding.[6, 48] The binding triggers conformational changes of STING and presumably causes the release of a C-terminal tail (CTT), which recruits and activates downstream kinase TBK1.[6, 49] Although the structure of STING has been largely revealed by X-ray crystallography, the structure of the CTT remains unknown. It has been proposed based on molecular simulation results that the TCC of STING likely formed a structure that could be recognized by TBK1 as a substrate.[50] The phosphorylation of the STING CTT by TBK1 allows the recruitment of transcription factor IRF3, as the phosphorylated STING binds to the positively charged moiety of IRF3.[49] IRF3 gets phosphorylated by TBK1, and forms the activated homo-dimer which further induces the expression of type-I interferon (IFN α/β) and other cytokines in the nuclei (**Figure 1.2**).[51] Beside the TBK1-IRF3 pathway, STING was also able to activate other signaling pathways, including NF-κB and STAT6, however the detailed mechanisms are still being investigated. [51-53]

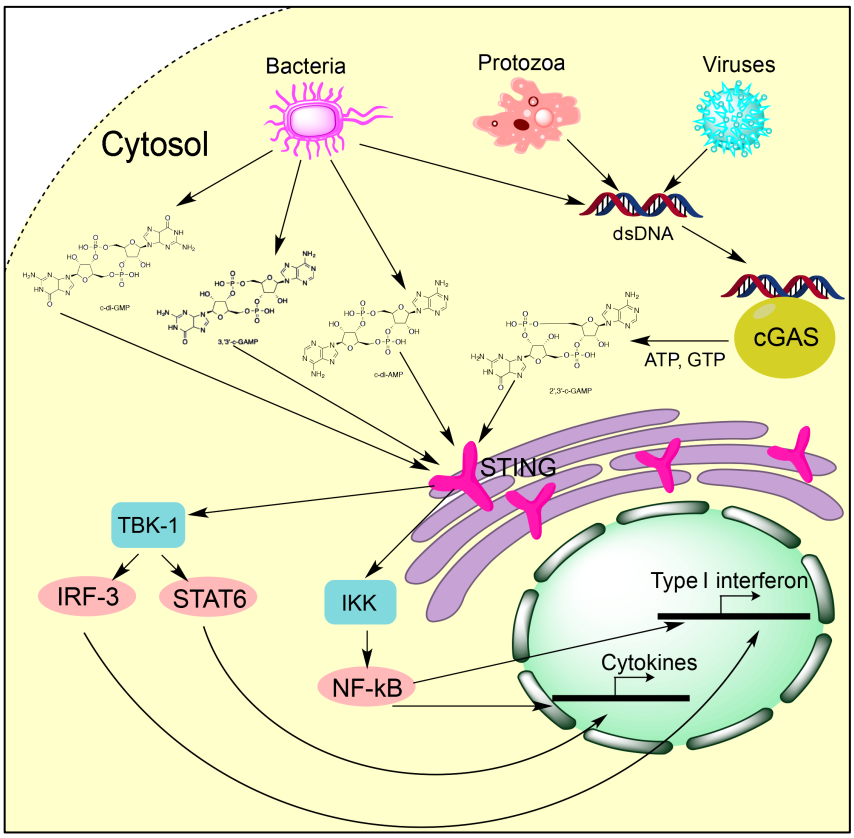

Figure 1.2 Innate immune response induced by cyclic dinucleotides.

Besides the canonical CDNs that act as PAMPs during bacterial infection, host cells also produce an endogenous CDN, which also plays an important role in innate immune responses against pathogens.[54] This endogenous CDN is a hybrid cyclic-GMP-AMP compound, but different from the bacterial 3',3'-cGAMP, it features a non-canonical structure of a 2'-5' G-pA linker and a 3'-5' A-pG linker.[4-5, 54-55] This 2',3'-c-GAMP is produced by cyclic GMP-AMP cyclase (cGAS) upon binding of cytoplasmic dsDNA.[56-58] Detecting cytoplasmic nucleic acid has been an important strategy of the innate immune system to sense a broad range of pathogens, although in some cases it could lead to self-recognition, which is often associated with autoinflammatory and autoimmune diseases.[59] As a recently discovered cytosolic dsDNA sensor, cGAS

appeared to be essential for type-I IFN induction during dsDNA viruses and retroviruses infections.[6, 51] Upon binding to dsDNA, cGAS goes through conformational rearrangements, and becomes an active enzyme to produce 2',3'-c-GAMP.[58] The endogenous CDN activates the STING-TBK1 signaling pathway and lead to the induction of type-I IFN. So far STING is the only known downstream receptor for 2',3'-c-GAMP as well as the bacterial CDNs. Although some human STING (hSTING) variants exhibit higher binding affinity to the 2',3'-c-GAMP than the bacterial CDNs, only modestly increased amount of type-I IFN was observed.[48]

1.4 Makers and breakers of cyclic dinucleotides

The cellular concentration of c-di-GMP is tightly regulated by DGCs contain GGDEF domain and PDEs with EAL or HD-GYP domain, as described in Error! Reference source not found.. Structural analysis of DGC PleD from *C. crescentus* revealed that two catalytic GGDEF domains act cooperatively to synthesize c-di-GMP with one GTP molecule bound to each domain.[60-61] The product c-di-GMP could bind to the allosteric site of DGCs and provides negative feedback regulation to DGC catalysis, which might help establish precise cellular threshold concentrations of c-di-GMP.[60, 62] PDEs contain EAL domain cleaves c-di-GMP to the linear dinucleotide pGpG in the presence of divalent metal ion Mg^{2+} or Mn^{2+}, however are strongly inhibited by Ca^{2+} or Zn^{2+}, whereas PDEs with HD-GYP domain cleaves c-di-GMP directly to two GMP residues.[63] pGpG can be further hydrolyzed to guanosine monophosphate (GMP) residues by other non-c-di-GMP specific PDEs.[64-65] Although a great number of DGCs and PDEs have been predicted by sequencing analysis, only a small number of them have demonstrated their physiological functions under laboratory

conditions.[66-68] Some recent studies have indicated that some PDEs remain inactive under laboratory conditions due to the lack of proper input signals from the environment.[66]

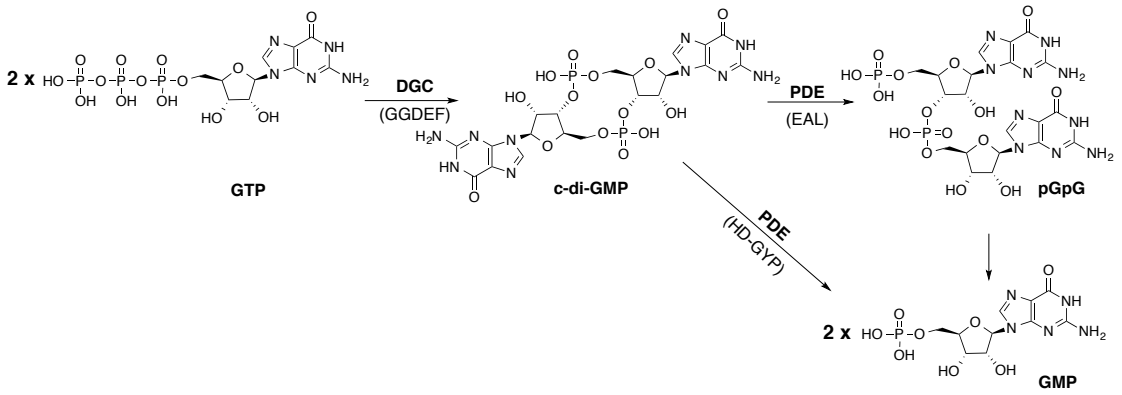

Figure 1.3 Biosynthesis and hydrolysis of c-di-GMP. C-di-GMP is synthesized by DGCs with GGDEF domain from two GTP residues, and hydrolyzed to linear pGpG by PDEs with EAL domain or two GMP by PDEs with HD-GYP domain. pGpG could also be further hydrolyzed to GMP by ribonucleases that are not CDN-specific.

Different from c-di-GMP synthesis, where a large number of GGDEF domain-containing proteins have been identified, only a few DACs have been discovered in bacteria and archaea.[3] c-di-AMP is synthesized from two ATP or ADP residues by DACs, and the first DAC domain was identified in DisA (DNA integrity scanning protein A) by X-ray crystallography.[31, 69] So far there have been four classes of DACs identified: DisA, CdaA, CdaS and CdaM.[3] c-di-AMP produced by different classes of DACs has been shown to play different physiological roles in bacteria. For example, DisA was known as a DNA-scanning protein that helps maintaining DNA integrity by regulating the sporulation progress through c-di-AMP.[69-70] When DNA lesion was detected, DisA pauses at the lesion site and haults the production of c-di-AMP, which leads to a rapid decrease in the cellular concentration of c-di-AMP and causes a delay

in the sporulation process.[69] When the DNA damage is repaired, DisA produces c-di-AMP to restart the sporulation.[69] Conserved motifs are also found in all DACs, most commonly DGA an RHR motifs, however no structural or sequence similarities was found between DACs and the GGDEF domaining-containing GACs, indicating that the c-di-AMP signaling pathways are independent from c-di-GMP signaling pathways.[3]

Three classes of c-di-AMP-specific PDEs have been identified: GdpP, Pde2 and PgpH.[71-72] GdpP contains the catalytic domain DHH/DHH1 and is able to cleave c-di-AMP with high specificity into linear pApA, which can be further degraded to to adenosine monophosphate (AMP) residues.[71-74] Interestingly, pApA was found to be involved in a negative feedback loop that inhibits GdpP-mediated c-di-AMP hydrolysis.[75] Pde2 is a cytoplasmic protein that also contains DHH/DHH1domain, however it preferentially degrades pApA into 2 AMP though it's also able to degrade c-di-AMP.[75-76] Another class of c-di-AMP-specific PDE is pgpH, which contains a catalytic HD domain and cleaves c-di-AMP to AMP with high specificity. [40, 72]

The latest-discovered bacterial CDN, 3',3'-cGAMP was found by Mekalanos and colleagues from *V. cholerae.*[42] This hybrid molecule is synthesized by dinucleotide cyclase DncV. DncV is able to recognize both GTP and ATP at the acceptor and donor binding pockets, and therefore is able to produce c-di-GMP, c-di-AMP as well when fed with only GTP or ATP in vitro. However, when both GTP and ATP were presented, the hybrid compound is the major product, similar to DncV's main product in vivo.[54, 77] Structural and biochemical studies have revealed that the synthesis of 3',3'-c-GAMP adopted a sequential reaction mechanism, where an pppA(3'-5')pG intermediate is formed in the first step of the catalysis and then released and rebound to the pocket in

the reverse direction to form the second phosphodiester bond.[78-79] Recently, Hammond and colleagues discovered that the hybrid promiscuous (HyPr) subfamily of GGDEF enzymes was also able to produce 3',3'-c-GAMP in addition to c-di-AMP and c-di-GMP when both GTP and ATP were present, although further investigations are needed to illustrate the mechanism of these enzymes.[80] Although several classes of PDEs have been identified with high specificity for c-di-GMP or c-di-AMP in various types of bacteria , 3',3'-c-GAMP specific PDEs have only been identified in *V. Cholerae* so far.[81] Jiang and colleagues identified three HD-GYP domain-containing enzymes, v-cGAP1, v-cGAP2 and v-cGAM3, that specifically breaks 3',3'-c-GAMP in *V. Cholerae.*[81] Interestingly, v-cGAP1 behaves as both PDE and 5'-phosphotase, as it breaks breaks 3',3'-c-GAMP first into 5'-pApG, then removes the 5'-phosphate group and generate ApG as final product.[81] This activity was only observed for v-cGAP1, as v-cGAP2 and v-cGAM3 only hydrolyze 3',3'-c-GAMP into 5'-pApG.[81]

The mammalian dinucleotide cyclase cGAS also has two nucleotide binding pockets and produces the non-canonical 2',3'-c-GAMP in sequential reactions similar to DncV, but is not known to produce any form of c-di-GMP or c-di-AMP. Different from DncV-mediated 3',3'-c-GAMP synthesis, cGAS first catalyzes the formation of the non-canonical phosphodiester bond and releases pppG(2'–5')pA intermediate, which then rebound to cGAS in the reverse direction and form the canonical linker.[78] cGAS also requires activation by dsDNA either in vitro or in vivo. Structural studies have shown that cGAS went through conformational rearrangements upon dsDNA binding in order to form catalytically accessible and competent nucleotide-binding pockets. [5] Despite the low sequence similarity (below 10% identity), the structure of

bacterial DncV demonstrated remarkable similarity to that of mammalian cGAS, which has led to an evolutional connection between the signaling systems of eukaryotes and prokaryotes.[78] The dominant cellular hydrolase of 2',3'-c-GAMP was identified by Mitchison and colleagues.[82] Previously known to hydrolyze ATP to AMP and PPi, the ectonucleotide pyrophosphatase/phosphodiesterase (ENPP1) was identified to be the dominant hydrolase for 2',3'-c-GAMP.[82] Besides degrading 2',3'-c-GAMP to AMP and GMP residues, ENPP1 was also known to hydrolyze c-di-AMP to AMP, though the reaction was considerably slower to hydrolysis meadiated by CdnP (a c-di-AMP-specific PDE).[83] These discoveries indicates that ENPP1 plays an key role in regulating the dsDNA-cGAS-STING signaling pathway, although detailed analysis needs to be done to better understand the catalytic mechanism of it.[82-83]

1.5 The conformational flexibility of cyclic dinucleotides

CDN signaling pathways have been extensively studied in recent years and complexes of CDN-related enzymes and receptors have been identified in addition to numerous signaling mechanisms. Indeed the conformational flexibility of CDNs contributed greatly to their versatility in signaling transduction.[84] The structure of intercalated c-di-GMP was revealed as early as 1990 by X-ray crystallography, which demonstrated the conformational flexibility of cyclic dinucleotides.[85] The four guanine bases from two c-di-GMP molecules were found stacking on top of each other to form a intercalated unit, with a Mg^{2+} coordinated to the two central bases.[85] More recent NMR analysis of c-di-GMP in buffered solution has demonstrated that at physiological concentration (low micromolar) c-di-GMP undergoes fast exchange between monomeric form and intercalated dimeric form with an equilibrium constant around

1mM.[86] Co-crystallization of cyclic dinucleotides and proteins/RNA riboswitches have revealed more diverse structures cyclic dinucleotides could adopt when bound to enzymes or receptors (**Figure 1.4**).[84] Beside adjusting the distance between the two nucleobases in the CDN monomer from a completely extended conformation where the two nucleobases pointing opposite directions, to a tightly closed U-shape molecule (**Figure 1.4a–d**), CDNs can also form dimers and tetramers during signal transduction (**Figure 1.4e–f**). The intercalated dimer of c-di-GMP was found to be important in the negative feedback regulation of some GGDEF domain-containing DGCs, as it binds to the inhibition site (I-site) of DGCs, and exhibits allosteric inhibition of c-di-GMP synthesis (**Figure 1.4e)**.[62] Tetrameric form of c-di-GMP was recently identified in complex with the C-terminal domain (CTD) of transcription factor BldD by X-ray crystallography.[21] Structural analysis illustrated that the tetrameric c-di-GMP induces the dimerization of BldD by linking the two subunits together through their CTDs, which further initiates the expression of multiple genes involved in *Streptomyces* sporulation.[21] The presence of higher oligomeric forms of c-di-GMP at millimolar concentration have been proposed based on NMR, UV spectroscopy and circular dichroism (CD) spectroscopy, however such oligomers have not been identified under physiological conditions.[21, 86-87]

Common techniques used in analyzing the conformation of CDNs include NMR, X-ray chrystallography, UV spectroscopy and CD spectroscopy, however, none of these techniques could illustrate the conformational changes CDNs undergo during biochemical processes. Fluorescent analogs of CDNs have been developed in order to

reflect the conformational changes of CDNs in real-time (discussed in the next chapter).[88]

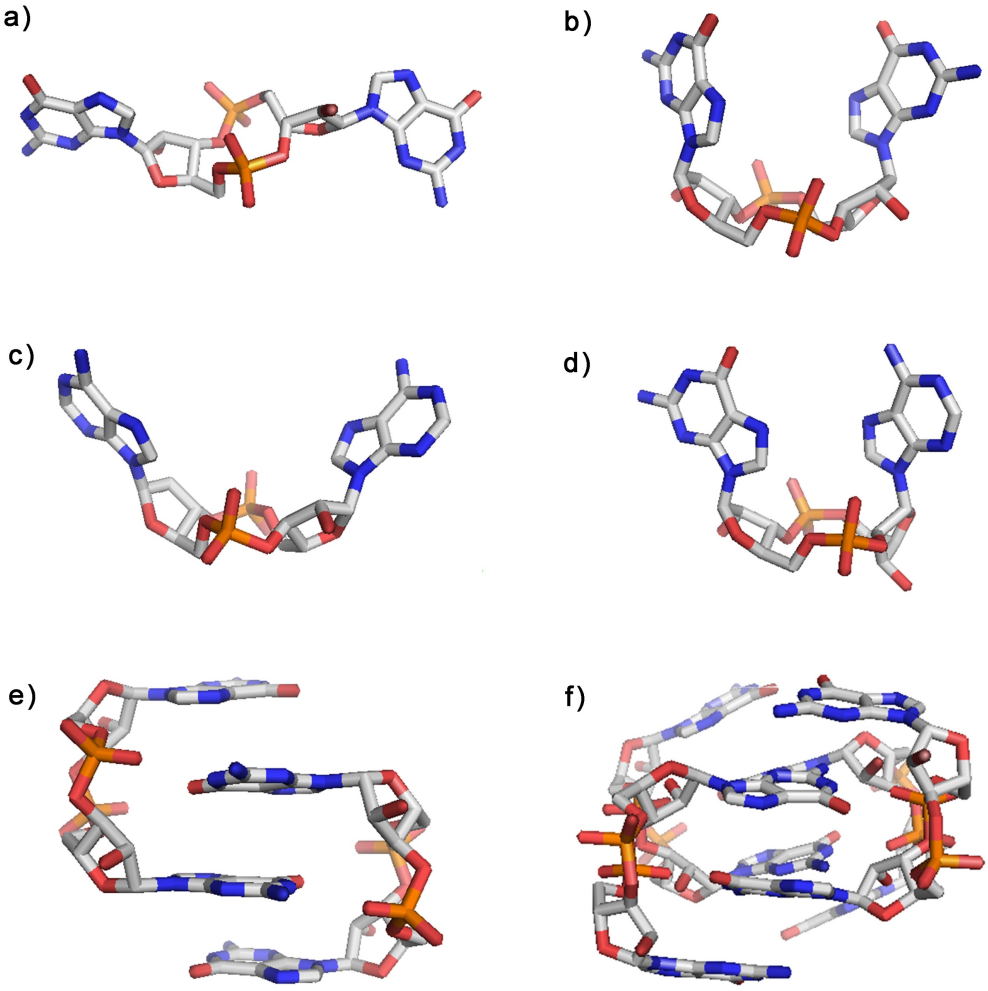

Figure 1.4 Conformational flexibility of cyclic dinucleotides. a) c-di-GMP in extended "open" conformation in the binding pocket of EAL domain-containing PDE, PBD 3gfz. b) c-di-GMP in the binding pocket of PilZ domain, PBD 2rde. c) c-di-AMP in the binding pocket of riboswitch ydaO, PBD 4qlm. d) 2',3'-c-GAMP in the binding pocket of hSTING, PBD 5bqx. e) Intercalated dimer of c-di-GMP in the binding pocket of the I-site of GGDEF domain, PBD 1w25. f) Tetrameric form of c-di-GMP in the CTD of transcription factor BldD, PDB 5khd.

1.6 Potential therapeutic applications of cyclic dinucleotides

The immunostimulatory effect of CDNs has made these small molecules very popular for potential therapeutic applications. CDNs induce potent type-I IFN and other cytokines production by directly binding and activating the ER-located receptor STING. Studies analyzing the adjuvant properties of different CDNs have been conducted even before the STING signaling pathway was illustrated.[89] The broad proinflammatory cytokine profile CDNs elicited has made them great adjuvant candidates for the development of vaccines against intracellular pathogenic infection such as HSV, HIV and *Mycobacterium tuberculosis*.[7, 90-92] In addition to infectious diseases, activation of STING signaling pathways has also been associated with cancer immunity.[93-95] Studies have shown that STING pathway is essential for radiation-induced antitumor immunity.[96] Tumor-derived DNA induces IFN-β production in tumor-infiltrating dendritic cells (DCs) in a STING-dependent manner, which further promote antitumor T cell response.[97] Great efforts have been made to produce degradation-resistance CDN analogs in order to enhance their potency as STING agonists.[95, 98] STING agonist formulated cancer vaccines have been tested in combination with other immunotherapeutic strategies such as PD-1 blockade in several clinic trials in order to enhance the efficacy of cancer treatment.[99-100]

1.7 References

1. Danilchanka, O.; Mekalanos, J. J., Cyclic dinucleotides and the innate immune response. *Cell* **2013,** *154* (5), 962-70.

2. Jenal, U.; Reinders, A.; Lori, C., Cyclic di-GMP: second messenger extraordinaire. *Nat Rev Microbiol* **2017,** *15* (5), 271-284.

3. Fahmi, T.; Port, G. C.; Cho, K. H., c-di-AMP: An Essential Molecule in the Signaling Pathways that Regulate the Viability and Virulence of Gram-Positive Bacteria. *Genes (Basel)* **2017,** *8* (8).

4. Zhang, X.; Shi, H.; Wu, J.; Zhang, X.; Sun, L.; Chen, C.; Chen, Z. J., Cyclic GMP-AMP containing mixed phosphodiester linkages is an endogenous high-affinity ligand for STING. *Molecular cell* **2013,** *51* (2), 226-235.

5. Gao, P.; Ascano, M.; Wu, Y.; Barchet, W.; Gaffney, Barbara L.; Zillinger, T.; Serganov, Artem A.; Liu, Y.; Jones, Roger A.; Hartmann, G.; Tuschl, T.; Patel, Dinshaw J., Cyclic [G(2′,5′)pA(3′,5′)p] Is the Metazoan Second Messenger Produced by DNA-Activated Cyclic GMP-AMP Synthase. *Cell* **2013,** *153* (5), 1094-1107.

6. Chen, Q.; Sun, L.; Chen, Z. J., Regulation and function of the cGAS–STING pathway of cytosolic DNA sensing. *Nature Immunology* **2016,** *17*, 1142.

7. Libanova, R.; Becker, P. D.; Guzman, C. A., Cyclic di-nucleotides: new era for small molecules as adjuvants. *Microb Biotechnol* **2012,** *5* (2), 168-76.

8. Ross, P.; Weinhouse, H.; Aloni, Y.; Michaeli, D.; Weinberger-Ohana, P.; Mayer, R.; Braun, S.; de Vroom, E.; van der Marel, G. A.; van Boom, J. H.; Benziman, M., Regulation of cellulose synthesis in Acetobacter xylinum by cyclic diguanylic acid. *Nature* **1987,** *325*, 279-281.

9. D'Argenio, D. A.; Miller, S. I., Cyclic di-GMP as a bacterial second messenger. *Microbiology* **2004,** *150* (Pt 8), 2497-502.

10. Jenal, U., Cyclic di-guanosine-monophosphate comes of age: a novel secondary messenger involved in modulating cell surface structures in bacteria? *Current Opinion in Microbiology* **2004,** *7* (2), 185-191.

11. Jenal, U.; Malone, J., Mechanisms of Cyclic-di-GMP Signaling in Bacteria. *Annual Review of Genetics* **2006,** *40* (1), 385-407.

12. Römling, U.; Amikam, D., Cyclic di-GMP as a second messenger. *Current Opinion in Microbiology* **2006,** *9* (2), 218-228.

13. Römling, U.; Gomelsky, M.; Galperin, M. Y., C-di-GMP: the dawning of a novel bacterial signalling system. *Molecular Microbiology* **2005,** *57* (3), 629-639.

14. Romling, U.; Galperin, M. Y.; Gomelsky, M., Cyclic di-GMP: the first 25 years of a universal bacterial second messenger. *Microbiol Mol Biol Rev* **2013,** *77* (1), 1-52.

15. Tuckerman, J. R.; Gonzalez, G.; Sousa, E. H. S.; Wan, X.; Saito, J. A.; Alam, M.; Gilles-Gonzalez, M.-A., An Oxygen-Sensing Diguanylate Cyclase and Phosphodiesterase Couple for c-di-GMP Control. *Biochemistry* **2009,** *48* (41), 9764-9774.

16. Hengge, R., Trigger phosphodiesterases as a novel class of c-di-GMP effector proteins. *Philosophical Transactions of the Royal Society B: Biological Sciences* **2016,** *371* (1707), 20150498.

17. Boehm, A.; Kaiser, M.; Li, H.; Spangler, C.; Kasper, C. A.; Ackermann, M.; Kaever, V.; Sourjik, V.; Roth, V.; Jenal, U., Second Messenger-Mediated Adjustment of Bacterial Swimming Velocity. *Cell* **2010,** *141* (1), 107-116.

18. Habazettl, J.; Allan, M. G.; Jenal, U.; Grzesiek, S., Solution Structure of the PilZ Domain Protein PA4608 Complex with Cyclic di-GMP Identifies Charge Clustering as Molecular Readout. *Journal of Biological Chemistry* **2011,** *286* (16), 14304-14314.

19. Schumacher, M. A.; Zeng, W., Structures of the activator of K. pneumonia biofilm formation, MrkH, indicates PilZ domains involved in c-di-GMP and DNA binding. *Proceedings of the National Academy of Sciences* **2016,** *113* (36), 10067-10072.

20. Krasteva, P. V.; Fong, J. C. N.; Shikuma, N. J.; Beyhan, S.; Navarro, M. V. A. S.; Yildiz, F. H.; Sondermann, H., Vibrio cholerae VpsT Regulates Matrix Production and Motility by Directly Sensing Cyclic di-GMP. *Science* **2010,** *327* (5967), 866-868.

21. Tschowri, N.; Schumacher, Maria A.; Schlimpert, S.; Chinnam, Naga b.; Findlay, Kim C.; Brennan, Richard G.; Buttner, Mark J., Tetrameric c-di-GMP Mediates Effective Transcription Factor Dimerization to Control Streptomyces Development. *Cell* **2014,** *158* (5), 1136-1147.

22. Baraquet, C.; Harwood, C. S., Cyclic diguanosine monophosphate represses bacterial flagella synthesis by interacting with the Walker A motif of the enhancer-

binding protein FleQ. *Proceedings of the National Academy of Sciences* **2013,** *110* (46), 18478-18483.

23. Hengge, R., Cyclic-di-GMP Reaches Out into the Bacterial RNA World. *Science Signaling* **2010,** *3* (149), pe44-pe44.

24. Duerig, A.; Abel, S.; Folcher, M.; Nicollier, M.; Schwede, T.; Amiot, N.; Giese, B.; Jenal, U., Second messenger-mediated spatiotemporal control of protein degradation regulates bacterial cell cycle progression. *Genes & Development* **2009,** *23* (1), 93-104.

25. Valentini, M.; Filloux, A., Biofilms and Cyclic di-GMP (c-di-GMP) Signaling: Lessons from Pseudomonas aeruginosa and Other Bacteria. *The Journal of biological chemistry* **2016,** *291* (24), 12547-12555.

26. Christen, M.; Kulasekara, H. D.; Christen, B.; Kulasekara, B. R.; Hoffman, L. R.; Miller, S. I., Asymmetrical Distribution of the Second Messenger c-di-GMP upon Bacterial Cell Division. *Science* **2010,** *328* (5983), 1295-1297.

27. Kulasekara, B. R.; Kamischke, C.; Kulasekara, H. D.; Christen, M.; Wiggins, P. A.; Miller, S. I., c-di-GMP heterogeneity is generated by the chemotaxis machinery to regulate flagellar motility. *eLife* **2013,** *2*, e01402-e01402.

28. Trampari, E.; Stevenson, C. E. M.; Little, R. H.; Wilhelm, T.; Lawson, D. M.; Malone, J. G., Bacterial Rotary Export ATPases Are Allosterically Regulated by the Nucleotide Second Messenger Cyclic-di-GMP. *Journal of Biological Chemistry* **2015,** *290* (40), 24470-24483.

29. Roelofs, K. G.; Jones, C. J.; Helman, S. R.; Shang, X.; Orr, M. W.; Goodson, J. R.; Galperin, M. Y.; Yildiz, F. H.; Lee, V. T., Systematic Identification of Cyclic-di-GMP Binding Proteins in Vibrio cholerae Reveals a Novel Class of Cyclic-di-GMP-Binding ATPases Associated with Type II Secretion Systems. *PLOS Pathogens* **2015,** *11* (10), e1005232.

30. Richter, A. M.; Povolotsky, T. L.; Wieler, L. H.; Hengge, R., Cyclic-di-GMP signalling and biofilm-related properties of the Shiga toxin-producing 2011 German outbreak Escherichia coli O104:H4. *EMBO Molecular Medicine* **2014,** *6* (12), 1622.

31. Witte, G.; Hartung, S.; Büttner, K.; Hopfner, K.-P., Structural Biochemistry of a Bacterial Checkpoint Protein Reveals Diadenylate Cyclase Activity Regulated by DNA Recombination Intermediates. *Molecular Cell* **2008,** *30* (2), 167-178.

32. Witte, C. E.; Archer, K. A.; Rae, C. S.; Sauer, J.-D.; Woodward, J. J.; Portnoy, D. A., Chapter 8 - Innate Immune Pathways Triggered by Listeria monocytogenes and Their Role in the Induction of Cell-Mediated Immunity. In *Advances in Immunology*, Unanue, E. R.; Carrero, J. A., Eds. Academic Press: 2012; Vol. 113, pp 135-156.

33. Luo, Y.; Helmann, J. D., Analysis of the role of Bacillus subtilis σM in β-lactam resistance reveals an essential role for c-di-AMP in peptidoglycan homeostasis. *Molecular Microbiology* **2012,** *83* (3), 623-639.

34. Corrigan, R. M.; Abbott, J. C.; Burhenne, H.; Kaever, V.; Gründling, A., c-di-AMP Is a New Second Messenger in Staphylococcus aureus with a Role in Controlling Cell Size and Envelope Stress. *PLOS Pathogens* **2011,** *7* (9), e1002217.

35. Corrigan, R. M.; Campeotto, I.; Jeganathan, T.; Roelofs, K. G.; Lee, V. T.; Gründling, A., Systematic identification of conserved bacterial c-di-AMP receptor proteins. *Proceedings of the National Academy of Sciences of the United States of America* **2013,** *110* (22), 9084-9089.

36. Gundlach, J.; Rath, H.; Herzberg, C.; Mäder, U.; Stülke, J., Second Messenger Signaling in Bacillus subtilis: Accumulation of Cyclic di-AMP Inhibits Biofilm Formation. *Frontiers in microbiology* **2016,** *7*, 804-804.

37. Bai, Y.; Yang, J.; Zarrella, T. M.; Zhang, Y.; Metzger, D. W.; Bai, G., Cyclic Di-AMP Impairs Potassium Uptake Mediated by a Cyclic Di-AMP Binding Protein in Streptococcus pneumoniae. *Journal of Bacteriology* **2014,** *196* (3), 614.

38. Corrigan, R. M.; Gründling, A., Cyclic di-AMP: another second messenger enters the fray. *Nature Reviews Microbiology* **2013,** *11*, 513.

39. Gundlach, J.; Herzberg, C.; Kaever, V.; Gunka, K.; Hoffmann, T.; Weiß, M.; Gibhardt, J.; Thürmer, A.; Hertel, D.; Daniel, R.; Bremer, E.; Commichau, F. M.; Stülke, J., Control of potassium homeostasis is an essential function of the second messenger cyclic di-AMP in Bacillus subtilis. *Science Signaling* **2017,** *10* (475), eaal3011.

40. Sureka, K.; Choi, Philip H.; Precit, M.; Delince, M.; Pensinger, D. A.; Huynh, TuAnh N.; Jurado, Ashley R.; Goo, Young A.; Sadilek, M.; Iavarone, Anthony T.; Sauer, J.-D.; Tong, L.; Woodward, Joshua J., The Cyclic Dinucleotide c-di-AMP Is an Allosteric Regulator of Metabolic Enzyme Function. *Cell* **2014,** *158* (6), 1389-1401.

41. Whiteley, A. T.; Garelis, N. E.; Peterson, B. N.; Choi, P. H.; Tong, L.; Woodward, J. J.; Portnoy, D. A., c-di-AMP modulates Listeria monocytogenes central metabolism to regulate growth, antibiotic resistance and osmoregulation. *Molecular Microbiology* **2017,** *104* (2), 212-233.

42. Davies, B. W.; Bogard, R. W.; Young, T. S.; Mekalanos, J. J., Coordinated regulation of accessory genetic elements produces cyclic di-nucleotides for V. cholerae virulence. *Cell* **2012,** *149* (2), 358-70.

43. Nelson, J. W.; Sudarsan, N.; Phillips, G. E.; Stav, S.; Lünse, C. E.; McCown, P. J.; Breaker, R. R., Control of bacterial exoelectrogenesis by c-AMP-GMP. *Proceedings of the National Academy of Sciences* **2015,** *112* (17), 5389.

44. Severin, G. B.; Ramliden, M. S.; Hawver, L. A.; Wang, K.; Pell, M. E.; Kieninger, A.-K.; Khataokar, A.; O'Hara, B. J.; Behrmann, L. V.; Neiditch, M. B.; Benning, C.; Waters, C. M.; Ng, W.-L., Direct activation of a phospholipase by cyclic GMP-AMP in El Tor Vibrio cholerae</em&gt. *Proceedings of the National Academy of Sciences* **2018,** *115* (26), E6048.

45. Kellenberger, C. A.; Wilson, S. C.; Hickey, S. F.; Gonzalez, T. L.; Su, Y.; Hallberg, Z. F.; Brewer, T. F.; Iavarone, A. T.; Carlson, H. K.; Hsieh, Y.-F.; Hammond, M. C., GEMM-I riboswitches from Geobacter sense the bacterial second messenger cyclic AMP-GMP. *Proceedings of the National Academy of Sciences* **2015,** *112* (17), 5383.

46. Iwasaki, A.; Medzhitov, R., Regulation of Adaptive Immunity by the Innate Immune System. *Science* **2010,** *327* (5963), 291.

47. Burdette, D. L.; Monroe, K. M.; Sotelo-Troha, K.; Iwig, J. S.; Eckert, B.; Hyodo, M.; Hayakawa, Y.; Vance, R. E., STING is a direct innate immune sensor of cyclic di-GMP. *Nature* **2011,** *478* (7370), 515-8.

48. Gao, P.; Ascano, M.; Zillinger, T.; Wang, W.; Dai, P.; Serganov, A. A.; Gaffney, B. L.; Shuman, S.; Jones, R. A.; Deng, L.; Hartmann, G.; Barchet, W.; Tuschl, T.; Patel,

D. J., Structure-function analysis of STING activation by c[G(2',5')pA(3',5')p] and targeting by antiviral DMXAA. *Cell* **2013,** *154* (4), 748-62.

49. Liu, S.; Cai, X.; Wu, J.; Cong, Q.; Chen, X.; Li, T.; Du, F.; Ren, J.; Wu, Y.-T.; Grishin, N. V.; Chen, Z. J., Phosphorylation of innate immune adaptor proteins MAVS, STING, and TRIF induces IRF3 activation. *Science* **2015,** *347* (6227), aaa2630.

50. Tsuchiya, Y.; Jounai, N.; Takeshita, F.; Ishii, K. J.; Mizuguchi, K., Ligand-induced Ordering of the C-terminal Tail Primes STING for Phosphorylation by TBK1. *EBioMedicine* **2016,** *9*, 87-96.

51. Margolis, S. R.; Wilson, S. C.; Vance, R. E., Evolutionary Origins of cGAS-STING Signaling. *Trends Immunol* **2017,** *38* (10), 733-743.

52. Chen, H.; Sun, H.; You, F.; Sun, W.; Zhou, X.; Chen, L.; Yang, J.; Wang, Y.; Tang, H.; Guan, Y.; Xia, W.; Gu, J.; Ishikawa, H.; Gutman, D.; Barber, G.; Qin, Z.; Jiang, Z., Activation of STAT6 by STING Is Critical for Antiviral Innate Immunity. *Cell* **2011,** *147* (2), 436-446.

53. Abe, T.; Barber, G. N., Cytosolic-DNA-Mediated, STING-Dependent Proinflammatory Gene Induction Necessitates Canonical NF-κB Activation through TBK1. *Journal of Virology* **2014,** *88* (10), 5328.

54. Diner, E. J.; Burdette, D. L.; Wilson, S. C.; Monroe, K. M.; Kellenberger, C. A.; Hyodo, M.; Hayakawa, Y.; Hammond, M. C.; Vance, R. E., The innate immune DNA sensor cGAS produces a noncanonical cyclic dinucleotide that activates human STING. *Cell Rep* **2013,** *3* (5), 1355-61.

55. Ablasser, A.; Goldeck, M.; Cavlar, T.; Deimling, T.; Witte, G.; Rohl, I.; Hopfner, K. P.; Ludwig, J.; Hornung, V., cGAS produces a 2'-5'-linked cyclic dinucleotide second messenger that activates STING. *Nature* **2013,** *498* (7454), 380–4.

56. Wu, J.; Sun, L.; Chen, X.; Du, F.; Shi, H.; Chen, C.; Chen, Z. J., Cyclic GMP-AMP is an endogenous second messenger in innate immune signaling by cytosolic DNA. *Science* **2013,** *339* (6121), 826-30.

57. Sun, L.; Wu, J.; Du, F.; Chen, X.; Chen, Z. J., Cyclic GMP-AMP Synthase Is a Cytosolic DNA Sensor That Activates the Type I Interferon Pathway. *Science* **2013,** *339*, 786-791.

58. Zhang, X.; Wu, J.; Du, F.; Xu, H.; Sun, L.; Chen, Z.; Brautigam, Chad A.; Zhang, X.; Chen, Zhijian J., The Cytosolic DNA Sensor cGAS Forms an Oligomeric Complex with DNA and Undergoes Switch-like Conformational Changes in the Activation Loop. *Cell Reports* **2014,** *6* (3), 421-430.

59. Barbalat, R.; Ewald, S. E.; Mouchess, M. L.; Barton, G. M., Nucleic Acid Recognition by the Innate Immune System. *Annual Review of Immunology* **2011,** *29* (1), 185-214.

60. Chan, C.; Paul, R.; Samoray, D.; Amiot, N. C.; Giese, B.; Jenal, U.; Schirmer, T., Structural basis of activity and allosteric control of diguanylate cyclase. *Proceedings of the National Academy of Sciences of the United States of America* **2004,** *101* (49), 17084-17089.

61. Wassmann, P.; Chan, C.; Paul, R.; Beck, A.; Heerklotz, H.; Jenal, U.; Schirmer, T., Structure of BeF3−-Modified Response Regulator PleD: Implications for Diguanylate Cyclase Activation, Catalysis, and Feedback Inhibition. *Structure* **2007,** *15* (8), 915-927.

62. Christen, B.; Christen, M.; Paul, R.; Schmid, F.; Folcher, M.; Jenoe, P.; Meuwly, M.; Jenal, U., Allosteric Control of Cyclic di-GMP Signaling. *Journal of Biological Chemistry* **2006,** *281* (42), 32015-32024.

63. Bellini, D.; Caly, D. L.; McCarthy, Y.; Bumann, M.; An, S.-Q.; Dow, J. M.; Ryan, R. P.; Walsh, M. A., Crystal structure of an HD-GYP domain cyclic-di-GMP phosphodiesterase reveals an enzyme with a novel trinuclear catalytic iron centre. *Molecular Microbiology* **2014,** *91* (1), 26-38.

64. Cohen, D.; Mechold, U.; Nevenzal, H.; Yarmiyhu, Y.; Randall, T. E.; Bay, D. C.; Rich, J. D.; Parsek, M. R.; Kaever, V.; Harrison, J. J.; Banin, E., Oligoribonuclease is a central feature of cyclic diguanylate signaling in Pseudomonas aeruginosa *Proceedings of the National Academy of Sciences* **2015,** *112* (36), 11359.

65. Orr, M. W.; Donaldson, G. P.; Severin, G. B.; Wang, J.; Sintim, H. O.; Waters, C. M.; Lee, V. T., Oligoribonuclease is the primary degradative enzyme for pGpG in Pseudomonas aeruginosa that is required for cyclic-di-GMP turnover. *Proceedings of the National Academy of Sciences* **2015,** *112* (36), E5048.

66. Reinders, A.; Hee, C.-S.; Ozaki, S.; Mazur, A.; Boehm, A.; Schirmer, T.; Jenal, U., Expression and Genetic Activation of Cyclic Di-GMP-Specific Phosphodiesterases in Escherichia coli. *Journal of Bacteriology* **2016,** *198* (3), 448.

67. Hengge, R.; Galperin, M. Y.; Ghigo, J.-M.; Gomelsky, M.; Green, J.; Hughes, K. T.; Jenal, U.; Landini, P., Systematic Nomenclature for GGDEF and EAL Domain-Containing Cyclic Di-GMP Turnover Proteins of Escherichia coli. *Journal of Bacteriology* **2016,** *198* (1), 7.

68. García, B.; Latasa, C.; Solano, C.; Portillo, F. G.-d.; Gamazo, C.; Lasa, I., Role of the GGDEF protein family in Salmonella cellulose biosynthesis and biofilm formation. *Molecular Microbiology* **2004,** *54* (1), 264-277.

69. Oppenheimer-Shaanan, Y.; Wexselblatt, E.; Katzhendler, J.; Yavin, E.; Ben-Yehuda, S., c-di-AMP reports DNA integrity during sporulation in Bacillus subtilis. *EMBO reports* **2011,** *12* (6), 594-601.

70. Bejerano-Sagie, M.; Oppenheimer-Shaanan, Y.; Berlatzky, I.; Rouvinski, A.; Meyerovich, M.; Ben-Yehuda, S., A Checkpoint Protein That Scans the Chromosome for Damage at the Start of Sporulation in Bacillus subtilis. *Cell* **2006,** *125* (4), 679-690.

71. Rao, F.; See, R. Y.; Zhang, D.; Toh, D. C.; Ji, Q.; Liang, Z.-X., YybT Is a Signaling Protein That Contains a Cyclic Dinucleotide Phosphodiesterase Domain and a GGDEF Domain with ATPase Activity. *Journal of Biological Chemistry* **2010,** *285* (1), 473-482.

72. Huynh, T. N.; Luo, S.; Pensinger, D.; Sauer, J.-D.; Tong, L.; Woodward, J. J., An HD-domain phosphodiesterase mediates cooperative hydrolysis of c-di-AMP to affect bacterial growth and virulence. *Proceedings of the National Academy of Sciences* **2015,** *112* (7), E747.

73. Woodward, J. J.; Iavarone, A. T.; Portnoy, D. A., c-di-AMP Secreted by Intracellular Listeria monocytogenes Activates a Host Type I Interferon Response. *Science* **2010,** *328* (5986), 1703.

74. Huynh, T. N.; Woodward, J. J., Too much of a good thing: regulated depletion of c-di-AMP in the bacterial cytoplasm. *Current Opinion in Microbiology* **2016,** *30*, 22-29.

75. Bowman, L.; Zeden, M. S.; Schuster, C. F.; Kaever, V.; Gründling, A., New Insights into the Cyclic Di-adenosine Monophosphate (c-di-AMP) Degradation Pathway and the Requirement of the Cyclic Dinucleotide for Acid Stress Resistance in Staphylococcus aureus. *Journal of Biological Chemistry* **2016,** *291* (53), 26970-26986.

76. Bai, Y.; Yang, J.; Eisele, L. E.; Underwood, A. J.; Koestler, B. J.; Waters, C. M.; Metzger, D. W.; Bai, G., Two DHH Subfamily 1 Proteins in Streptococcus pneumoniae Possess Cyclic Di-AMP Phosphodiesterase Activity and Affect Bacterial Growth and Virulence. *Journal of Bacteriology* **2013,** *195* (22), 5123.

77. Davies, Bryan W.; Bogard, Ryan W.; Young, Travis S.; Mekalanos, John J., Coordinated Regulation of Accessory Genetic Elements Produces Cyclic Di-Nucleotides for V. cholerae Virulence. *Cell* **2012,** *149* (2), 358-370.

78. Kranzusch, P. J.; Lee, A. S. Y.; Wilson, S. C.; Solovykh, M. S.; Vance, R. E.; Berger, J. M.; Doudna, J. A., Structure-guided reprogramming of human cGAS dinucleotide linkage specificity. *Cell* **2014,** *158* (5), 1011-1021.

79. Kato, K.; Ishii, R.; Hirano, S.; Ishitani, R.; Nureki, O., Structural Basis for the Catalytic Mechanism of DncV, Bacterial Homolog of Cyclic GMP-AMP Synthase. *Structure* **2015,** *23* (5), 843-850.

80. Hallberg, Z. F.; Wang, X. C.; Wright, T. A.; Nan, B.; Ad, O.; Yeo, J.; Hammond, M. C., Hybrid promiscuous (Hypr) GGDEF enzymes produce cyclic AMP-GMP (3′, 3′ -cGAMP). *Proceedings of the National Academy of Sciences* **2016,** *113* (7), 1790.

81. Gao, J.; Tao, J.; Liang, W.; Zhao, M.; Du, X.; Cui, S.; Duan, H.; Kan, B.; Su, X.; Jiang, Z., Identification and characterization of phosphodiesterases that specifically degrade 3′3′-cyclic GMP-AMP. *Cell Research* **2015,** *25*, 539.

82. Li, L.; Yin, Q.; Kuss, P.; Maliga, Z.; Millán, J. L.; Wu, H.; Mitchison, T. J., Hydrolysis of 2′3′-cGAMP by ENPP1 and design of nonhydrolyzable analogs. *Nature Chemical Biology* **2014,** *10*, 1043.

83. Dey, R. J.; Dey, B.; Zheng, Y.; Cheung, L. S.; Zhou, J.; Sayre, D.; Kumar, P.; Guo, H.; Lamichhane, G.; Sintim, H. O.; Bishai, W. R., Inhibition of innate immune cytosolic surveillance by an M. tuberculosis phosphodiesterase. *Nature Chemical Biology* **2016,** *13*, 210.

84. Krasteva, P. V.; Sondermann, H., Versatile modes of cellular regulation via cyclic dinucleotides. *Nat Chem Biol* **2017,** *13* (4), 350-359.

85. Egli, M.; Gessner, R. V.; Williams, L. D.; Quigley, G. J.; van der Marel, G. A.; van Boom, J. H.; Rich, A.; Frederick, C. A., Atomic-resolution structure of the cellulose synthase regulator cyclic diguanylic acid. *Proceedings of the National Academy of Sciences* **1990,** *87* (8), 3235.

86. Gentner, M.; Allan, M. G.; Zaehringer, F.; Schirmer, T.; Grzesiek, S., Oligomer formation of the bacterial second messenger c-di-GMP: reaction rates and equilibrium constants indicate a monomeric state at physiological concentrations. *J Am Chem Soc* **2012,** *134* (2), 1019-29.

87. Zhang, Z.; Kim, S.; Gaffney, B. L.; Jones, R. A., Polymorphism of the Signaling Molecule c-di-GMP. *Journal of the American Chemical Society* **2006,** *128* (21), 7015-7024.

88. Zhou, J.; Zheng, Y.; Roembke, B. T.; Robinson, Sarah M.; Opoku-Temeng, C.; Sayre, D. A.; Sintim, H. O., Fluorescent analogs of cyclic and linear dinucleotides as phosphodiesterase and oligoribonuclease activity probes. *RSC Adv.* **2017,** *7* (9), 5421-5426.

89. Dubensky, J., T. W. ; Kanne, D. B.; Leong, M. L., Rationale, progress and development of vaccines utilizing STING-activating cyclic dinucleotide adjuvants. *Ther Adv Vaccines* **2013,** *1* (4), 131–143.

90. Li, X. D.; Wu, J.; Gao, D.; Wang, H.; Sun, L.; Chen, Z. J., Pivotal roles of cGAS-cGAMP signaling in antiviral defense and immune adjuvant effects. *Science* **2013,** *341* (6152), 1390-4.

91. Van Dis, E.; Sogi, K. M.; Rae, C. S.; Sivick, K. E.; Surh, N. H.; Leong, M. L.; Kanne, D. B.; Metchette, K.; Leong, J. J.; Bruml, J. R.; Chen, V.; Heydari, K.; Cadieux, N.; Evans, T.; McWhirter, S. M.; Dubensky, T. W.; Portnoy, D. A.; Stanley, S. A., STING-Activating Adjuvants Elicit a Th17 Immune Response and Protect against Mycobacterium tuberculosis Infection. *Cell Reports* **2018,** *23* (5), 1435-1447.

92. Gao, D.; Wu, J.; Wu, Y.-T.; Du, F.; Aroh, C.; Yan, N.; Sun, L.; Chen, Z. J., Cyclic GMP-AMP Synthase Is an Innate Immune Sensor of HIV and Other Retroviruses. *Science* **2013,** *341* (6148), 903.

93. Barber, G. N., STING: infection, inflammation and cancer. *Nat Rev Immunol* **2015,** *15* (12), 760-70.

94. Curran, E.; Chen, X.; Corrales, L.; Kline, D. E.; Dubensky, T. W., Jr.; Duttagupta, P.; Kortylewski, M.; Kline, J., STING Pathway Activation Stimulates Potent Immunity against Acute Myeloid Leukemia. *Cell Rep* **2016,** *15* (11), 2357-66.

95. Corrales, L.; Glickman, L. H.; McWhirter, S. M.; Kanne, D. B.; Sivick, K. E.; Katibah, G. E.; Woo, S. R.; Lemmens, E.; Banda, T.; Leong, J. J.; Metchette, K.; Dubensky, T. W., Jr.; Gajewski, T. F., Direct Activation of STING in the Tumor Microenvironment Leads to Potent and Systemic Tumor Regression and Immunity. *Cell Rep* **2015,** *11* (7), 1018-30.

96. Deng, L.; Liang, H.; Xu, M.; Yang, X.; Burnette, B.; Arina, A.; Li, X.-D.; Mauceri, H.; Beckett, M.; Darga, T.; Huang, X.; Gajewski, Thomas F.; Chen, Zhijian J.; Fu, Y.-X.; Weichselbaum, Ralph R., STING-Dependent Cytosolic DNA Sensing Promotes Radiation-Induced Type I Interferon-Dependent Antitumor Immunity in Immunogenic Tumors. *Immunity* **2014,** *41* (5), 843-852.

97. Woo, S. R.; Fuertes, M. B.; Corrales, L.; Spranger, S.; Furdyna, M. J.; Leung, M. Y.; Duggan, R.; Wang, Y.; Barber, G. N.; Fitzgerald, K. A.; Alegre, M. L.; Gajewski, T. F., STING-dependent cytosolic DNA sensing mediates innate immune recognition of immunogenic tumors. *Immunity* **2014,** *41* (5), 830-42.

98. Li, L.; Yin, Q.; Kuss, P.; Maliga, Z.; Millan, J. L.; Wu, H.; Mitchison, T. J., Hydrolysis of 2'3'-cGAMP by ENPP1 and design of nonhydrolyzable analogs. *Nat Chem Biol* **2014,** *10* (12), 1043-8.

99. Fu, J.; Kanne, D. B.; Leong, M.; Glickman, L. H.; McWhirter, S. M.; Lemmens, E.; Mechette, K.; Leong, J. J.; Lauer, P.; Liu, W.; Sivick, K. E.; Zeng, Q.; Soares, K. C.; Zheng, L.; Portnoy, D. A.; Woodward, J. J.; Pardoll, D. M.; Dubensky Jr., T. W.; Kim, Y., STING agonist formulated cancer vaccines can cure established tumors resistant to PD-1 blockade. *Sci. Transl. Med.* **2015,** *7* (283), 283ra52.

100. Hanson, M. C.; Crespo, M. P.; Abraham, W.; Moynihan, K. D.; Szeto, G. L.; Chen, S. H.; Melo, M. B.; Mueller, S.; Irvine, D. J., Nanoparticulate STING agonists are potent lymph node–targeted vaccine adjuvants. *The Journal of Clinical Investigation* **2015,** *125* (6), 2532-2546.

2 Development of isomorphic fluorescent CDN analogs

2.1 Introduction of isomorphic fluorescent nucleosides in the Tor lab

Nucleosides are fundamental components for all living organisms. The deoxyribonucleosides, including deoxy-adenosine (dA), deoxy-guanosine (dG), thymidine (T), and deoxy-cytidine (dC), are basic components of deoxyribonucleic acids (DNA), whereas the four types of ribonucleosides, adenosine (A), guanosine (G), uridine (U), and cytidine (C), are essential components of ribonucleic acids (RNA) (**Figure 2.1**).[1] The minimal building blocks of DNA and RNA are nucleotides, which can be considered as nucleosides that are functionalized with a 5'-phosphate group. DNA is essential for the storage of genetic information, while RNA not only acts as messenger and transporter that convey the genetic information from DNA to protein, but could also demonstrate catalytic and regulatory functions.[2]

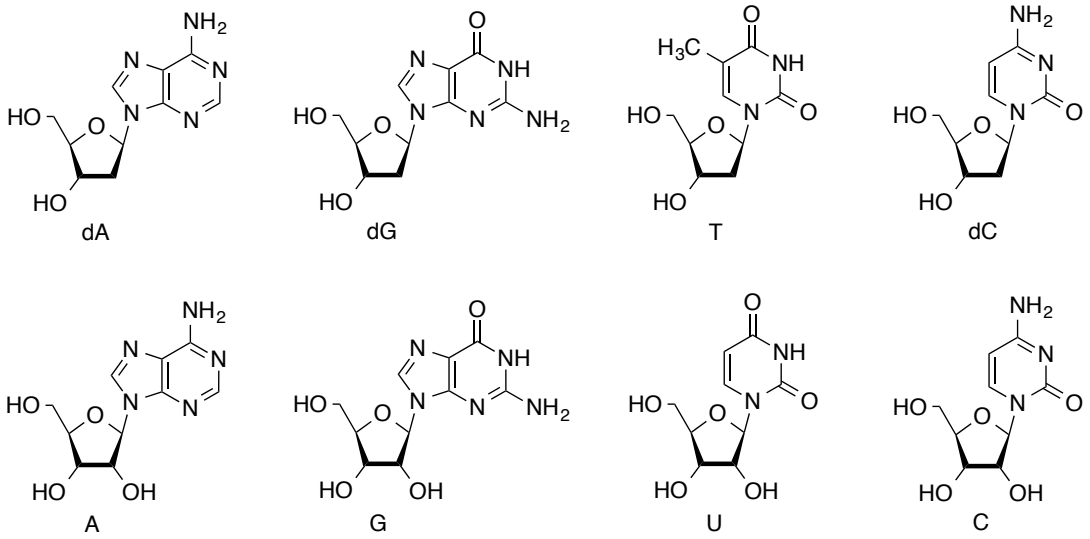

Figure 2.1 Canonical deoxyribonucleosides (dA, dG, T, dC) and ribonucleosides (A, G, U, C).

In addition to DNA and RNA, nucleosides and nucleotides can be also incorporated into enzyme cofactors (i.e. coenzyme A, SAM, NAD^+, and $NADP^+$) and second messengers that play essential roles in cell signaling, such as cyclic nucleotides (cGMP, cAMP) and CDNs (**Figure 2.2**).[3]

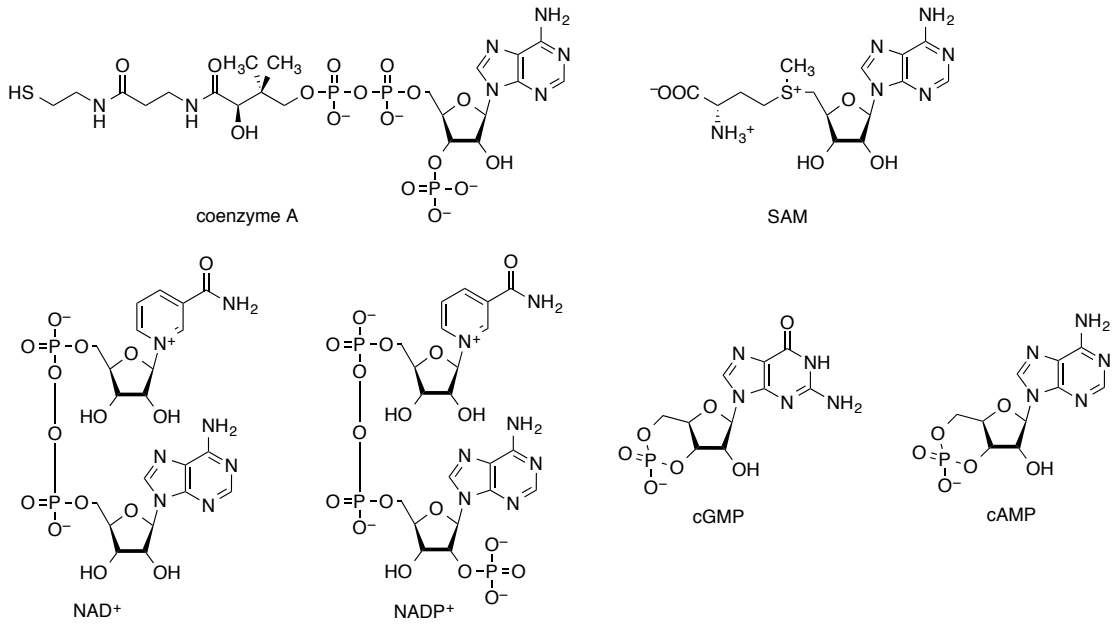

Figure 2.2 Enzyme cofactors and second messengers where nucleosides or nucleotides are incorporated.

Considering the wide range of biological and biochemical processes nucleosides and nucleotides are involved in, novel techniques and tools that could aid the investigations of these processes are greatly appreciated. Fluorescence-based techniques have been playing key roles in modern biochemical and biophysical research due to their high sensitivity and informativeness. However, due to the non-emissive nature of most canonical nucleosides, great efforts have been taken to develop applicable approaches so as to take advantage of fluorescence-based tools in nucleic acids research.[4] A well-known example is the application of fluorescent dye-labeled

terminators in Sanger sequencing, which are prepared by covalently attach fluorescent dyes (such as rhodamine and fluorescein) to dideoxynucleoside triphosphates (ddNTPs).[5-6] Replacing radioactively labeled terminators to fluorescently labeled ones greatly facilitated the development of automated sequencing. However, due to the structural perturbation, such labeling approach might not be applicable for detailed analysis where structural analogy to the native nucleotides is highly desired. Therefore, the development of fluorescent nucleosides with minimum perturbation to their hydrogen bonding patterns and overall dimension is of key importance. The desired fluorescent nucleoside analogs should have appreciably applicable photophysical properties (discussed in section 2.2) and close structural analogy to the native counterparts in order to ensure the biological meaningfulness of the readout.

The Tor group has been developing isomorphic fluorescent nucleosides and applying them in biophysical and biochemical studies of oligonucleotides and enzyme cofactors that involve nucleoside building blocks.[4, 7-8] Recent works of the Tor group feature the development of two families of isomorphic emissive ribonucleosides and corresponding ribonucleoside triphosphates (NTPs), the thiopheno ($^{th-}$) family and the isothiazolo ($^{tz-}$) family (**Figure 2.3**).[7-8] These two families of nucleoside analogs demonstrated distinctive photophysical properties and were able to form functional W–C base pairs.

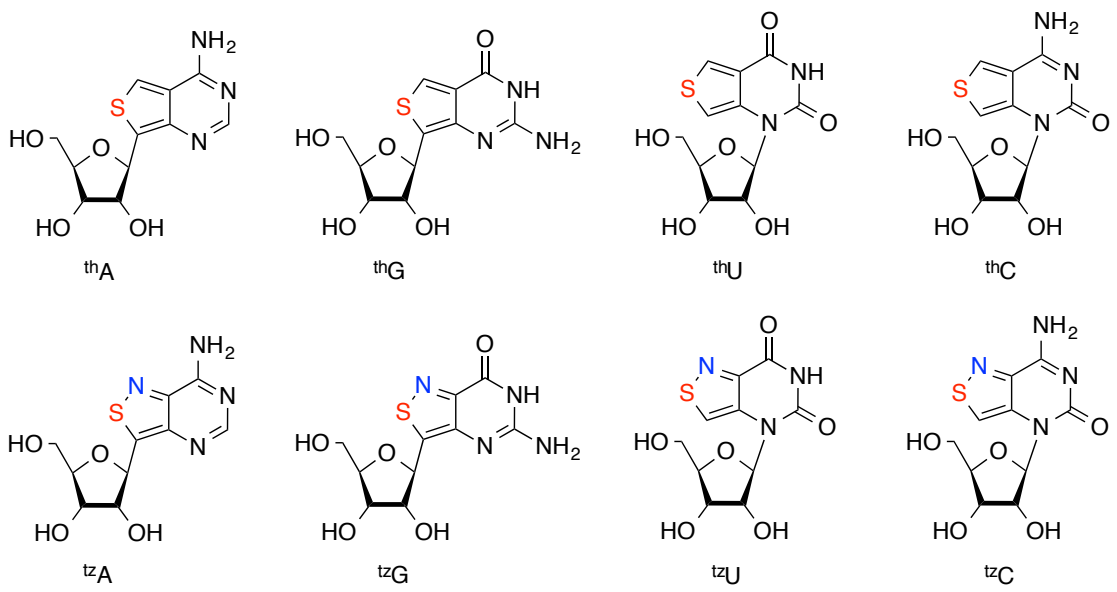

Figure 2.3 The thiopheno ([th-]) and the isothiazolo ([tz-]) families of ribonucleosides.

Several studies have taken advantage of the isomorphicity and/or desirable fluorescence properties of these molecules to investigate catalytic RNA and enzyme cofactors.[9-12] For example, mechanistic analysis of hammerhead ribozyme HH16 was conducted by incorporating [th]G at desired sites of the HH16 RNA.[9] Thanks to the isomorphicity of [th]G, instead of using traditional solid-phase synthesis to incorporate modified nucleosides at specific sites, we were able to achieve it by T7 RNA polymerase mediated transcription, which does not require the challenging nucleoside phosphoramidite synthesis.[9]

2.2 Photophysical properties

Fluorescence is a form of luminescence which describes the emission of light from any substance that has absorbed electromagnetic radiation (light).[13] In addition to the maximum absorption and emission wavelengths, several key values are often used

to describe photophysical properties of chromophores, including extinction coefficient (ε) and fluorescence quantum yield (Φ). [13]

The extinction coefficient is also referred to as molar absorptivity and is used to describe the efficiency of a substance in absorbing electromagnetic radiation.[13] Beer–Lambert law, which correlates absorbance with the concentration of a substance, is often used to define extinction coefficient. The commonly used form of Beer–Lambert law in experiments is shown as follow:

$$A = \varepsilon bc$$

Equation 2.1 Commonly used form of Beer–Lambert law equation.

where A is absorption, ε is the extinction coefficient which is wavelength-dependent (with unit L mol^{-1} cm^{-1}), b is the path length of the cuvette that contains the sample, c is the concentration of the sample in the cuvette (with unit mol L^{-1}).

Quantum yield is defined as the radio of the number of photons emitted to the number of photons absorbed, which can be represented by the ratio of fluorescence lifetime (τ) to excited state lifetime (τ_0), as described in the following equation:

$$\Phi = \tau / \tau_0$$

Equation 2.2 Equation of fluorescence quantum yield defined by the ratio of fluorescent lifetime to excited state lifetime.

where τ_0 reflects sum of all radiative and nonradiative processes that a chromophore undertakes decaying from excited state to the ground state, while τ represents the fraction of those processes that is responsible for emitting a photon.[13]

Without knowing the lifetimes of a chromophore, relative quantum yield can be generated in experiment by employing a chromophore of known quantum yield as a standard and apply the same experimental parameters to measure the florescence of both the standard and the sample.[8] The equation of relative quantum yield is listed below:

$$\Phi = \Phi_{STD} \frac{I}{I_{STD}} \frac{OD_{STD}}{OD} \frac{n^2}{n_{STD}^2}$$

Equation 2.3 Relative fluorescent quantum yield equation.

where Φ is relative quantum yield of sample, Φ_{STD} is the quantum yield of the standard, I and I_{STD} are the integrated area under the emission spectrum of the sample and the standard at the respectively, OD and OD_{STD} are the optical density at the excitation wavelength for the sample and the standard, n and n_{STD} are the refractive index of the solvent to the sample and standard.

2.3 From fluorescent nucleosides to fluorescent CDNs

CDNs are important second messengers that are involved in bacterial pathogenesis and host innate immune response. Understanding the cyclization, hydrolysis and recognition of CDNs is of key importance to study CDN signaling pathways. Several types of fluorescent CDN analogs have been developed by synthetically incorporating previously known fluorescent nucleoside analogs into CDNs

(**Figure 2.4**).[14] These fluorescent CDN analogs were used to monitor the hydrolysis of CDNs with several types of PDEs, which demonstrated the potential of utilizing such fluorescent substrates in high-throughput screening for PDE inhibitors.[14] However, application of fluorescent CDN analogs in studying dinucleotide cyclases kinetics or receptor protein binding has not been reported. We speculate that the rigorous substrate recognition mechanism of these enzymes and receptor proteins might have limited the application of these fluorescent CDNs.

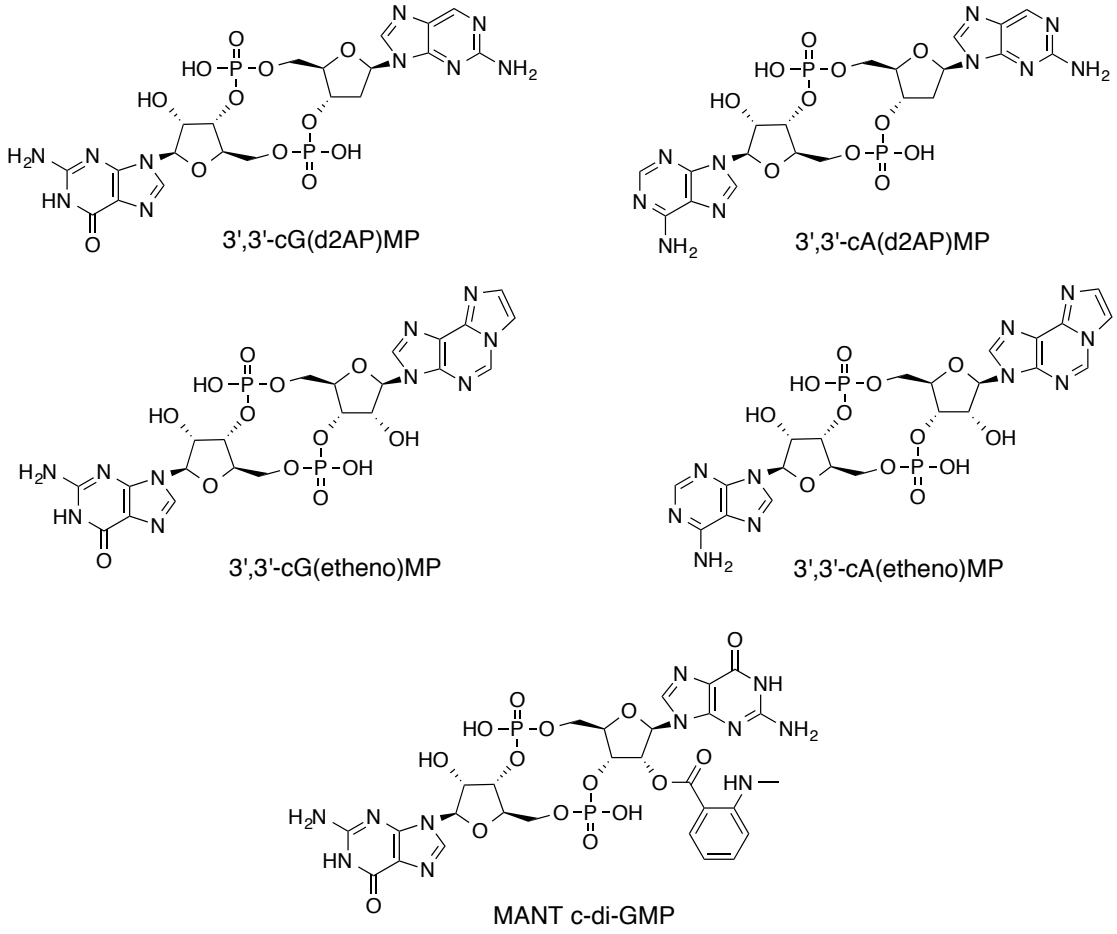

Figure 2.4 Fluorescent CDN analogs developed in previous studies.

Considering the high isomorphicity and isofunctionality the $^{th-}$ and $^{tz-}$ families of nucleosides have demonstrated, incorporating them into CDNs might allow the utilization of fluorescence-based techniques in directly monitoring the synthesis, hydrolysis and ligand-receptor interactions of CDNs in real-time. Moreover, due to the high sensitivity and simplicity of operation, such fluorescence-based techniques could be beneficial for high-throughput screening assays targeting inhibitors of enzymes or protein receptors involved in CDN signaling. As discussed in the previous chapter, various types of dinucleotide cyclases are responsible for converting two NTP (ATP and/or GTP) residues into the corresponding CDN in cells. Many of these enzymes, such as WspR, DisA, DncV and cGAS, also demonstrate remarkable activities in vitro, which provides a possible enzymatic approach of incorporating chemically-modified nucleosides into CDNs.

2.4 References

1. Crick, F., Central Dogma of Molecular Biology. *Nature* **1970,** *227* (5258), 561-563.

2. Chaffey, N., Alberts, B., Johnson, A., Lewis, J., Raff, M., Roberts, K. and Walter, P. Molecular biology of the cell. 4th edn. *Annals of Botany* **2003,** *91* (3), 401-401.

3. Geuther, R., A. L. LEHNINGER, Biochemistry. The Molecular Basis of Cell Structure and Function (2nd Edition). 1104 S., zahlr. Abb., zahlr. Tab. New York 1975. Worth Publ. Inc. $ 17.50. *Zeitschrift für allgemeine Mikrobiologie* **1977,** *17* (1), 86-87.

4. Sinkeldam, R. W.; Greco, N. J.; Tor, Y., Fluorescent Analogs of Biomolecular Building Blocks: Design, Properties, and Applications. *Chemical Reviews* **2010,** *110* (5), 2579-2619.

5. Prober, J.; Trainor, G.; Dam, R.; Hobbs, F.; Robertson, C.; Zagursky, R.; Cocuzza, A.; Jensen, M.; Baumeister, K., A system for rapid DNA sequencing with fluorescent chain-terminating dideoxynucleotides. *Science* **1987,** *238* (4825), 336-341.

6. Heiner, C. R.; Lee, L. G.; Khan, S. H.; Spurgeon, S. L.; Chen, S. M.; Menchen, S. M.; Rosenblum, B. B., New dye-labeled terminators for improved DNA sequencing patterns. *Nucleic Acids Research* **1997,** *25* (22), 4500-4504.

7. Shin, D.; Sinkeldam, R. W.; Tor, Y., Emissive RNA alphabet. *J Am Chem Soc* **2011,** *133* (38), 14912-5.

8. Rovira, A. R.; Fin, A.; Tor, Y., Chemical Mutagenesis of an Emissive RNA Alphabet. *J Am Chem Soc* **2015,** *137* (46), 14602-5.

9. Li, Y.; Fin, A.; McCoy, L.; Tor, Y., Polymerase-Mediated Site-Specific Incorporation of a Synthetic Fluorescent Isomorphic G Surrogate into RNA. *Angew Chem Int Ed Engl* **2017,** *56* (5), 1303-1307.

10. McCoy, L. S.; Shin, D.; Tor, Y., Isomorphic emissive GTP surrogate facilitates initiation and elongation of in vitro transcription reactions. *J Am Chem Soc* **2014,** *136* (43), 15176-84.

11. Hallé, F.; Fin, A.; Rovira, A. R.; Tor, Y., Emissive Synthetic Cofactors: Enzymatic Interconversions of tzA Analogues of ATP, NAD+, NADH, NADP+, and NADPH. *Angewandte Chemie International Edition* **2018,** *57* (4), 1087-1090.

12. Feldmann, J.; Li, Y.; Tor, Y., Emissive Synthetic Cofactors: A Highly Responsive NAD+ Analogue Reveals Biomolecular Recognition Features. *Chemistry – A European Journal 0* (0).

13. Masters, B. R., *Principles of Fluorescence Spectroscopy, Third Edition*. SPIE: 2008; Vol. 13.

14. Zhou, J.; Zheng, Y.; Roembke, B. T.; Robinson, Sarah M.; Opoku-Temeng, C.; Sayre, D. A.; Sintim, H. O., Fluorescent analogs of cyclic and linear dinucleotides as phosphodiesterase and oligoribonuclease activity probes. *RSC Adv.* **2017,** *7* (9), 5421-5426.

3 Enzyme-mediated synthesis of emissive cyclic dinucleotides analogs

3.1 Introduction

CDN analogues have greatly facilitated mechanistic, biochemical and structural studies, particularly in the context of CDN-binding riboswitches and protein receptors.[1-5] The biggest hindrance to such studies has frequently been the preparation of analogues, as they have been predominately stepwise synthesized using phosphoramidite chemistry.[1, 6-7]

Various dinucleotide cyclases are able to convert two NTPs into a CDN product. Among these enzymes, DncV was one of the most versatile cyclases. DncV mainly produces 3',3'-c-GAMP *in vivo*, however, when isolated and incubated with GTP or ATP *in vitro*, DncV was also able to produce c-di-GMP and c-di-AMP in the presence of Mg^{2+}.[8] Recent studies have demonstrated that with the presence of alternative divalent metal ions, such as Mn^{2+} and Co^{2+}, DncV was able to produce cyclic dinucleotides with modified sugar or phosphate moieties, as well as some conservatively modified nucleobases and purine nucleobases.[1] We thus employed DncV to produce emissive c-di-GMP and 3',3'-c-GAMP analogs with our thNTPs and ^{tz}NTPs. Beside DncV, several other dinucleotide cyclases have also demonstrated catalytic activity *in vitro*. In order to demonstrate the isomorphicity of our emissive NTP analogs, we have also tested c-di-AMP cyclase DisA with our $^{th-}$ and $^{tz-}$ families of NTP analogs.

3.2 Results

3.2.1 DncV-mediated synthesis of c-di-GMP analogs

To explore the enzymatic synthesis of c-di-GMP and its analogues, the bacterial enzyme DncV was incubated with GTP, thGTP and ^{tz}GTP (**Figure 3.1**), and the reactions were analyzed by HPLC and mass spectrometry (**Figure 3.2–3.3**, **Spectrum 3.1–3.4**). After 40 minutes incubation with 500 µM GTP, ^{tz}GTP or thGTP at 37 °C, c-di-GMP, c-di-^{tz}GMP and c-di-thGMP were obtained in 94%, 85% and 11% yield, respectively. DncV also produced the mixed c-G^{tz}GMP when incubated with 500 µM each of GTP and ^{tz}GTP (**Figure 3.3a**). When incubated with a mixture of 500 µM of GTP and thGTP, DncV also produces all three plausible products c-di-GMP, c-GthGMP and c-di-thGMP (**Figure 3.3b**).

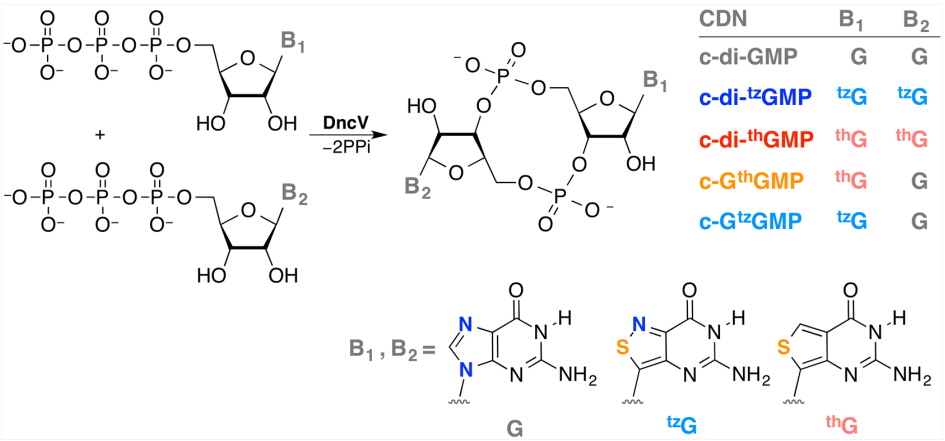

Figure 3.1 Enzymatic preparation of c-di-GMP analogues using DncV. Shown are the structure of guanosine and its thiopheno and isothiazolo surrogates.

Previous studies have illustrated that the catalytic mechanism of DncV involves a unique release-and-rebound process of the uncyclized dinucleotide intermediate. [9-10] To better analyze the ability of DncV to convert GTP and its analogues into the

corresponding CDNs, the reaction time course was analyzed, paying particular attention to the accumulation of intermediates. DncV was incubated with GTP, ^{tz}GTP and thGTP and the reactions were quenched with calf intestinal alkaline phosphatase (CIAP) at designated time points. The relative concentrations of the starting material (S), uncyclized intermediate (I) and product (P) were monitored by HPLC. The DncV-mediated synthesis of CDNs was kinetically analyzed according to the model shown in **Scheme 3.1**.

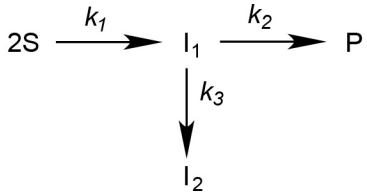

Scheme 3.1 Kinetic scheme of DncV-mediated CDN synthesis. S represents the starting NTP, I_1 and I_2 respectively represent intermediates pppNpN and degraded intermediate pNpN (I= I_1 + I_2), and P represents the product CDN.

The following differential equations were used to simulate the process:

$$d[S]/dt = -2k_1[S]^2$$

Equation 3.1 Differential equation for substrate (S) consumption.

$$d[I_1]/dt = k_1[S]^2 - k_2[I_1] - k_3[I_1]$$

Equation 3.2 Differential equation for first intermediate (I_1) accumulation.

$$d[P]/dt = k_2[I_1]$$

Equation 3.3 Differential equation for product (P) formation.

$$d[I_2]/dt = k_3[I_1]$$

Equation 3.4 Differential equation for second intermediate (I_2) formation.

All the differential equations were solved with ODE solver in MATLAB.

A small amount of uncyclized intermediate was observed during c-di-GMP synthesis (**Figure 3.2a–c**), and the calculated k_1, k_2 and k_3 values obtained were $(7.1\pm2.3)\times10^{-6}$ $\mu M^{-1}s^{-1}$, $(7.4\pm2.1)\times10^{-2}$ and $(6.4\pm0.3)\times10^{-4}$ s^{-1}, respectively (**Table 3.1**). When incubated with ^{tz}GTP, a larger amount of the intermediate was accumulated in the first 10 minutes resulting in an S-shaped product formation curve, which is common for consecutive reactions (**Figure 3.2d–f**)[11]. The calculated k_1, k_2 and k_3 were $(1.26 \pm 0.07) \times 10^{-6}$ $\mu M^{-1}s^{-1}$, $(3.4 \pm 0.2) \times 10^{-3}$ and $(1.3 \pm 0.1) \times 10^{-4}$ s^{-1}, respectively. DncV also converts thGTP to the corresponding c-di-thGMP albeit much slower when compared to its reactions with GTP and ^{tz}GTP, with k_1, k_2 and k_3 of $(3.08 \pm 0.03) \times10^{-7}$ $\mu M^{-1}s^{-1}$, $(2.32 \pm 0.05) \times 10^{-4}$ and $(2.91 \pm 0.01) \times 10^{-5}$ s^{-1}, respectively (**Figure 3.2g–i**).

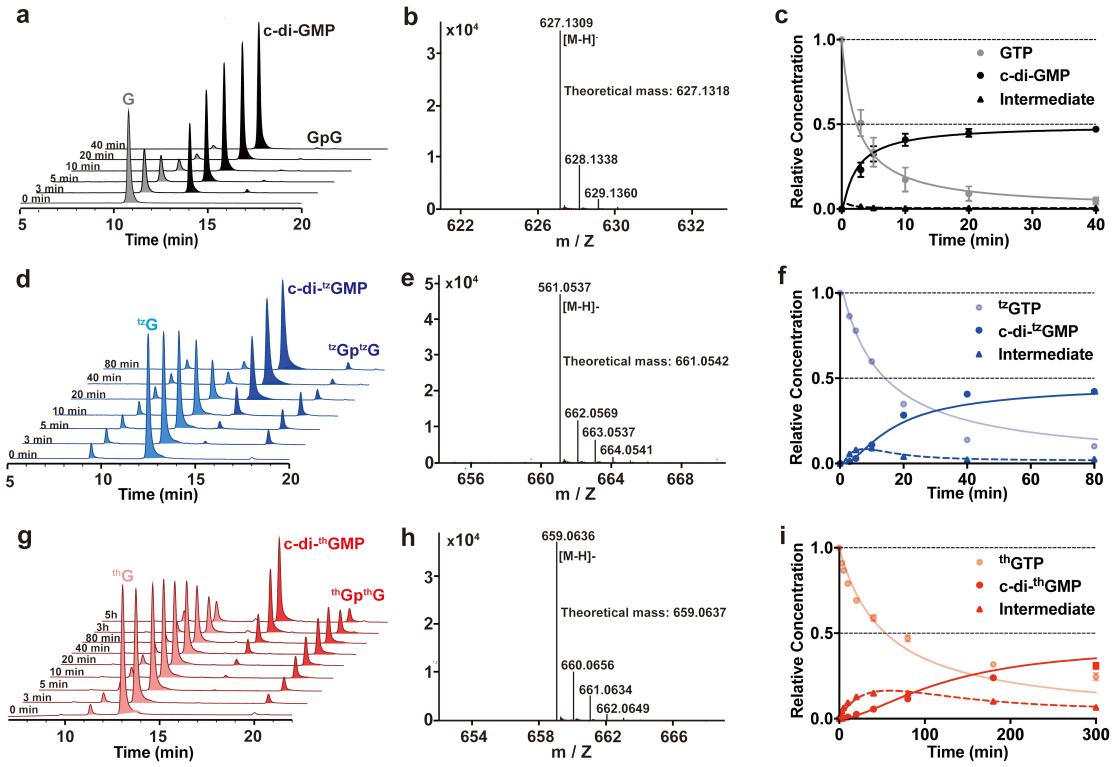

Figure 3.2 DncV-mediated enzymatic synthesis of c-di-GMP and its analogues c-di-^{tz}GMP and c-di-thGMP. (a)–(c) UV-monitored HPLC chromatograms of the DncV-mediated synthesis with GTP, ^{tz}GTP and thGTP, respectively; Aliquots were treated with calf intestinal alkaline phosphatase (CIAP) at designated times, therefore the starting materials were presented as G, ^{tz}G and thG, and intermediates were presented as GpG, ^{tz}Gp^{tz}G and thGpthG. (d)–(f) HR-MS of the intermediates from CIAP-treated reaction. (g)–(i) Kinetic analysis of the HPLC-integrated relative concentration and fitted curve of the starting material (measured as nucleosides), products and intermediates for the DncV-mediated reactions of GTP, ^{tz}GTP and thGTP, respectively. Assays were done in duplicates. Error bars indicate standard deviation (SD).

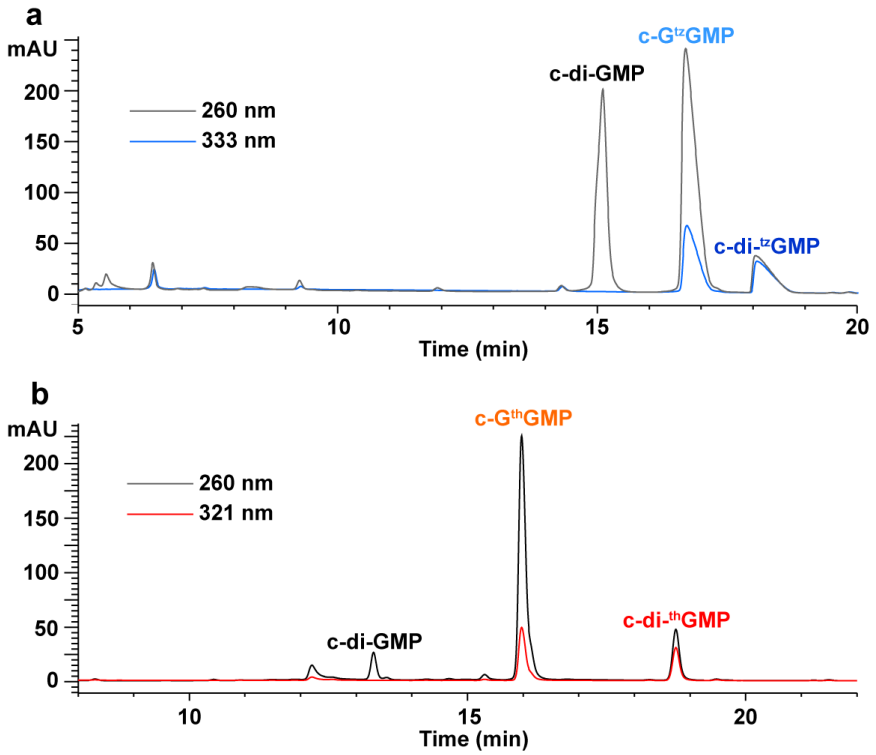

Figure 3.3 Enzymatic synthesis of c-G^{tz}GMP and c-GthGMP with DncV. HPLC analysis of reactions where DncV was incubate with 500 µM of (a) GTP and ^{tz}GTP, (b) GTP and thGTP, respectively. The HPLC separation method was described in the experimental section.

Table 3.1 Reaction rate constants of DncV-mediated CDN synthesis

	k_1($\mu M^{-1}s^{-1}$)	k_2(s^{-1})	k_3(s^{-1})
c-di-GMP	$(7.1 \pm 2.3) \times 10^{-6}$	$(7.4 \pm 2.1) \times 10^{-2}$	$(6.4 \pm 0.3) \times 10^{-4}$
c-di-^{tz}GMP	$(1.26 \pm 0.07) \times 10^{-6}$	$(3.4 \pm 0.2) \times 10^{-3}$	$(1.3 \pm 0.1) \times 10^{-4}$
c-di-thGMP	$(3.08 \pm 0.03) \times 10^{-7}$	$(2.32 \pm 0.05) \times 10^{-4}$	$(2.91 \pm 0.01) \times 10^{-5}$

After 5h of incubation, 62% of thGTP was converted to c-di-thGMP. Obvious accumulation of the reaction intermediate is seen for the first 80 minutes (**Figure 3.2g, i**). The relatively fast degradation of the intermediate compared to product formation (k_2/k_3 was 8.0 for c-di-thGMP synthesis, compared to 26 for c-di-^{tz}GMP and 116 for c-

di-GMP) resulted in relatively high concentration (13% after 300 min) of persistent uncyclized intermediate (**Figure 3.2i**).

3.3 DncV-mediated synthesis of 3',3'-c-GAMP analogs

When incubated with 1mM of ATP and GTP, DncV predominantly produces c-3',3'-c-GAMP after 2h of incubation at 37 ℃ (**Figure 3.4**, 81%). The reaction was quenched by removing all the termini phosphate groups with alkaline phosphatase (CIAP).

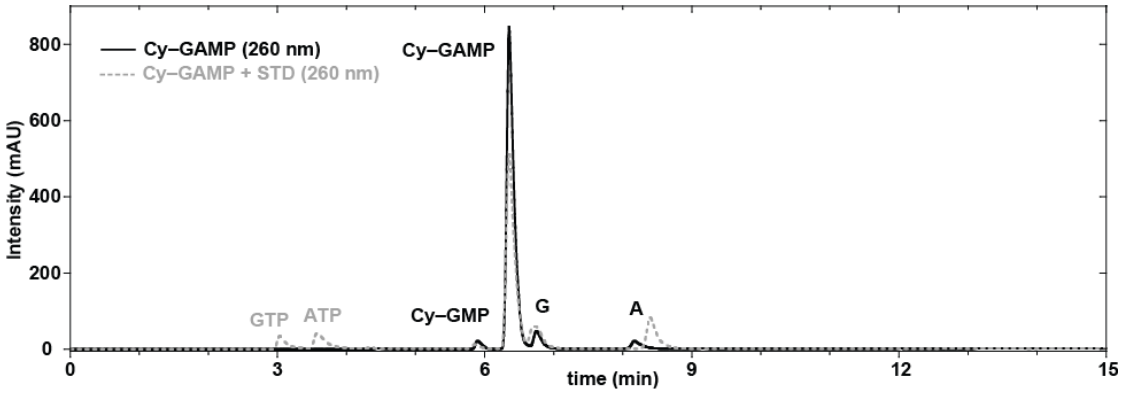

Figure 3.4 HPLC trace at 260 nm of reaction mixture containing 1mM of ATP, GTP, 2μM of DncV(solid black) and reaction coinjected with GTP, ATP, G and A.

In order to produce fluorescent 3',3'-c-GAMP analogs, ATP, GTP and their fluorescent analogs were incubated with DncV at 37 ℃ for 2h (**Table 3.2**). The reaction mixtures were analyzed by HPLC (**Figure 3.5**), and the identities of products were confirmed with high resolution mass spectroscopy (**Spectrum 3.5–3.8**). Though there were some challenges in the separation of the reaction mixtures, the major products of the heterodimeric cyclic dinucleotides were successfully isolated (**Figure 3.5**).

Table 3.2 DncV-mediated synthesis of emissive 3',3'-c-GAMP analogs

Entry	Starting material 0.5 mM	Major product	Other products observed
1	ATP, thGTP	c-thGAMP	c-di-AMP, c-di-thGMP
2	ATP, ^{tz}GTP	c-^{tz}GAMP	c-di-AMP
3	GTP, thATP	c-GthAMP	c-di-GMP, c-di-thAMP
4	GTP, ^{tz}ATP	c-G^{tz}AMP	c-di-GMP, c-di-^{tz}AMP

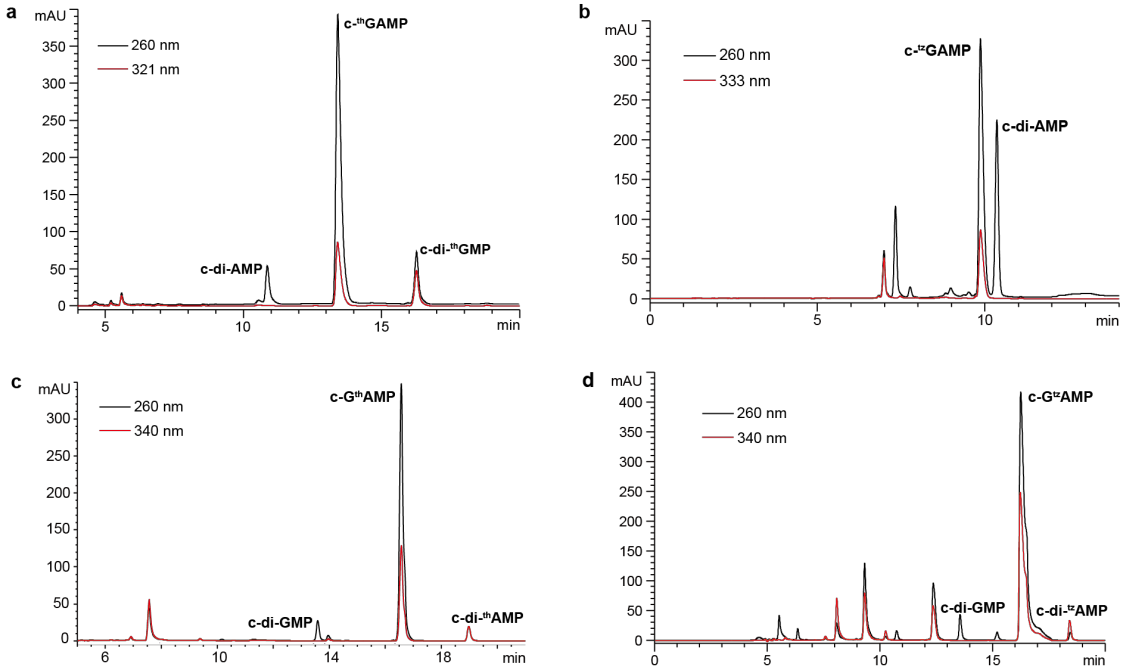

Figure 3.5 Enzymatic synthesis of c-GAMP analogs with DncV. HPLC analysis of (a) entry 1 in Table 3.2, (b) entry 2 in Table 3.2, (c) entry 3 in Table 3.2, (d) entry 4 in Table 3.2, respectively. The HPLC separation method was described in the methods section.

3.4 DisA-mediated synthesis of c-di-AMP analogs

DisA was the first identified DAC, and its catalytic activities have been demonstrated in previous studies. Therefore, DisA was employed to produce emissive c-di-AMP analogs.

As indicated in **Table 3.2**, ATP and/or thATP was incubated with 5.5 μM of DisA at 37 °C for 2h. In order to better quantify the starting material and any possible intermediates, alkaline phosphatase (CIAP) was added to each reaction to remove all termini phosphate groups. The reaction mixtures were then analyzed with HPLC. The reaction with only ATP (entry 1 in **Table 3.2**) went to almost full conversion, as demonstrated in **Figure 3.6**. DisA efficiently converted thATP into the corresponding cyclic dinucleotide (entry 2 in **Table 3.2,** 86%) with a comparable conversion yield to the native c-di-AMP (near 100%) formation (**Figure 3.7**, **Table 3.3**). Interestingly, in the presence of both the native and the thATP analog (**entry 3 in Table 3.2**), DisA yields comparable amount of c-di-AMP (37%) and c-AthAMP (31%) and additionally a slightly lower amount of c-di-thAMP (20%) indicating not a remarkable selectivity of the enzyme towards the native triphosphate (**Figure 3.8**). The identities of the products were confirmed by high-resolution mass spectroscopy (**Spectrum 3.9–3.11**).

Table 3.3 DisA mediated c-di-A(thA)MPs synthesis

Entry	DisA (5.5 µM)		Conversion					
	ATP/ thATP (mM)	Mg^{2+} (mM)	λ (nm)	c-AMP (%)	c-AthAMP (%)	c-thAMP (%)	A (%)	thA (%)
1	1 / 0	10	260	quant	-	-	0.0	-
2	0 / 1	10	260	-	-	86.1	-	13.9
			340	-	-	81.4	-	18.6
3	0.5 / 0.5	10	260	37.3	33.3	15.5	6.4	7.5
			340	0.0	54.5	34.9	0.0	10.6
			340*	37.3	30.7	19.6	6.4	5.9

Entries **1** and **2** were analyzed by HPCL method C, entry **3** was analyzed by HPCL method D. Conversion yields were calculated upon normalization of the HPLC peaks area by the extinction coefficients of the different compounds (supplementary information). *Normalized integrated peaks area considering the total area for the trace at 340 nm equal to 100% – (%Area of species absorbing at 260 nm but not at 340 nm).

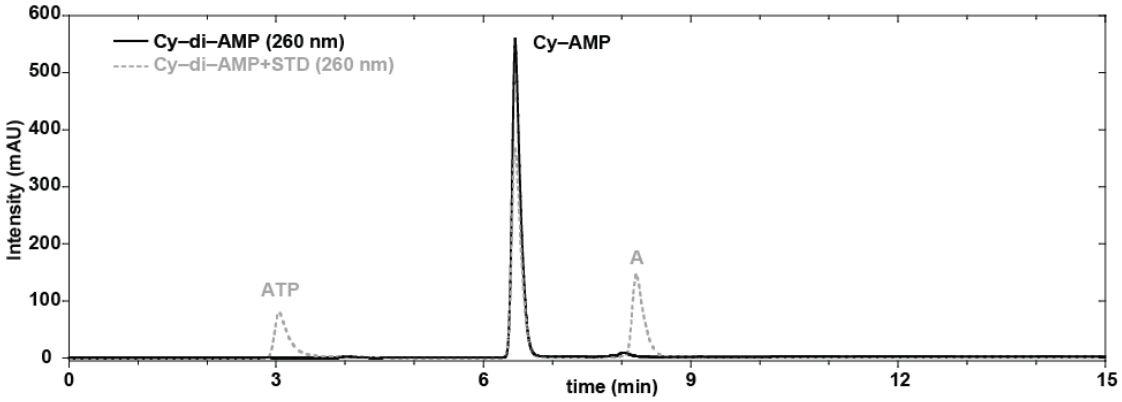

Figure 3.6 HPLC runs monitored at 260 nm of entry **1** (solid black) and entry **1** co-injected with ATP and A.

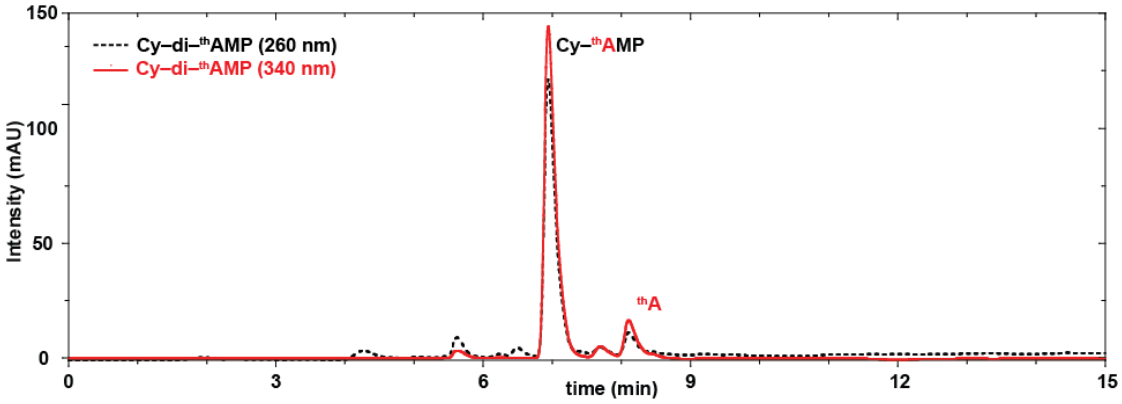

Figure 3.7 HPLC trace at 260 (dashed black) and 340 (solid red) nm of entry **2**.

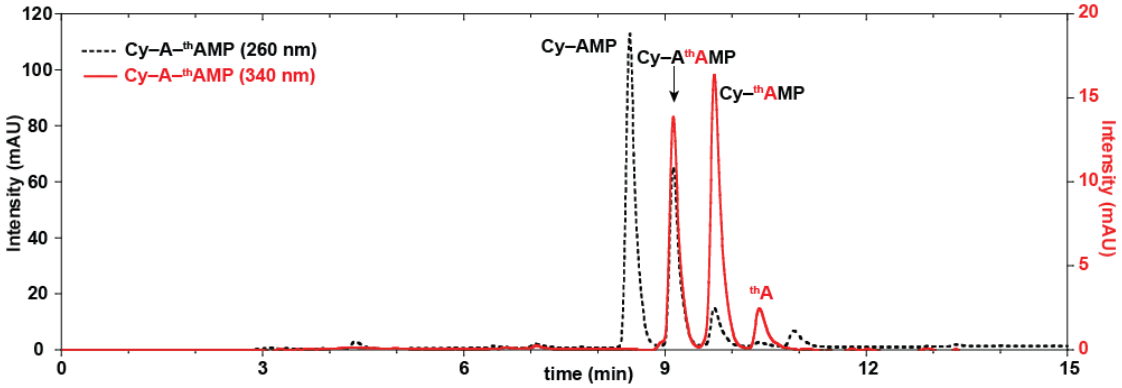

Figure 3.8 HPLC trace monitored at 260 (dashed black) and 340 (solid red) nm of entry **3**.

3.5 Discussion

We employed DncV and DisA to enzymatically produce a series of c-di-GMP, c-di-AMP and 3',3'-c-GAMP analogs. DncV primarily synthesizes 3',5-'c-GAMP *in vivo*, however, when provided with only GTP or ATP *in vitro*, it is also capable of making c-di-GMP and c-di-AMP [8-9]. Since DncV can accept both purine triphosphates, we postulated it could tolerate the thiopheno and isothiazolo G and A surrogates, members of our previously synthesized RNA alphabets (Fig. 1) [12-13]. The results have indeed confirmed this tolerance level, as DncV was able to recognize thGTP, ^{tz}GTP, thATP and ^{tz}ATP, and produce corresponding c-di-GMP and 3',3'-c-GAMP analogs. DisA was also able to produce c-di-thAMP and c-AthAMP with yields comparable to c-di-AMP synthesis.

The catalytic mechanism of DncV has been largely revealed by structural studies. During the enzymatic conversion of NTPs to CDNs, after the first 3',5'-phosphordiester bond was formed between the two NTP substrates, the uncyclized intermediate is

thought to be released and oppositely rebound to the enzyme, after which the second 3',5'-phosphodiester bond is then made [9-10, 14].

In order to gain some mechanistic insights of DncV catalysis, the kinetics of DncV-mediated synthesis of c-di-GMP analogs were analyzed in detail. The guanosine surrogates used have illustrated the key functional elements in the purine scaffold that affect the formation and consumption of the reaction intermediate. The kinetic constants listed in **Table 3.1** illustrate that forming the first phosphodiester linkage is the rate-limiting step for the synthesis of c-di-GMP, c-di-^{tz}GMP and c-di-thGMP as in all cases k_1 is much smaller than k_2. Furthermore, a certain amount of the uncyclized intermediate in all three reactions does not get entirely consumed (Fig. 2c, 2f, 2i). We speculate that the hydrolysis of the open intermediate pppNpN (I_1 in Scheme 1) to the uncyclizable pNpN (I_2 in Scheme 1) could take place (note that I_1 and I_2 were not experimentally differentiated in the kinetic analysis and are shown as $I = I_1 + I_2$ in Fig. 2c, 2f, 2i). Additionally, the consumption of thGTP in c-di-thGMP synthesis was observed to be slower than simulated, which could be explained by a non-productive DncV-mediated degradation of thGTP to thG monophosphate (pthG) without successfully forming the inter-nucleotide phosphodiester bond. The results above thus show that the absence of the nucleobase's N-7 significantly alters the reaction kinetics, though previous structural studies with DncV have not revealed direct contact between N-7 of GTP and any protein residues [9-10, 14].

3.6 Conclusions

We have exploited bacterial enzymes, DncV and DisA, which tolerates synthetic triphosphate analogues, for an unprecedented, one-step, efficient enzymatic synthesis

of novel site-specifically mutated CDNs. The enzymatic synthesis of CDNs demonstrated the isomorphicity of the emissive nucleotide analogs, and these CDN analogues produced provide insight into DncV catalytic mechanism.

3.7 Acknowledgements

Chapter 3, 4 and 5, in full, are currently being prepared for submission for publication for the material. Li, Y.; Fin, A; Ludford, P. T.; Rovira, A. R.; Tor, Y., Monitoring the formation and degradation of c-di-GMP analogs using fluorescence. The thesis author was the primary author of this material.

We thank Dr. Ming Chen Hammond for kindly providing us the DisA enzyme.

3.8 Supplementary information

3.8.1 Methods

For large scale synthesis of c-di-GMP analogs, 500 μM of guanosine 5'-triphosphates analogs were incubated with at 37 °C 2.3 μM of DncV in a buffer containing 0.1 M NaCl, 40 mM Tris pH 7.5 and 10 mM $MgCl_2$ for 2–5 hours. The reaction mixture was then heated at 90 °C for 5 minutes and chilled on ice for 15 minutes and filtered through a 0.22 μm filter. The supernatant was separated with HPLC method A. Collected HPLC fractions were lyophilized with Labconco FreeZone 2.5 lyophilizer and re-dissolved in autoclaved water. UV spectroscopy was used to determine the concentration of each solution with the following extinction coefficients: 26000 L mol^{-1} cm^{-1} for c-di-GMP (260 nm), 8370 L mol^{-1} cm^{-1} for c-di-^{tz}GMP (333 nm), 7470 L mol^{-1} cm^{-1} for c-di-thGMP (321 nm), 3735 L mol^{-1} cm^{-1} for c-GthGMP (333 nm), and 4185 L mol^{-1} cm^{-1} for c-G^{tz}GMP (333 nm).

For kinetics studies of c-di-GMP analog synthesis, 500 μM of guanosine 5'-triphosphates analogs were incubated at 37 °C with 2.3 μM of DncV in a buffer containing 0.1 M NaCl, 40 mM Tris pH 7.5 and 10 mM $MgCl_2$. 8 μL aliquots of reaction were taken out at designated time points, and added to quenching solution containing 30 μL of water and 1μL of alkaline phosphatase CIAP (Promega) and incubated at 37 °C for another 5 minutes. 30 μL of the mixture was subjected to HPLC analysis after filtration. The reaction mixture was separated by HPLC method B.

The same recipe of large-scale synthesis of c-di-GMP was used for the synthesis of c-di-GAMP and c-di-AMP analogs. For the synthesis of c-di-AMP analogs, after incubating at 37 °C for 2h, alkaline phosphatase (CIAP) was added to the reaction mixture, and the solution was incubated for another hour in order to remove the termini phosphate groups. c-GAMP analogs were purified with HPLC method A or C, c-di-AMP analogs were purified with HPLC method C or D.

HPLC method A: Synergi 4μ Fusion-RP 80A column (250 × 10 mm, 4 μm particle size) or Sepax Bio C-18 column (250 × 10mm, 5 μm particle size) with a gradient of 0.5–20% of 10 mM NH_4OAc, pH 7 in MeOH in 20 minutes on an Agilent 1200 series HPLC system (Agilent Technologies).

HPLC method B: Sepax Bio C-18 column (250 × 10mm, 5 μm particle size) with a gradient of 0.5% – 25% of 10 mM TEAA, pH7 in MeOH in 20min at 25 °C on an Agilent 1200 series HPLC system (Agilent Technologies).

HPLC method C: gradient 0-95% of MeOH in NH_4OAc (0.1 M, pH 7.00) over 20 minutes followed by isocratic elution for 3 minutes, 25 cm RP–18 analytical column,

50 °C, 1 ml/min flux. Monitored wavelength: 260, 321 and 340 nm. The collected fractions were frozen, lyophilized and re-dissolved in 10 µl of water for ESI analysis.

HPLC method D: gradient 0-30% of MeOH in NH_4OAc (0.1 M, pH 7.00) over 20 minutes followed by a gradient 30–95% over 5 minutes then isocratic elution for 3 minutes, 25 cm RP–18 analytical column, 50 °C, 1 ml/min flux. Monitored wavelength: 260, 321 and 340 nm. The collected fractions were frozen, lyophilized and re-dissolved in 10 µl of water for ESI analysis.

3.8.2 Supplementary spectra

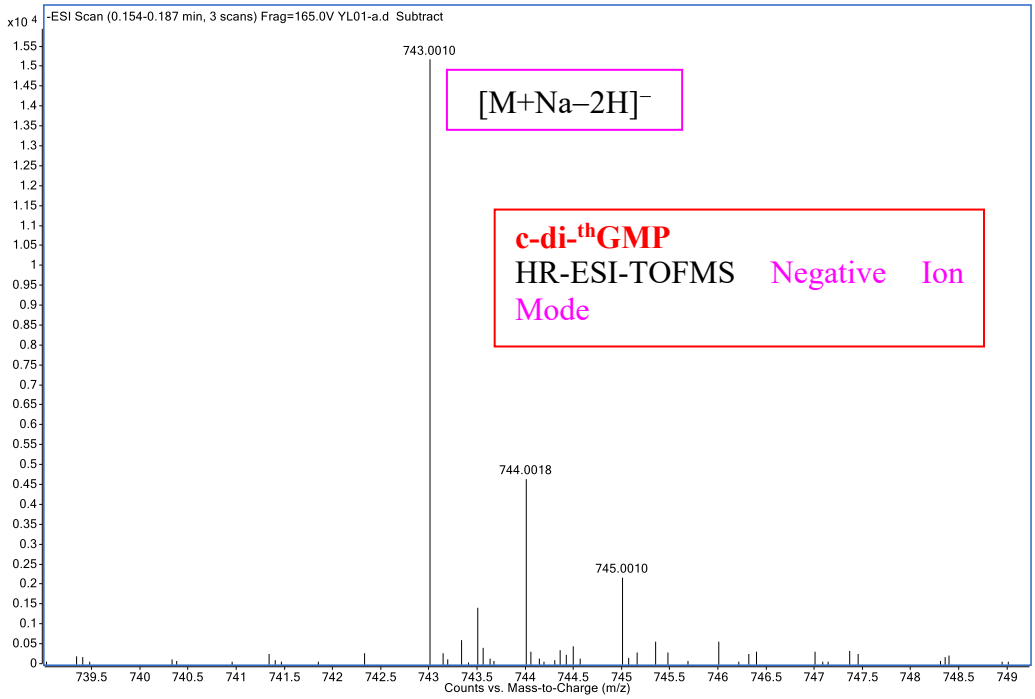

Spectrum 3.1 HR-ESI-TOFMS of c-di-thGMP. $[C_{22}\,H_{22}\,N_6\,O_{14}\,P_2\,S_2\,Na]^-$, calculated 743.0014, found 743.001, delta (ppm) –0.5.

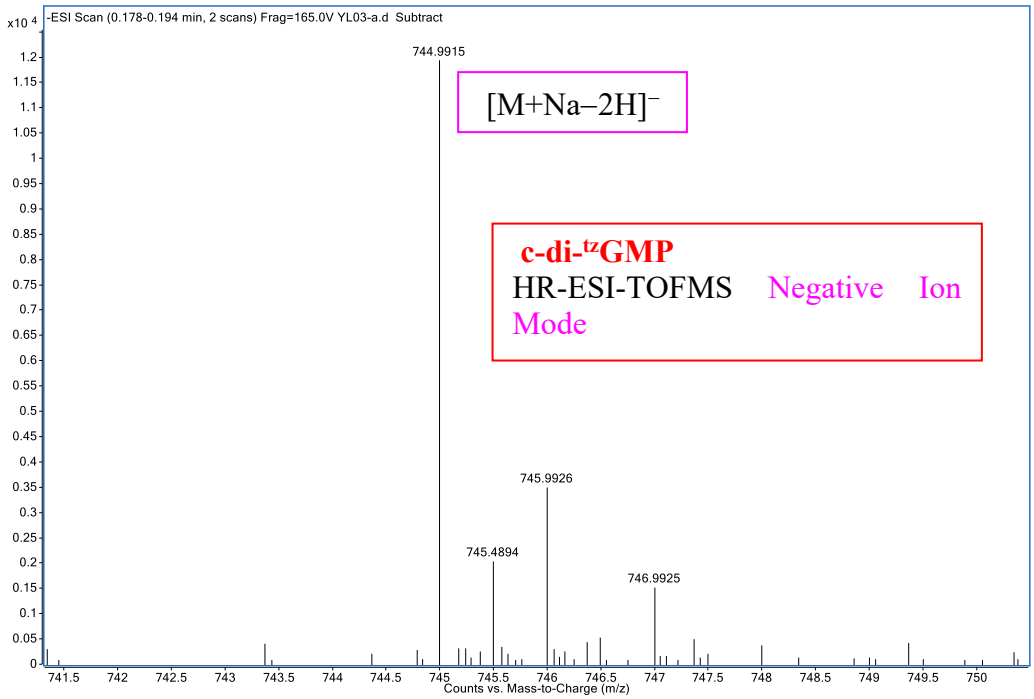

Spectrum 3.2 HR-ESI-TOFMS of c-di-^{tz}GMP. $[C_{20}\,H_{20}\,N_8\,O_{14}\,P_2\,S_2\,Na]^-$, calculated 744.9919, found 744.9915, delta (ppm) –0.5.

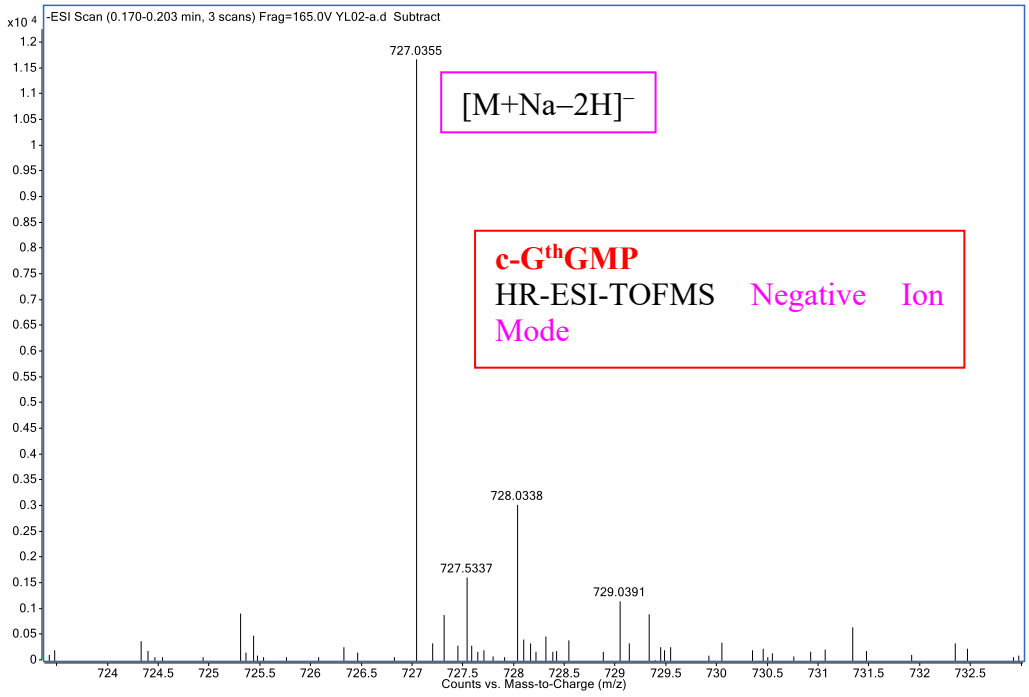

Spectrum 3.3 HR-ESI-TOFMS of c-GthGMP. $[C_{21}\,H_{22}\,N_8\,O_{14}\,P_2\,S\,Na]^-$, calculated 727.0355, found 727.0355, delta (ppm) 0.0.

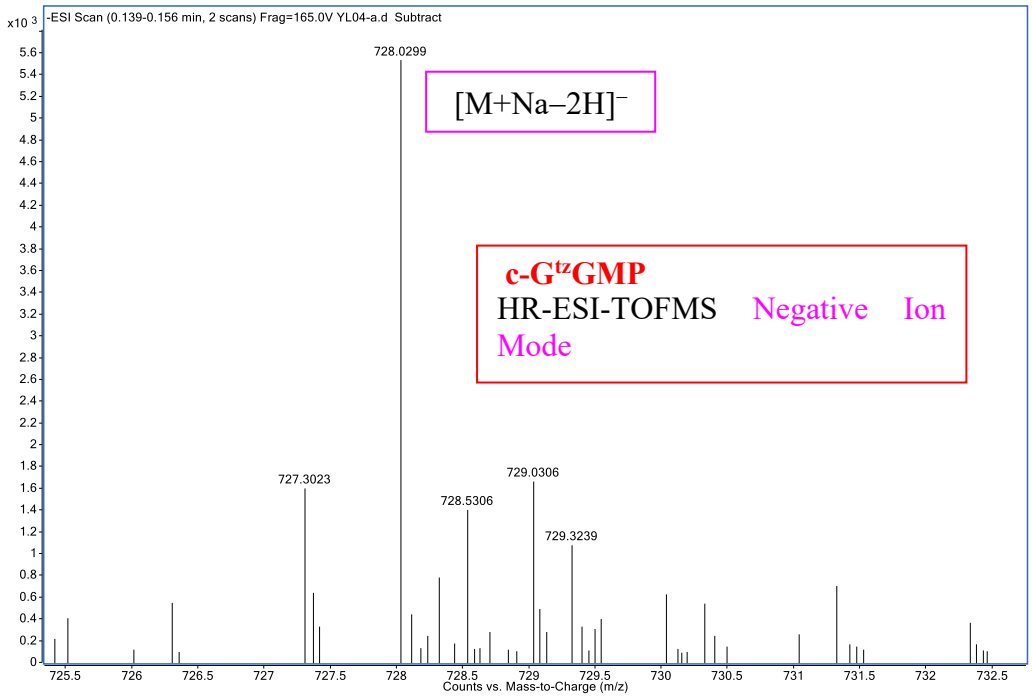

Spectrum 3.4 HR-ESI-TOFMS of c-G^{tz}GMP. [C_{20} H_{21} N_9 O_{14} P_2 S Na]$^-$, calculated 728.0307, found 728.0299, delta (ppm) –1.1.

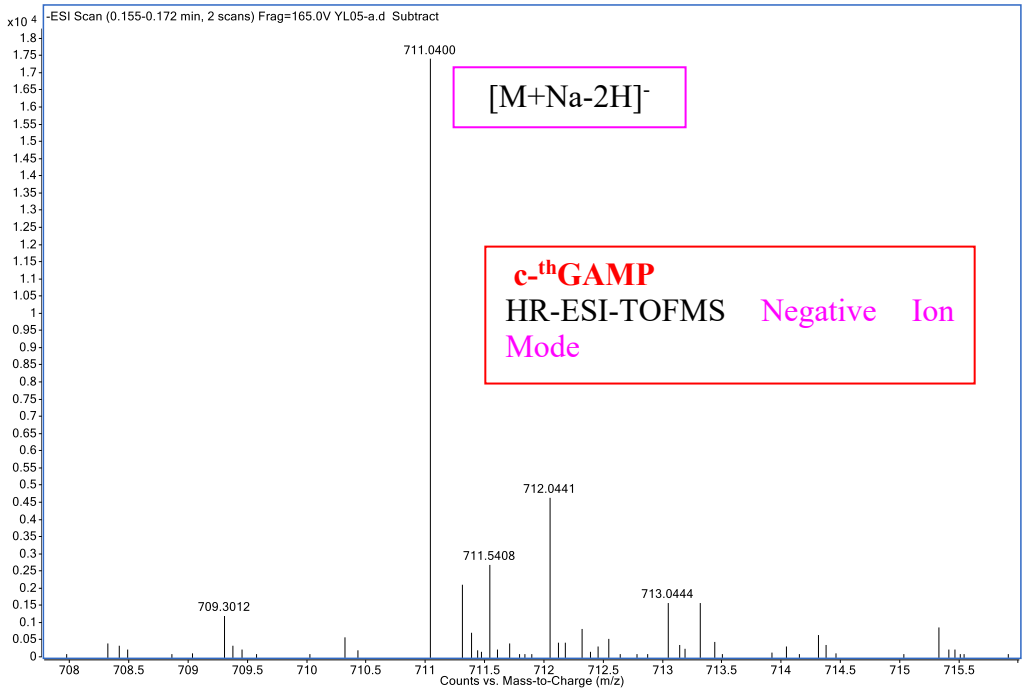

Spectrum 3.5 HR-ESI-TOFMS of 3'3'-c-thGAMP. [C_{21} H_{22} N_8 O_{13} P_2 S Na]$^-$, calculated 711.0405, found 711.0400, delta (ppm) –0.7.

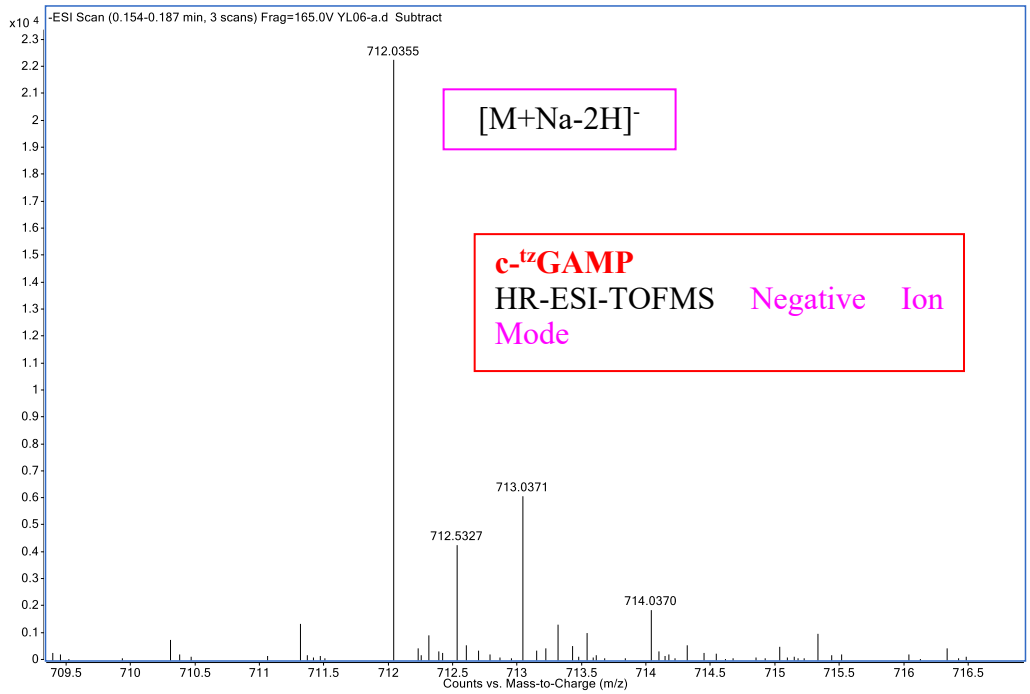

Spectrum 3.6 HR-ESI-TOFMS of 3'3'-c-^{tz}GAMP. $[C_{20}H_{21}N_9O_{13}P_2SNa]^-$, calculated 712.0358, found 712.0355, delta (ppm) –0.4.

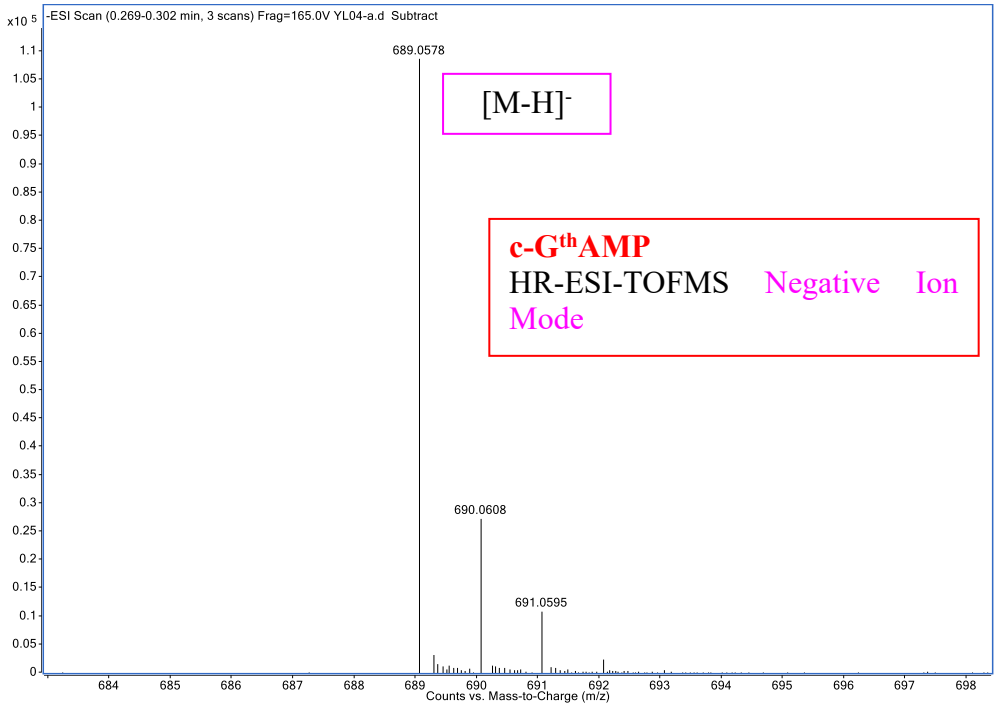

Spectrum 3.7 HR-ESI-TOFMS of 3'3'-c-GthAMP. $[C_{21}H_{23}N_8O_{13}P_2S]^-$, calculated 689.0586, found 689.0578, delta (ppm) –1.2.

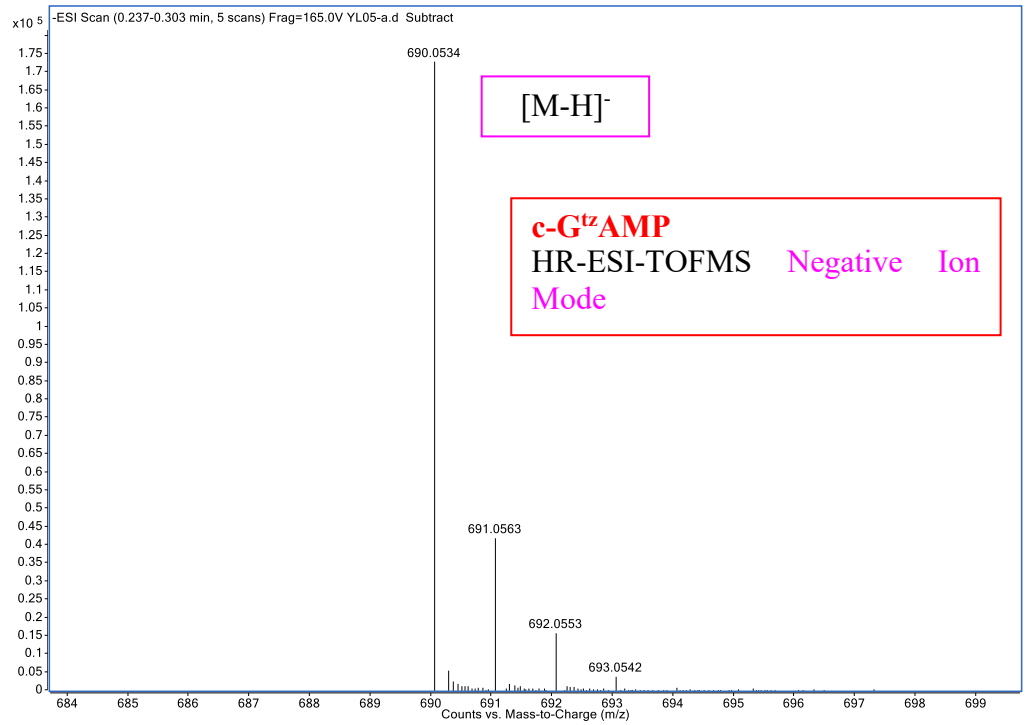

Spectrum 3.8 HR-ESI-TOFMS of 3'3'-c-G^{tz}AMP. $[C_{20}H_{22}N_9O_{13}P_2S]^-$, calculated 690.0538, found 690.0534, delta (ppm) –0.6.

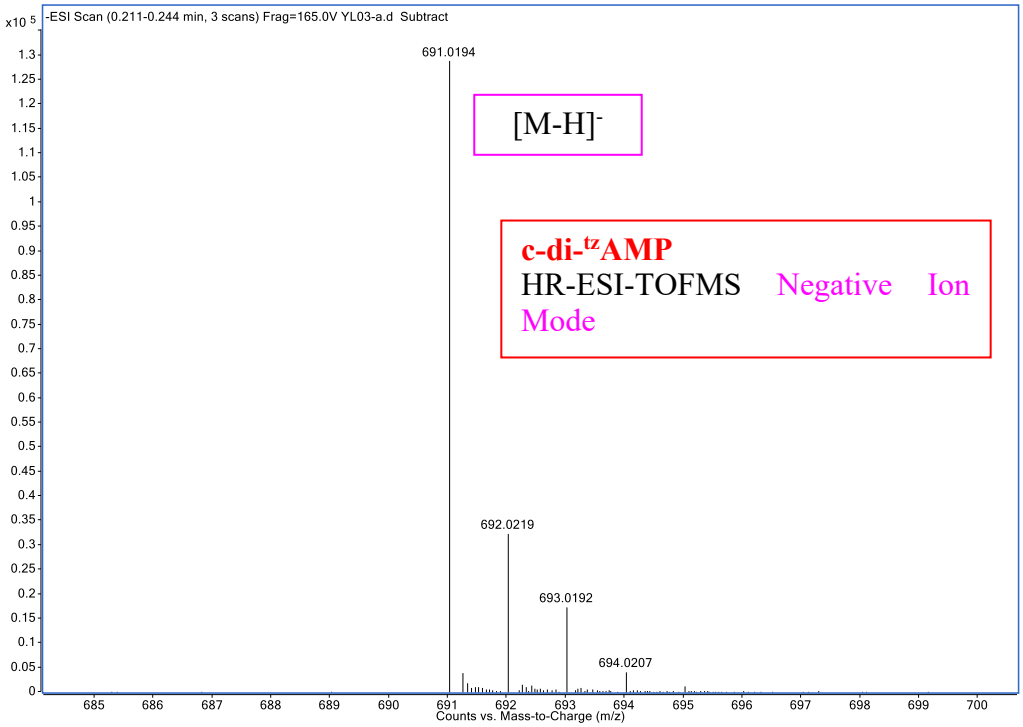

Spectrum 3.9 HR-ESI-TOFMS of c-di-^{tz}AMP. $[C_{20}H_{21}N_8O_{12}P_2S_2]^-$, calculated 691.0201, found 691.0194, delta (ppm) –1.0.

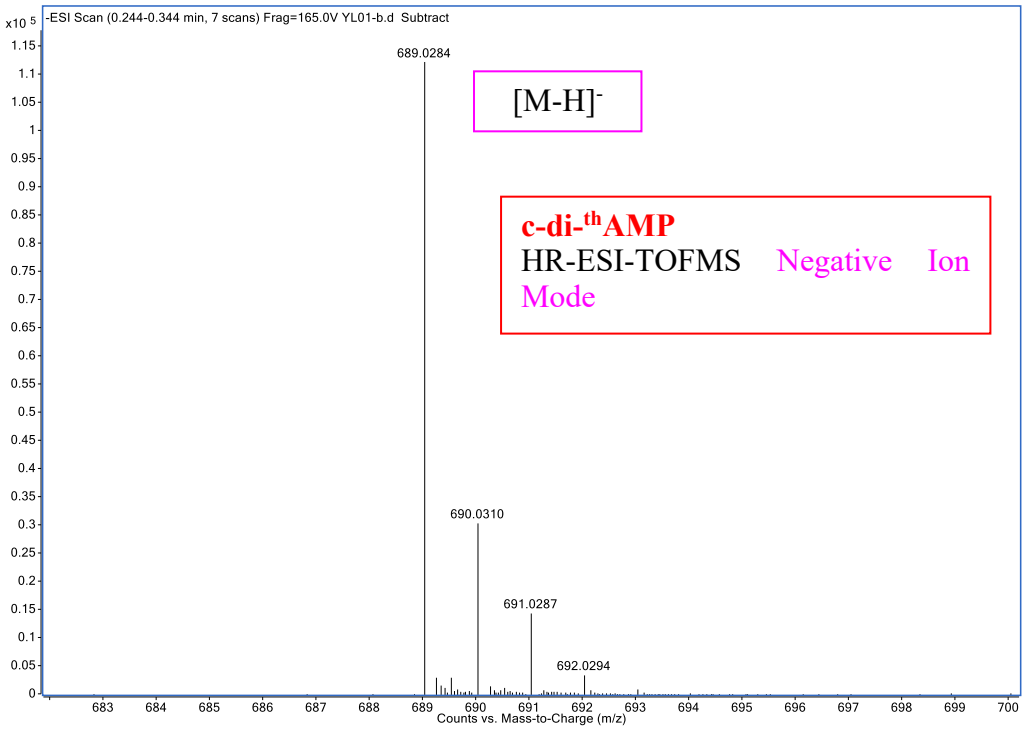

Spectrum 3.10 HR-ESI-TOFMS of c-di-thAMP. $[C_{22}\ H_{23}\ N_6\ O_{12}\ P_2\ S_2]^-$, calculated 689.0296, found 689.0284, delta (ppm) –1.7.

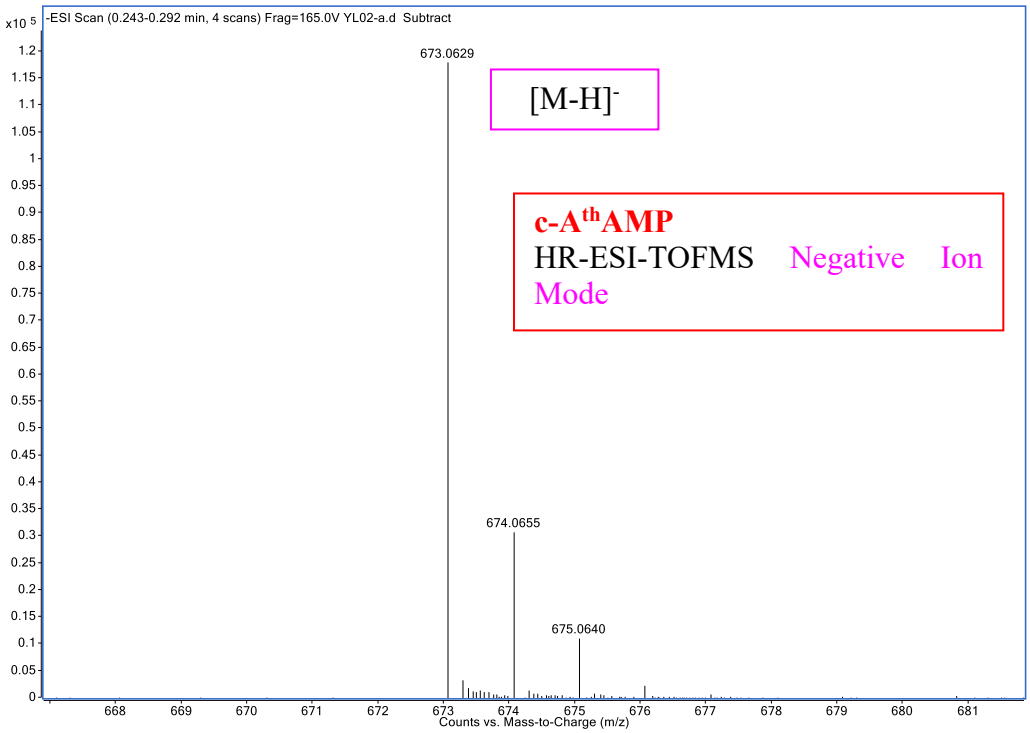

Spectrum 3.11 HR-ESI-TOFMS of c-AthAMP. $[C_{21}\ H_{23}\ N_8\ O_{12}\ P_2\ S\ ]^-$, calculated 673.0637, found 673.0629, delta (ppm) –1.2.

3.9 References

1. Launer-Felty, K. D.; Strobel, S. A., Enzymatic synthesis of cyclic dinucleotide analogs by a promiscuous cyclic-AMP-GMP synthetase and analysis of cyclic dinucleotide responsive riboswitches. *Nucleic Acids Res* **2018,** *46* (6), 2765-2776.

2. Luo, Y.; Zhou, J.; Watt, S. K.; Lee, V. T.; Dayie, T. K.; Sintim, H. O., Differential binding of 2'-biotinylated analogs of c-di-GMP with c-di-GMP riboswitches and binding proteins. *Mol Biosyst* **2012,** *8* (3), 772-8.

3. Shanahan, C. A.; Gaffney, B. L.; Jones, R. A.; Strobel, S. A., Differential analogue binding by two classes of c-di-GMP riboswitches. *J Am Chem Soc* **2011,** *133* (39), 15578-92.

4. Shanahan, C. A.; Strobel, S. A., The bacterial second messenger c-di-GMP: probing interactions with protein and RNA binding partners using cyclic dinucleotide analogs. *Org Biomol Chem* **2012,** *10* (46), 9113-29.

5. Zhou, J.; Zheng, Y.; Roembke, B. T.; Robinson, Sarah M.; Opoku-Temeng, C.; Sayre, D. A.; Sintim, H. O., Fluorescent analogs of cyclic and linear dinucleotides as phosphodiesterase and oligoribonuclease activity probes. *RSC Adv.* **2017,** *7* (9), 5421-5426.

6. Clivio, P.; Coantic-Castex, S.; Guillaume, D., (3'-5')-Cyclic dinucleotides: synthetic strategies and biological potential. *Chem Rev* **2013,** *113* (10), 7354-401.

7. Wang, C.; Sinn, M.; Stifel, J.; Heiler, A. C.; Sommershof, A.; Hartig, J. S., Synthesis of All Possible Canonical (3′–5′-Linked) Cyclic Dinucleotides and Evaluation of Riboswitch Interactions and Immune-Stimulatory Effects. *Journal of the American Chemical Society* **2017,** *139* (45), 16154-16160.

8. Davies, B. W.; Bogard, R. W.; Young, T. S.; Mekalanos, J. J., Coordinated regulation of accessory genetic elements produces cyclic di-nucleotides for V. cholerae virulence. *Cell* **2012,** *149* (2), 358-70.

9. Kato, K.; Ishii, R.; Hirano, S.; Ishitani, R.; Nureki, O., Structural Basis for the Catalytic Mechanism of DncV, Bacterial Homolog of Cyclic GMP-AMP Synthase. *Structure* **2015,** *23* (5), 843-850.

10. Zhu, D.; Wang, L.; Shang, G.; Liu, X.; Zhu, J.; Lu, D.; Wang, L.; Kan, B.; Zhang, J. R.; Xiang, Y., Structural biochemistry of a Vibrio cholerae dinucleotide cyclase reveals cyclase activity regulation by folates. *Mol Cell* **2014,** *55* (6), 931-7.

11. Espenson, J. E., *Chemical kinetics and reaction mechanisms*. 2nd ed.; McGraw-Hill: New York, 1995; p 70-100.

12. Shin, D.; Sinkeldam, R. W.; Tor, Y., Emissive RNA alphabet. *J Am Chem Soc* **2011,** *133* (38), 14912-5.

13. Rovira, A. R.; Fin, A.; Tor, Y., Chemical Mutagenesis of an Emissive RNA Alphabet. *J Am Chem Soc* **2015,** *137* (46), 14602-5.

14. Ming, Z.; Wang, W.; Xie, Y.; Ding, P.; Chen, Y.; Jin, D.; Sun, Y.; Xia, B.; Yan, L.; Lou, Z., Crystal structure of the novel di-nucleotide cyclase from Vibrio cholerae (DncV) responsible for synthesizing a hybrid cyclic GMP-AMP. *Cell Res* **2014,** *24* (10), 1270-3.

4 Mechanistic studies facilitated by systematically-modified c-di-GMP analogs

4.1 Introduction

Since the biological role of c-di-GMP was first discovered in 1987, the landscape representing the signaling mechanisms and biological significance of CDNs has continued to expand. [1-5] Among the discovered bacterial CDNs (c-di-GMP, c-di-AMP and 3',3'-c-GAMP), c-di-GMP is the most studied, and has been recognized as a ubiquitous cytoplasmic secondary messenger in bacteria that regulates various important biological processes, including biofilm formation, motility and virulence.[2, 6-7] As its impact on pathogenic bacteria and eukaryotic cells is gradually being recognized, [4-5, 8] shedding light on the enzymatic pathways involved in its production, degradation and recognition is of significance. Synthetic analogues play unique roles in this endeavor since, unlike traditional biochemical or structural tools, systematic molecular "surgery" has the ability to unravel key recognition elements as well as producing ligands with unique cellular performance signatures. [9-13]

Beside the cyclases that synthesize c-di-GMP, PDEs that hydrolyze it to linear pGpG or GMP are key to controlling its global and local concentration in bacteria, which further modulate bacterial biofilm formation and virulence. [2, 4, 14-15] rocR is a PDE that contains an EAL domain and specifically recognizes and cleaves c-di-GMP into a dinucleotide monophosphate pGpG. [16-17] It is one of the most active and well-studied PDEs found in *P. aeruginosa*, and is essential for acute infections caused by this bacterium. [16, 18]

4.2 Results

To shed light on the substrate–enzyme interaction of the c-di-GMP phosphodiesterase (PDE) rocR, which down regulates c-di-GMP by hydrolyzing it to the linear pGpG (**Figure 4.1**), c-di-GMP, c-di-^{tz}GMP, c-di-thGMP, c-GthGMP and c-G^{tz}GMP were incubated with the enzyme, and the relative concentration of starting material (CDN) and product (pNpN) at designated time points was monitored by HPLC (**Figure 4.2**), and the identity of the products was confirmed by LC-ESI-TOFMS (**Spectrum 4.1–4.6**).

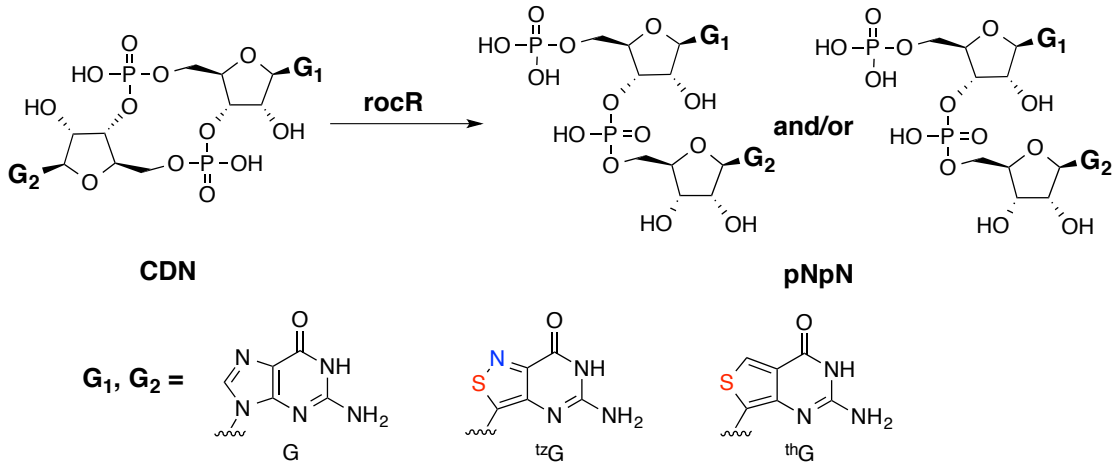

Figure 4.1 rocR-mediated hydrolysis of c-di-GMP and its analogs using. Shown are the structure of guanosine and its thiopheno and isothiazolo surrogates.

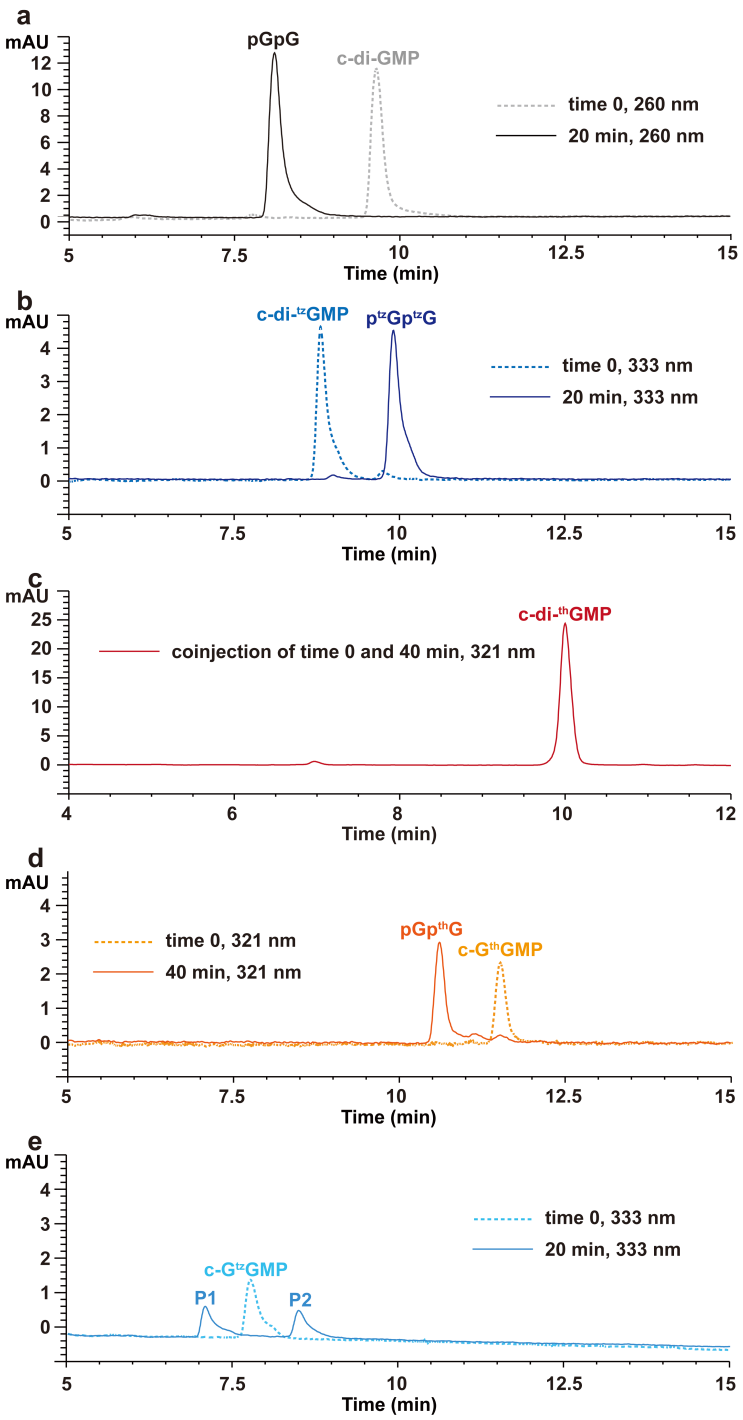

Figure 4.2 HPLC traces of CDN hydrolysis mediated by PDE rocR. RocR (100 nM) was incubated with 10 μM of (a) c-di-GMP, (b) c-di-^{tz}GMP, (c) c-di-thGMP, (d) c-GthGMP and (e) c-G^{tz}GMP, and the reactions were quenched using 100 mM $CaCl_2$ at designated time point and analyzed by HPLC following the gradient described in the method section.

It has been previously demonstrated that the rocR cleavage reaction follows a classic Michaelis-Menten kinetics, [15-16] which can be described in **Scheme 4.1a**. For the cleavage of mixed c-di-GMP analogues, where two isomeric products could be formed (pN_1pN_2 and pN_2pN_1) the cleavage reaction was described shown in **Scheme 4.1b**.

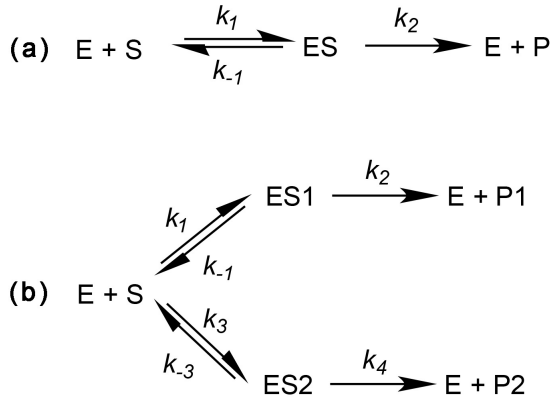

Scheme 4.1 Kinetics scheme of rocR-mediated hydrolysis of CDNs. E stands for the enzyme S stands for the starting CDN, and P stands for the product. (a) Kinetics scheme of rocR-mediated hydrolysis of c-di-GMP, c-di-^{tz}GMP and c-di-thGMP. (b) Kinetics scheme of rocR-mediated hydrolysis of c-G^{tz}GMP and c-GthGMP.

c-di-GMP was completely cleaved by rocR to pGpG in about 5 minutes with k_1 = 17 ± 13 $\mu M^{-1}s^{-1}$ and k_2 = 0.36 ± 0.03 s^{-1} (**Figure 4.3a**). Enzymatic cleavage of c-di-^{tz}GMP was slower compared to c-di-GMP, but went to completion within 20 min (**Figure 4.3b**) with k_1 = 0.034 ± 0.003 $\mu M^{-1}s^{-1}$ and k_2 = 0.32 ± 0.01 s^{-1}. On the other hand, no cleaved of c-di-thGMP was observed even after 40 min of incubation with rocR (**Figure 4.3c**). The rocR-mediated cleavage of the mixed c-GthGMP yielded a single product (**Figure 4.3d**), which could either be pGpthG or pthGpG, while two products were observed for c-G^{tz}GMP (**Figure 4.2**), illustrating that both pGp^{tz}G and p^{tz}GpG were produced (**Figure 4.3e**). Overall, a gradually reduced hydrolysis rate was observed

as the structures progressively deviated from the parent CDN in the order: c-di-GMP, c-di-^{tz}GMP, c-G^{tz}GMP, c-GthGMP and lastly c-di-thGMP (**Figure 4.3f**).

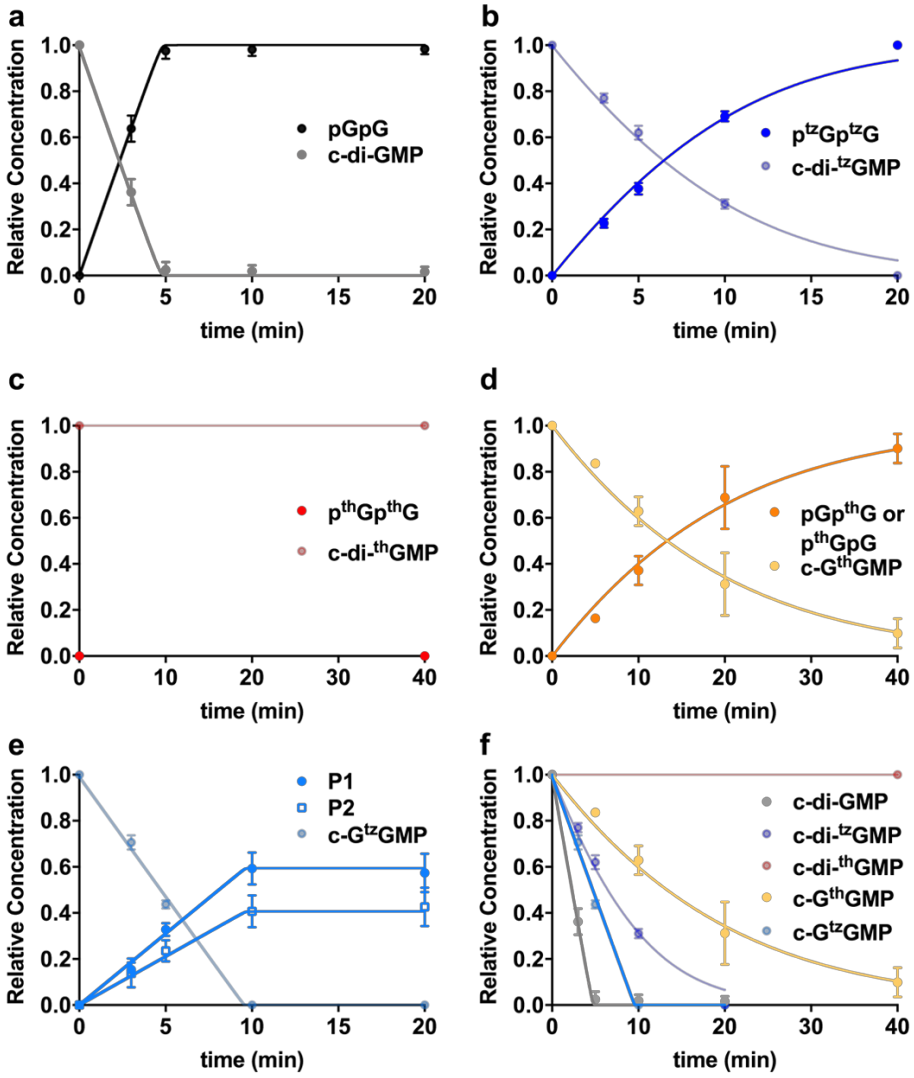

Figure 4.3 Kinetics analyses of rocR-mediated cleavage of c-di-GMP analogues. The enzyme (100 nM) was incubated with 10 µM of (a) c-di-GMP, (b) c-di-^{tz}GMP, (c) c-di-thGMP, (d) c-GthGMP and (e) c-G^{tz}GMP and the reactions were quenched using 100 mM $CaCl_2$ at designated time point and analyzed by HPLC. Assays were done in duplicates. Error bars indicate SD.

Table 4.1 Reaction rate constants for rocR-mediated CDNs cleavage

	k_1 ($\mu M^{-1}s^{-1}$)	k_{-1} (s^{-1})	k_2 (s^{-1})	k_3 ($\mu M^{-1}s^{-1}$)	k_{-3} (s^{-1})	k_4 (s^{-1})
c-di-GMP	17±13	1.2±0.3	0.36±0.03	NA	NA	NA
c-di-^{tz}GMP	0.034±0.003	0.042±0.003	0.32±0.01	NA	NA	NA
c-GthGMP	0.012±0.003	0.043±0.002	0.34±0.01	NA	NA	NA
c-G^{tz}GMP	18±1	0.12±0.03	0.25±0.05	18±1	0.14±0.01	0.12±0.03

4.3 Discussion

It has been established that rocR follows Michaelis-Menten kinetics [15-16]. **Scheme 4.1a** was therefore used to analyze the reaction kinetics, where k_1 and k_{-1} describe the enzyme/substrate association and dissociation, respectively, while k_2 reflects the cleavage reaction. When "asymmetrical" mixed c-di-GMP analogues are treated with rocR, the enzyme could, in principle, recognize and cleave either phosphodiester bonds, producing pN_1pN_2 and pN_2pN_1. Assuming the two products result from different binding orientation of the heterodimeric CDNs, **Scheme 4.1b** is thus introduced to model the cleavage reactions, where k_1, k_{-1} and k_2 reflect the association/dissociation and cleavage of the heterodimeric CDN in one orientation (ES1), respectively, and k_3, k_{-3} and k_4 reflect the other (ES2). The observed kinetics of rocR-mediated hydrolyses of CDN analogues indicates that the presence of N-7 on at least one nucleobase is necessary for efficient recognition and cleavage. The enzyme did not produce observable amounts of c-di-thGMP cleavage products after 40 min, while the majority of c-di-^{tz}GMP got cleaved within 20 min, indicating that altering both N-7 positions is detrimental to rocR-mediated hydrolytic cleavage. With a single N-7-containing nucleobase such as in the mixed c-GthGMP, only one phosphodiester bond can be recognized and cleaved by rocR. In contrast, the mixed c-G^{tz}GMP, where donor

nitrogens are present on both nucleobases, rocR was able to recognize the CDN from both orientations, which lead to cleavage of either phosphodiester bond and the release of pGp^{tz}G and p^{tz}GpG (**Figure 4.3e**).

The kinetic observations articulated above could possibly be explained by the high degree of conservation of a Q residue in chain β1 of EAL-domain containing PDEs (aa161 in rocR, aa16 in Ykul). [15, 18-19] The structure of Ykul-bound c-di-GMP shows the amide group of Q16 (similar to Q161 of rocR) to be hydrogen bonded to the N-7 of the guanosine found 5' to the cleavage site. [19] Indeed, mutation of rocR's Q161caused a 5-fold decrease in k_{cat}, and 2-fold increase in K_M, indicating that Q161 is involved in substrate recognition. [15] We thus speculate that the cleavage product of c-GthGMP is pGpthG and submit that there is little bias in rocR binding of c-G^{tz}GMP in either orientation, as $k_1 = k_3$, and $k_{-1} = k_{-3}$ (**Table 4.1**). The difference in the final percentage of the two products P1 (58 %) and P2 (42 %) (**Scheme 4.1b**) is likely caused by different efficiencies for the phosphodiester bond cleavage, as k_2 (0.25 ± 0.05 s^{-1}) is bigger than k_4 (0.12 ± 0.03 s^{-1}).

4.4 Conclusions

Synthetic analogs have been widely used in mechanistic studies of enzyme-mediated reactions, as systematic molecular "surgery" has the ability to unravel key recognition elements. The importance of N-7 in c-di-GMP for rocR recognition was revealed by comparing the reaction kinetics of rocR-mediated hydrolysis of c-di-GMP analogs. Such strategy could be used in the mechanistic studies for other enzymes or catalytic RNA. The fluorescence signal change might not be significant for the rocR-mediated hydrolysis, as the CDN is only cleaved to the linear pNpN. However, it would

be worthy to try monitoring this process with steady state fluorescence spectroscopy, as the reaction kinetics is independent to the absolute values of change in signal.

4.5 Acknowledgements

Chapter 3, 4 and 5, in full, are currently being prepared for submission for publication for the material. Li, Y.; Fin, A; Ludford, P. T.; Rovira, A. R.; Tor, Y., Monitoring the formation and degradation of c-di-GMP analogs using fluorescence. The thesis author was the primary author of this material.

4.6 Supplementary information

4.6.1 Methods

Cloning and protein expression

PA3977 (rocR) gene fragment with 5'-NdeI and 3'-HindIII cleavage sites was purchase from Integrated DNA Technologies (gBlock® Gene Fragments). The GOI and pet28b vector were digested with NdeI and HindIII to create matching sticky ends. The digested vector was also treated with CIAP (Promega) to avoid self-ligation. The digested GOI and vector were then ligated with T4 DNA ligase (New England Biolabs) following standard protocols. The insertion was confirmed by Sanger sequencing (GenScript). Plasmids containing the gene of interest were transformed into Escherichia coli BL21(DE3) competent cells respectively for protein expression according to previous publications [20-21].

CDN hydrolysis with rocR

10 μM of CDN was incubated with 100 nM of rocR in a buffer containing 100 mM Tris-HCl, pH 8, 20 mM KCl, 25 mM $MgCl_2$ at 37 °C. Aliquots of the reaction mixture were taken out at designated time points and quenched with 100 mM $CaCl_2$.

All aliquots were filtered before subjected to reverse-phase HPLC analysis. The reaction mixture was separated by Sepax Bio C-18 column (250 × 10mm, 5 µm particle size) with a gradient of 0.1–15% of 10 mM NH_4OAc, pH7 in MeOH in 12 minutes at 25 °C or 50 °C (only for reactions of c-G^{tz}GMP and c-di-^{tz}GMP) on an Agilent 1200 series HPLC system (Agilent Technologies).

4.6.2 Supplementary spectra

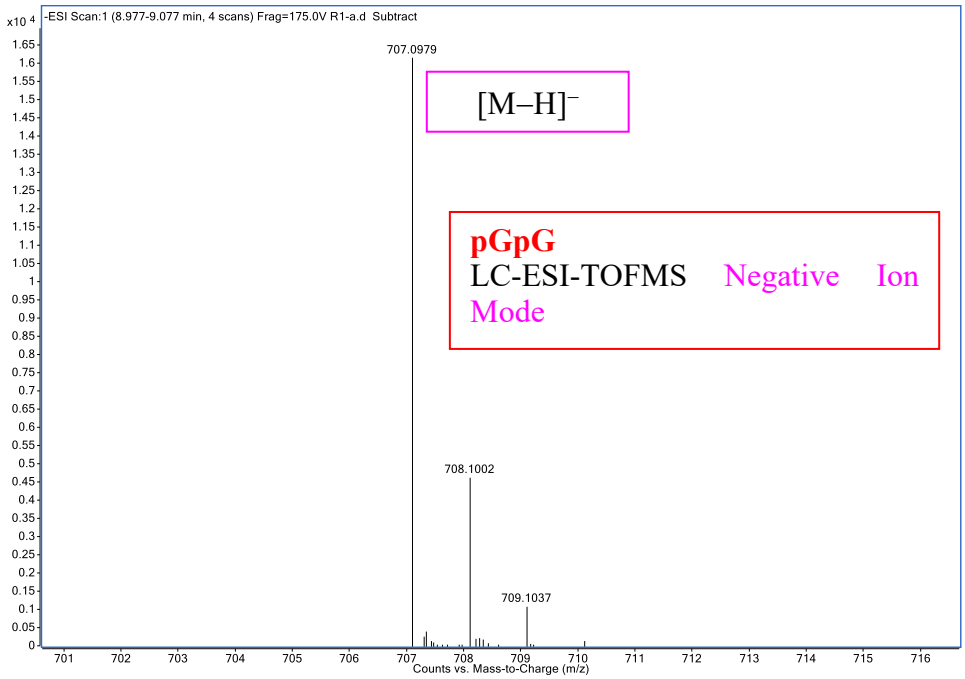

Spectrum 4.1 LC-ESI-TOFMS of pGpG. $[C_{20}\,H_{25}\,N_{10}\,O_{15}\,P_2]^-$, calculated 707.0982, found 707.0979, delta (ppm) –0.4. LC separation method was similar as reported in the method section for rocR hydrolysis analysis.

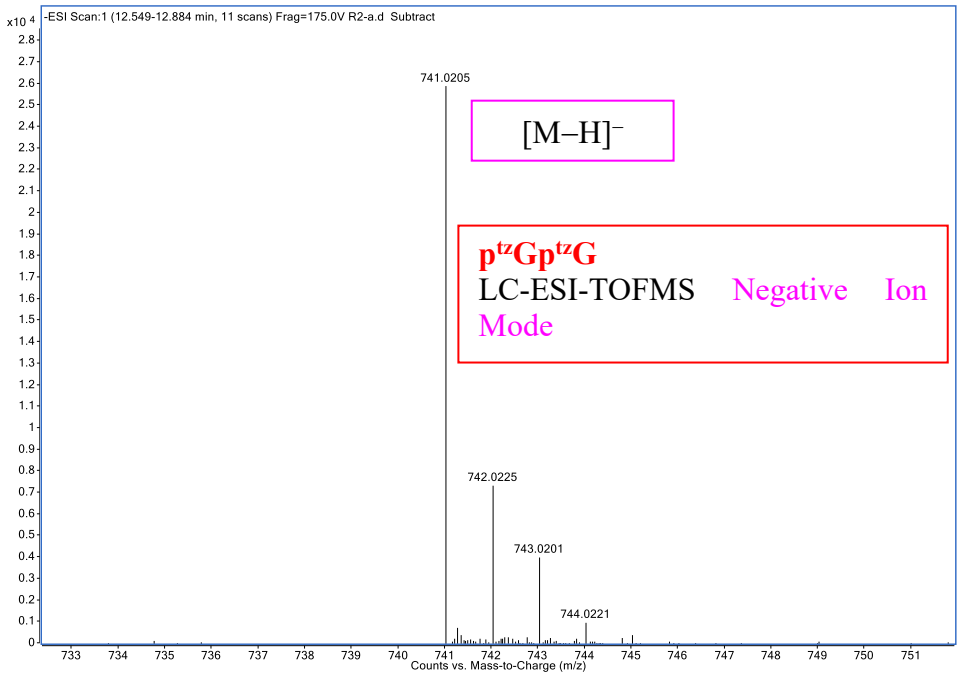

Spectrum 4.2 LC-ESI-TOFMS of $p^{tz}Gp^{tz}G$. $[C_{20}H_{23}N_8O_{15}S_2P_2]^-$, calculated 741.0205, found 741.0205, delta (ppm) 0.0. LC separation method was similar as reported in the method section for rocR hydrolysis analysis.

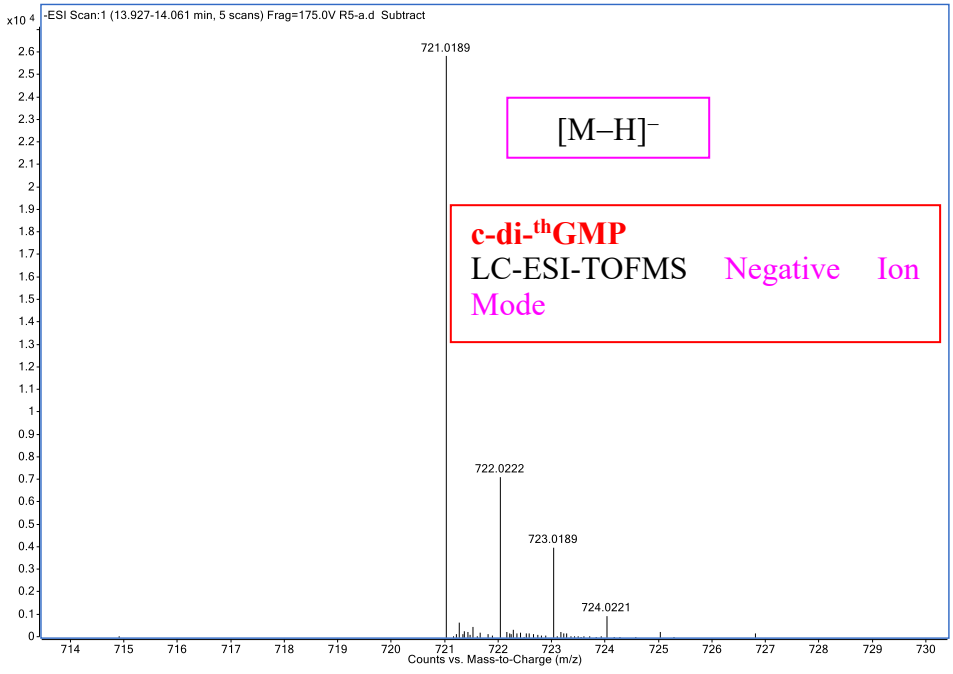

Spectrum 4.3 LC-ESI-TOFMS of c-di-thGMP. $[C_{22}H_{23}N_6O_{14}P_2S_2]^-$, calculated 721.0194, found 721.0189, delta (ppm) –0.7. LC separation method was similar as reported in the method section for rocR hydrolysis analysis.

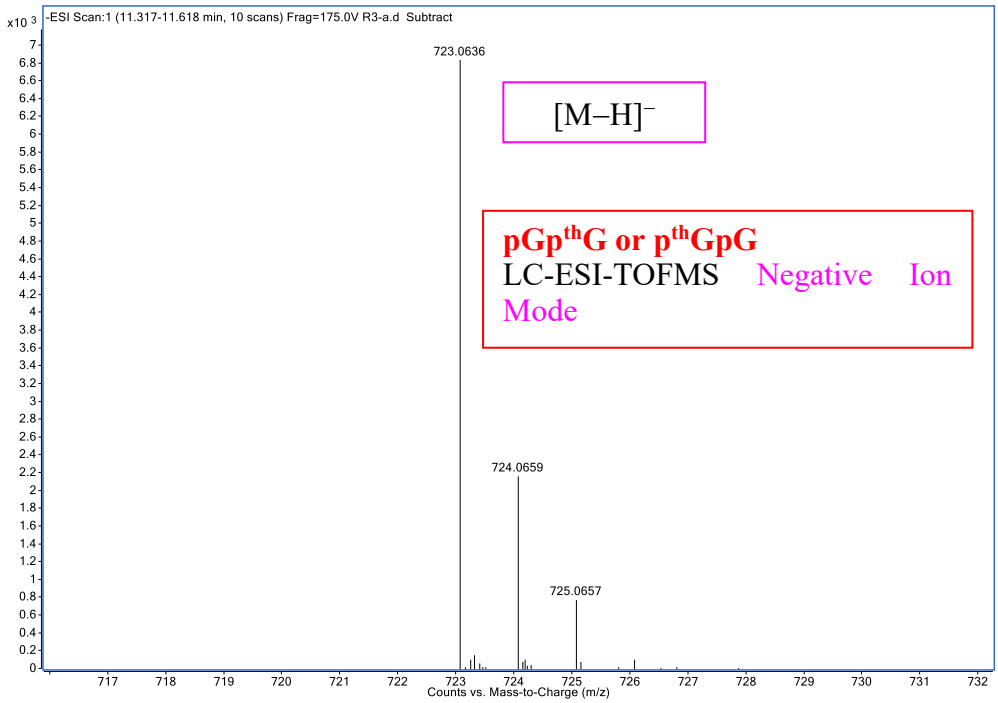

Spectrum 4.4 LC-ESI-TOFMS of pGpthG or pthGpG. $[C_{21}H_{25}N_8O_{15}P_2S]^-$, calculated 723.0641, found 723.0636, delta (ppm) –0.7. LC separation method was similar as reported in the method section for rocR hydrolysis analysis.

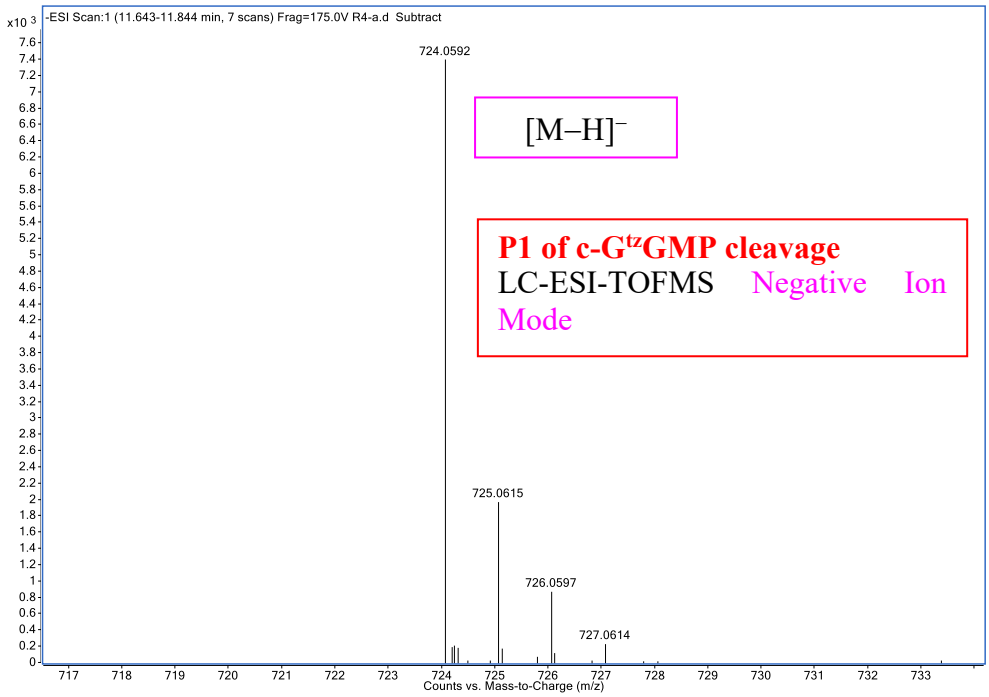

Spectrum 4.5 LC-ESI-TOFMS of P1 of c-G^{tz}GMP cleavage. $[C_{20}H_{24}N_9O_{15}P_2S]^-$, calculated 724.0593, found 724.0592, delta (ppm) –0.1. LC separation method was similar as reported in the method section for rocR hydrolysis analysis.

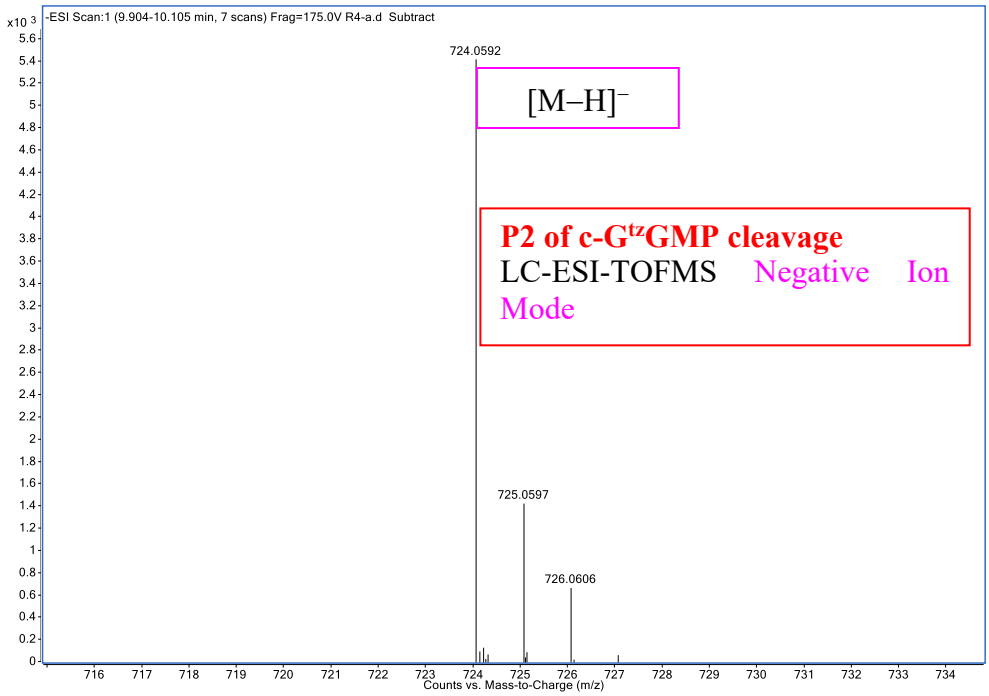

Spectrum 4.6 LC-ESI-TOFMS of P2 of c-G^{tz}GMP cleavage. $[C_{20}\,H_{24}\,N_9\,O_{15}\,P_2S]^-$, calculated 724.0593, found 724.0592, delta (ppm) –0.1. LC separation method was similar as reported in the method section for rocR hydrolysis analysis.

4.7 References

1. Ross, P.; Weinhouse, H.; Aloni, Y.; Michaeli, D.; Weinberger-Ohana, P.; Mayer, R.; Braun, S.; de Vroom, E.; van der Marel, G. A.; van Boom, J. H.; Benziman, M., Regulation of cellulose synthesis in Acetobacter xylinum by cyclic diguanylic acid. *Nature* **1987,** *325*, 279-281.

2. Romling, U.; Galperin, M. Y.; Gomelsky, M., Cyclic di-GMP: the first 25 years of a universal bacterial second messenger. *Microbiol Mol Biol Rev* **2013,** *77* (1), 1-52.

3. Libanova, R.; Becker, P. D.; Guzman, C. A., Cyclic di-nucleotides: new era for small molecules as adjuvants. *Microb Biotechnol* **2012,** *5* (2), 168-76.

4. Jenal, U.; Reinders, A.; Lori, C., Cyclic di-GMP: second messenger extraordinaire. *Nat Rev Microbiol* **2017,** *15* (5), 271-284.

5. Kalia, D.; Merey, G.; Nakayama, S.; Zheng, Y.; Zhou, J.; Luo, Y.; Guo, M.; Roembke, B. T.; Sintim, H. O., Nucleotide, c-di-GMP, c-di-AMP, cGMP, cAMP,

(p)ppGpp signaling in bacteria and implications in pathogenesis. *Chem Soc Rev* **2013,** *42* (1), 305-41.

6. Tamayo, R.; Pratt, J. T.; Camilli, A., Roles of cyclic diguanylate in the regulation of bacterial pathogenesis. *Annu Rev Microbiol* **2007,** *61*, 131-48.

7. Yan, W.; Qu, T.; Zhao, H.; Su, L.; Yu, Q.; Gao, J.; Wu, B., The effect of c-di-GMP (3'-5'-cyclic diguanylic acid) on the biofilm formation and adherence of Streptococcus mutans. *Microbiol Res* **2010,** *165* (2), 87-96.

8. Krasteva, P. V.; Sondermann, H., Versatile modes of cellular regulation via cyclic dinucleotides. *Nat Chem Biol* **2017,** *13* (4), 350-359.

9. Clivio, P.; Coantic-Castex, S.; Guillaume, D., (3'-5')-Cyclic dinucleotides: synthetic strategies and biological potential. *Chem Rev* **2013,** *113* (10), 7354-401.

10. Roembke, B. T.; Zhou, J.; Zheng, Y.; Sayre, D.; Lizardo, A.; Bernard, L.; Sintim, H. O., A cyclic dinucleotide containing 2-aminopurine is a general fluorescent sensor for c-di-GMP and 3',3'-cGAMP. *Mol Biosyst* **2014,** *10* (6), 1568-75.

11. Shanahan, C. A.; Strobel, S. A., The bacterial second messenger c-di-GMP: probing interactions with protein and RNA binding partners using cyclic dinucleotide analogs. *Org Biomol Chem* **2012,** *10* (46), 9113-29.

12. Zhou, J.; Zheng, Y.; Roembke, B. T.; Robinson, Sarah M.; Opoku-Temeng, C.; Sayre, D. A.; Sintim, H. O., Fluorescent analogs of cyclic and linear dinucleotides as phosphodiesterase and oligoribonuclease activity probes. *RSC Adv.* **2017,** *7* (9), 5421-5426.

13. Foletti, C.; Kramer, R. A.; Mauser, H.; Jenal, U.; Bleicher, K. H.; Wennemers, H., Functionalized Proline-Rich Peptides Bind the Bacterial Second Messenger c-di-GMP. *Angewandte Chemie International Edition* **2018,** *57* (26), 7729-7733.

14. Rossello, J.; Lima, A.; Gil, M.; Rodriguez Duarte, J.; Correa, A.; Carvalho, P. C.; Kierbel, A.; Duran, R., The EAL-domain protein FcsR regulates flagella, chemotaxis and type III secretion system in Pseudomonas aeruginosa by a phosphodiesterase independent mechanism. *Sci Rep* **2017,** *7* (1), 10281.

15. Rao, F.; Yang, Y.; Qi, Y.; Liang, Z. X., Catalytic mechanism of cyclic di-GMP-specific phosphodiesterase: a study of the EAL domain-containing RocR from Pseudomonas aeruginosa. *J Bacteriol* **2008,** *190* (10), 3622-31.

16. Zheng, Y.; Tsuji, G.; Opoku-Temeng, C.; Sintim, H. O., Inhibition of P. aeruginosa c-di-GMP phosphodiesterase RocR and swarming motility by a benzoisothiazolinone derivative. *Chemical Science* **2016,** *7* (9), 6238-6244.

17. Schmidt, A. J.; Ryjenkov, D. A.; Gomelsky, M., The ubiquitous protein domain EAL is a cyclic diguanylate-specific phosphodiesterase: enzymatically active and inactive EAL domains. *J Bacteriol* **2005,** *187* (14), 4774-81.

18. Chen, M. W.; Kotaka, M.; Vonrhein, C.; Bricogne, G.; Rao, F.; Chuah, M. L.; Svergun, D.; Schneider, G.; Liang, Z. X.; Lescar, J., Structural insights into the regulatory mechanism of the response regulator RocR from Pseudomonas aeruginosa in cyclic Di-GMP signaling. *J Bacteriol* **2012,** *194* (18), 4837-46.

19. Minasov, G.; Padavattan, S.; Shuvalova, L.; Brunzelle, J. S.; Miller, D. J.; Basle, A.; Massa, C.; Collart, F. R.; Schirmer, T.; Anderson, W. F., Crystal structures of YkuI and its complex with second messenger cyclic Di-GMP suggest catalytic mechanism of phosphodiester bond cleavage by EAL domains. *J Biol Chem* **2009,** *284* (19), 13174-84.

20. Barajas, J. F.; Finzel, K.; Valentic, T. R.; Shakya, G.; Gamarra, N.; Martinez, D.; Meier, J. L.; Vagstad, A. L.; Newman, A. G.; Townsend, C. A.; Burkart, M. D.; Tsai, S. C., Structural and Biochemical Analysis of Protein-Protein Interactions Between the Acyl-Carrier Protein and Product Template Domain. *Angew Chem Int Ed Engl* **2016,** *55* (42), 13005-13009.

21. Barajas, J. F.; Shakya, G.; Moreno, G.; Rivera, H., Jr.; Jackson, D. R.; Topper, C. L.; Vagstad, A. L.; La Clair, J. J.; Townsend, C. A.; Burkart, M. D.; Tsai, S. C., Polyketide mimetics yield structural and mechanistic insights into product template domain function in nonreducing polyketide synthases. *Proc Natl Acad Sci U S A* **2017,** *114* (21), E4142-E4148.

5 Biophysical application of fluorescent cyclic dinucleotides analogs

5.1 Introduction

Investigations of the *in vitro* biosynthesis and hydrolysis of CDN often rely on high performance liquid chromatography (HPLC) and radioisotope labeling. While both techniques are reliable and informative, neither of them can be used to monitor biochemical processes in real-time, regardless of the time-consuming experimental procedures. The difficulties and cost in handling radioactive material have also promoted the development of alternative techniques.

Steady-state fluorescence spectroscopy has been widely used for biophysical analysis. Using synthetic fluorescent CDNs containing previously developed emissive nucleosides to monitor PDE-mediated c-di-GMP hydrolysis with emission spectra has been demonstrated.[1] However, applying such strategy to the study of dinucleotide cyclases demands high isomorphicity of the NTP substrates.

The isomorphicity of our fluorescent NTP and CDN analogs has been demonstrated in the previous chapters, specifically for DncV-mediated CDN synthesis where thGTP and ^{tz}GTP were both accepted as surrogates of GTP. Based on the resolved structure of c-di-GMP in solution, the stacking of the two nucleobases could very likely result in fluorescence quenching when thG or ^{tz}G was incorporated.[2] Therefore, when thGTP or ^{tz}GTP were used as substrates for DncV-mediated CDN cyclization, a decay of fluorescence intensity of the reaction mixture should be observed as the cyclic dinucleotides being formed. Such a change of signal is directly correlated with the

cyclization process, and thus can be used to monitor the process in real-time and analyze the reaction kinetics.

5.2 Results

5.2.1 Photophysical properties of fluorescent CDN analogs

The fundamental photophysical properties of the fluorescent CDN analogs, including the maximum absorption wavelength (λ_{abs}^{max}) and emission wavelength (λ_{em}^{max}), fluorescence quantum yield (Φ), were derived from spectral data shown in **Figure 5.1** and listed in **Table 5.1**. The molar extinction coefficients (ε) at λ_{abs}^{max} of the fluorescent CDNs were calculated from then molar extinction coefficients of the nucleosides at that wavelength using the following equation:

$$\varepsilon_{CDN} = (\varepsilon_1 + \varepsilon_2) \times (1\text{-}10\%)$$

Equation 5.1 Equation for CDN molar extinction coefficient calculation.

where ε_1 and ε_2 represent the molar extinction coefficients of the two nucleosides incorporated in the CDN.

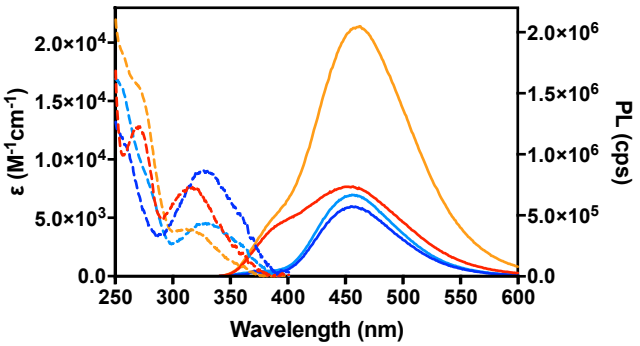

Figure 5.1 Absorption spectra (dashed lines) and emission spectra (solid lines) of c-di-thGMP (red), c-di-^{tz}GMP (indigo), c-GthGMP (orange) c-GtzGMP (light blue) dissolved in water. The emission spectra were normalized with excitation intensity of OD 0.1.

The maximum absorption and emission wavelengths did not shift much (< 5 nm) when thG and ^{tz}G were incorporated in corresponding cyclic dinucleotides. Yet when comparing the quantum yields of the fluorescent CDNs to those of the monomeric nucleosides (**Table 5.1**), the emissive guanosine analogs appeared to be significantly quenched when incorporated into corresponding cyclic dinucleotides. thG turns out to be a better quencher for itself than guanosine, as the quantum yield of c-di-thGMP was about 17% of that of thG, whereas c-GthGMP is 39%. The self-quenching effect of ^{tz}G resulted in the low quantum yield of c-di-^{tz}GMP (16% of Φ^{tz}_{G}), which is comparable to that of c-G^{tz}GMP (19% of Φ^{tz}_{G}).

Table 5.1 Photophysical properties of emissive nucleosides and CDN analogs.

	λ_{abs}^{max} (nm)	ε (M^{-1} cm^{-1})	λ_{em}^{max} (nm)	Φ	Φε
[1] thG	321	4150	453	4.6×10^{-1}	1909
[1] ^{tz}G	333	4870	459	2.5×10^{-1}	1203
c-di-thGMP	317	7470	457	7.7×10^{-2}	575
c-di-^{tz}GMP	331	8766	456	3.9×10^{-2}	342
c-GthGMP	317	3535	458	1.8×10^{-1}	636
c-G^{tz}GMP	331	4383	456	4.8×10^{-2}	210

[1] Values for thG and ^{tz}G were obtained from previous publications.

5.2.2 Monitoring DncV-mediated synthesis of c-di-GMP analogs with fluorescence

After observing the significant quenching thG or ^{tz}G in corresponding CDNs, we sought to utilize this effect to monitor the synthesis of c-di-GMP with fluorescence. In order to compare fluorescence-monitored and HPLC-monitored reaction kinetics, experimental conditions of the DncV-mediated reactions were held the same for both analyses. Aliquots of reaction mixtures were treated with calf intestinal alkaline phosphatase (CIAP) at designated times, and emission spectra were taken after each

sample was diluted in cuvette. Rewardingly, significant decrease in the fluorescence intensity was observed as the reactions proceed for the synthesis of all four fluorescent c-di-GMP analogs (**Figure 5.2**).

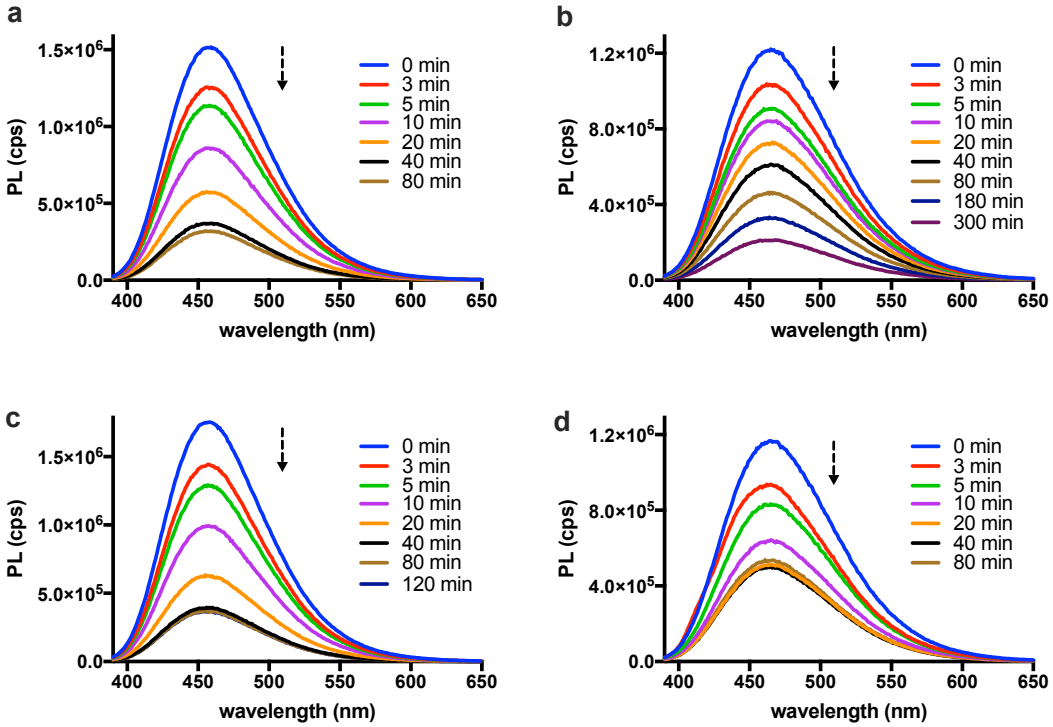

Figure 5.2 DncV-mediated cyclization monitored by emission spectra for c-di-^{tz}GMP (a), c-di-thGMP (b), c-G^{tz}GMP (c) and c-GthGMP (d). Excitation wavelength was 380nm for all emission spectra.

When the reactions were monitored with HPLC, a second-order consecutive reaction model (**Scheme 3.1)** was used to describe DncV-mediated synthesis of c-di-GMP and its analogs, where 2 NTPs (S) were converted to an intermediate pppNpN (I_1), which could be further converted to the cyclized CDN (P). A small amount of I_1 could also be converted to the inert second intermediate pNpN (I_2) instead of successfully cyclized into CDN. When simulated with **Equation 3.1–3.4**, k_1, k_2 and k_3 were derived. In order to demonstrate the good agreement between fluorescence and HPLC-monitored kinetics, we first used the *k* values determined by HPLC analysis and experimentally

determined *a* values to fit the fluorescence data (**Figure 5.3,** Model 2 in **Table 5.2, 5.3**). In order to correlate the fluorescence signal with the concentrations of different species presented in the reactions, we introduced fluorescence conversion factor (*a*) to our simulation system in addition to the previously used differential equations (**Equation 3.1–3.4)**. The fluorescence conversion factor serves as a "bridge" between the integrated fluorescent intensity (area under the emission spectrum) and the concentration of a given chromophore at a given condition, and can be calculated from measured emission spectrum using the following equation:

$$FL_{int} = a[C]$$

Equation 5.2 Equation for fluorescence conversion factor calculation.

where FL_{int} stands for the integration of the area under the emission spectrum of a given chromophore, [C] stands for concentration of the chromophore. All the *a* values for emissive CDN analogs were listed in **Table 5.4**. **Equation 5.3** was used to correlate the recorded fluorescence spectrum with the concentrations of different species in the reaction mixture:

$$FL_{int} = a_1[S] + a_2[I_1] + a_3[P] + a_4[I_2]$$

Equation 5.3 Equation for converting concentration to fluorescence signal.

where FL_{int} stands for the integration of the area under the emission spectrum of the sample, a_1–a_4 represent the fluorescence conversion factors of I, I_1, P and I_2. Due to the similar quenching effect of intermediate and the product, we assumed that $a_2 = a_3 = a_4$. The fitted-curve was in excellent agreement to the experimental data for c-di-^{tz}GMP synthesis **(Figure 5.3a)** with R^2 = 0.988 (**Table 5.2**). For c-di-thGMP synthesis, the

observed fluorescence signal decreased much faster than simulated in the first 40 minutes **(Figure 5.3b)**, which resulted in a smaller R^2 (0.824) for this simulation (**Table 5.3**).

In order to demonstrate that the DncV-mediated catalytic process can be monitor directly with fluorescence without any assistance of HPLC analysis, the reaction was simplified to a pseudo-second order reaction for c-di-^{tz}GMP and c-di-thGMP synthesis (Model 3 in **Table 5.2, 5.3**):

$$2S \xrightarrow{k_{app}} P_{app}$$

Scheme 5.1 Scheme of pseudo-second order reaction.

where S stands for the starting material, P_{app} (apparent product) stands for the sum of all the species that demonstrate similar photophysical properties as the CDN product ($P_{app} = I_1 + I_2 + P$).

The following equation was used to correlate fluorescence signal with concentration of species:

$$FL_{int} = a_1[S] + a_3[P_{app}]$$

Equation 5.4 Equation for converting concentration to fluorescence signal in pseudo-second order reaction.

where FL_{int} represents the integration of the area under the emission spectrum of the sample, a_1 and a_3 represent the fluorescence conversion factors of S and P.

Rewardingly, using Model 3, the simulated curve fits the experimental data of c-di-^{tz}GMP with R^2 =0.993, and derived k_{app}=1.57 M^{-1} s^{-1}, which is very close to the k_1 derived from HPLC analysis (1.26 M^{-1} s^{-1}) (**Table 5.5**). For c-di-thGMP synthesis, the

k_{app} value derived from the pseudo-second order simulation was slightly bigger than the k_1 values derived from HPLC analysis (0.530 and 0.308 M^{-1} s^{-1}, respectively), but overall the two k values were still comparable (**Table 5.3**).

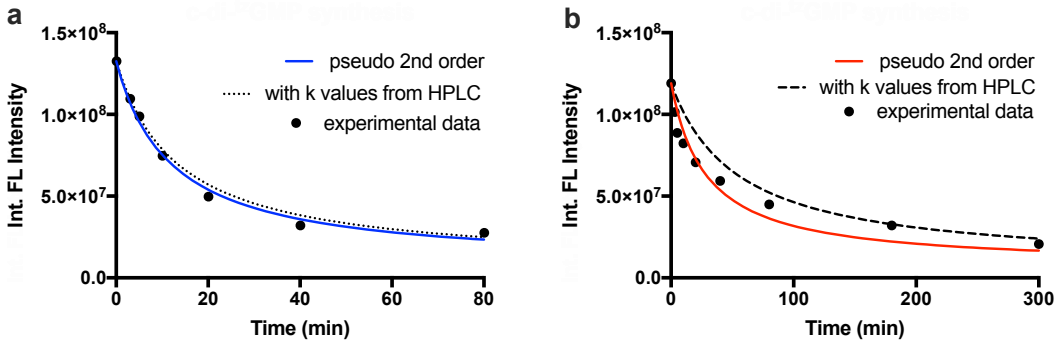

Figure 5.3 Kinetics analysis of DncV-mediated synthesis of c-di-^{tz}GMP (a), and c-di-thGMP (b). The integrated emission intensity (black dots), fitted curves of second-order consecutive reaction with k values from HPLC analysis (black dashed lines), and fitted curves of pseudo second order reactions (solid colored lines).

Table 5.2 Reaction rate constants and coefficients of determination for c-di-^{tz}GMP synthesis simulated with different models.

	[1] Model 1	[2] Model 2	[3] Model 3
k_1 (M^{-1} s^{-1})	1.26 ± 0.07	1.26 ± 0.07	-
kapp (M^{-1} s^{-1})	-	-	1.57± 0.15
R^2	0.971	0.988	0.993

[1] Second-order consecutive reaction monitored with HPLC analysis, only R^2 for the fitted curve of the starting material was shown.
[2] Second-order consecutive reaction monitored with emission spectra, k values derived from Model 1 was used for curve-fitting
[3] Pseudo-second order reaction monitored with emission spectra.

Table 5.3 Reaction rate constants and coefficients of determination for c-di-thGMP synthesis simulated with different models.

	[1]Model 1	[2]Model 2	[3]Model 3
k_1(M^{-1} s^{-1})	$(3.08 \pm 0.03) \times 10^{-1}$	$(3.08 \pm 0.03) \times 10^{-1}$	-
kapp (M^{-1} s^{-1})	-	-	$(5.30 \pm 0.49) \times 10^{-1}$
R^2	0.949	0.824	0.939

[1] Second-order consecutive reaction monitored with HPLC analysis, only R^2 for the fitted curve of the starting material was shown.
[2] Second-order consecutive reaction monitored with emission spectra, k values derived from Model 1 was used for curve-fitting
[3] Pseudo-second order reaction monitored with emission spectra.

Table 5.4 Fluorescence coefficients of emissive CDN analogs

	[1] a_1 ($\times 10^{11}$)	[2] $a_3=a_2=a_4$ ($\times 10^{11}$)
c-di-^{tz}GMP	2.75	0.29
c-di-thGMP	2.18	0.28
c-G^{tz}GMP	3.14	0.29
c-GthGMP	2.28	0.67

[1] a_1 was measured by taking emission spectrum of ^{tz}GTP or thGTP at known concentration at the experimental conditions and calculated using Equation 5.2.

[2] a_3 was measured by taking emission spectrum of each CDN at known concentration at the experimental conditions and calculated using Equation 5.2.

Due to the complexity of DncV-mediated synthesis of c-G^{tz}GMP and c-GthGMP, we were not able to monitor those reactions with HPLC. These reactions lead to the production of three products with the heterodimers being the major products (**Figure 3.3**), and could involve multiple types of intermediates. In order to monitor these reactions with fluorescence, we focused on the formation of the main product, and simplified the reaction with the scheme below:

$$S_n + S_e \xrightarrow{k_{app}} P_{app}$$

Scheme 5.2 Scheme of DncV-mediated synthesis of c-G^{tz}GMP or c-GthGMP.

where S_n, S_e represents the non-emissive (GTP) and emissive substrate (^{tz}GTP or thGTP) respectively, P_{app} stands for the sum of all the species that demonstrate similar photophysical properties as the major CDN product (c-G^{tz}GMP or c-GthGMP).

Since S_n does not contribute to the fluorescence signal, the reaction can be further simplified as below:

$$S_e \xrightarrow{k_{app}} P_{app}$$

Scheme 5.3 Scheme of DncV-mediated synthesis of c-G^{tz}GMP or c-GthGMP simplified as pseudo-first order reaction.

Equation 5.4 was used to correlate fluorescence signal with concentration. Considering the complexity of the actual reaction, instead of using the experimentally determined value for simulation, a_3 was treated as a variable and was calculated based on the best-fitted curves. The k_{app}, calculated a_3, coefficients of determination (R^2), and experimentally measured a_3 were listed in **Table 5.5** for c-G^{tz}GMP and c-GthGMP synthesis. The curves fitted excellently to the experimental data, as indicated by the R^2 values, however, the calculated a_3 values were bigger than the experimentally measured a_3, indicating that in additional to the major product, other species in the reaction mixture could also contribute to the overall fluorescence signal.

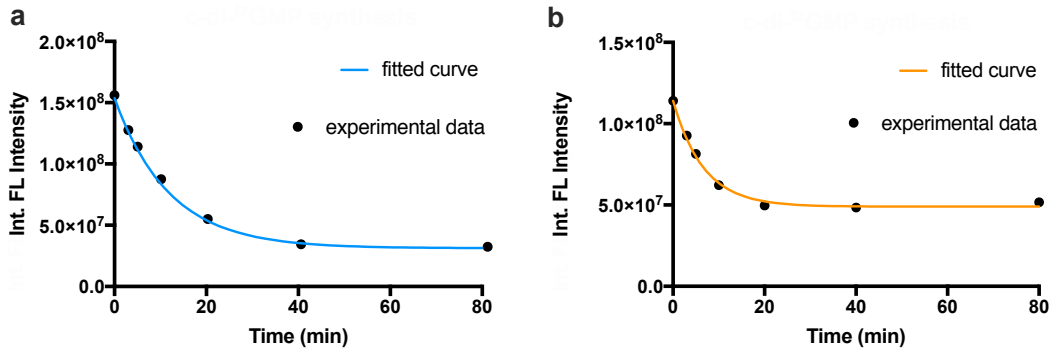

Figure 5.4 Kinetics analysis of DncV-mediated synthesis of c-G^{tz}GMP (a), and c-GthGMP (b). The integrated emission intensity (black dots), fitted curves using pseudo first order reaction model (solid colored lines) were shown.

Table 5.5 Reaction rate constants and coefficients of determination for DncV-mediated c-G^{tz}GMP synthesis.

	c-G^{tz}GMP synthesis	c-GthGMP synthesis
kapp (s^{-1})	$(1.37 \pm 0.06) \times 10^{-3}$	$(2.57 \pm 0.12) \times 10^{-3}$
a_3 calculated ($\times 10^{11}$)	0.64	0.93
R^2	0.999	0.994
a_3 measured ($\times 10^{11}$)	0.29	0.67

5.3 Discussion

It has been previously demonstrated that either as a free nucleoside or incorporated in oligonucleotides, thG exists in an equilibrium of two ground-state tautomers with significantly shifted absorption and emission spectra at physiological pH.[3] The shoulder peaks in the emission spectra of c-di-thGMP and c-GthGMP indicated the presence of the two tautomers of thG in corresponding CDNs (**Figure 5.1**). According to previous studies, the blue-shifted tautomer is likely thG-H3, with λ_{abs}^{max} = 313 nm, λ_{em}^{max} = 400 nm, and the red-shifted tautomer is likely thG-H1, with λ_{abs}^{max} = 334 nm, λ_{em}^{max} = 470 nm. The overall absorption and emission spectra are the result of the linear combination of the two tautomeric forms of thG. We speculate that such tautomerization is also presented in c-di-thGMP and c-GthGMP.

Fluorescence quenching of fluorophores incorporated in oligonucleotides by proximal nucleobases has been intensively studied.[4] For example, 2-aminopurine (2-AP) is statically quenched when stacked with purine bases in DNA.[5] The major contributor for such quenching effect is the distance-dependent electron transfer from the 2-AP to the adjacent purine residues.[6] The obvious quenching effect of the emissive nucleotides in cyclic dinucleotides is likely resulted from the same processes. Since the distance-dependent quenching is closely associated with the cyclization reaction processes, especially the formation of the first phosphodiester linker, we sought to utilize the quenching of fluorescence to monitor the cyclization reaction.

When monitoring the process with emission spectra, not all the species in the reaction mixtures could be distinguished due to the similarity in quenching effect for some species. As shown in **Figure 5.5**, the intermediate and the product might demonstrate similar photophysical properties, as the distance between the two nucleobases in those two species (D_2, D_3) might not be significantly different, especially when compared to that of the starting material (D_1). In summary, since $D_1 >> D_2 \approx D_3$, the recorded change in fluorescence intensity is mainly caused by the formation of the intermediate. Therefore in **Equation 5.3**, $a_2 = a_3 = a_4$. Since photophysical properties can be affected by reaction conditions, such as pH, ion strength and temperature, the *a* values have to be measured under the exact same condition as the reaction. In addition to previous studies where fluorescent CDN analogs were used to monitor PDE-mediated hydrolysis,[1] our hypothesis was also supported by the excellent agreement between fluorescence and HPLC-monitored kinetics (**Figure 5.3**).

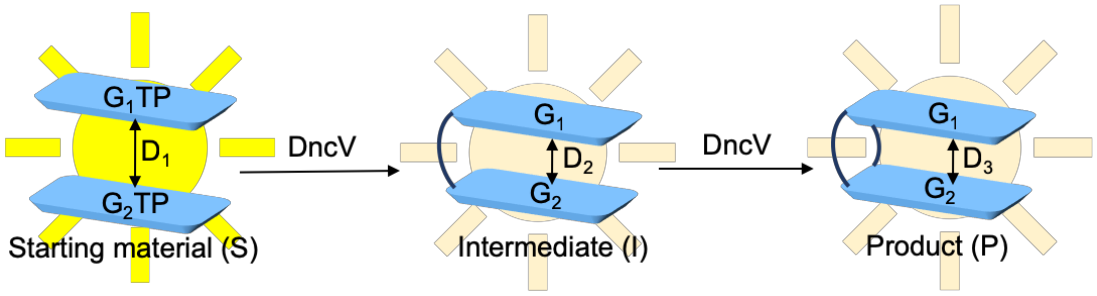

Figure 5.5 Hypothetical model of fluorescence quenching upon DncV-mediated cyclization.

Based on our hypothesis, k_{app} in **Scheme 5.1–5.3** should be comparable to k_1 in **Scheme 3.1**, as the major contributor to the change in fluorescence signal is the formation of the first intermediate (I_1).

The synthesis of the homodimeric CDNs was simplified to pseudo-second order reaction, as the photophysical properties of the intermediates and the product are not significantly different. Our simulations using pseudo-second order kinetics were in excellent agreement with the experimental data, and the derived k_{app} was comparable to k_1 calculated from HPLC analysis using second-order consecutive reaction model. In the synthesis of c-di-thGMP, the fluorescence signal decreased significantly faster than predicted by the fitted-curve in the first 40 minutes. This might be caused by other quenching effect of thG, such as interaction between thGTP and the intermediates.

Although HPLC analysis appears to be very informative in terms of isolating and quantifying different species in the reaction mixture, it cannot be used to monitor the reaction processes in real-time, and the analysis process is extremely time-consuming. Careful optimization of the solvent gradient is also needed in order to get good separation, which might not be practical for some complicated reactions. For example, in the synthesis of c-G^{tz}GMP, three products can be isolated from HPLC, however, it would be very challenging to separate all the intermediates, including

pppGp^{tz}G, ppp^{tz}GpG, pppGpG and ppp^{tz}GptzG, as well as the starting material GTP and ^{tz}GTP. Therefore, monitoring such reactions with fluorescence is a great advantage. We monitored the reactions by focusing on the formation of the major product, which contains reactions one emissive nucleotide and one non-emissive nucleotide. By simplifying the reaction to pseudo-first order reaction, k_{app} was calculated, which should reflect the rate of ^{tz}GTP consumption. Considering that the overall fluorescence signal is a combination of the signals from all the species in the reaction mixture, it is understandable that the calculated a_3 is slightly larger than experimentally measured values (**Table 5.5**).

5.4 Conclusions

DncV-mediated cyclization of CDNs was successfully monitored with steady state fluorescence spectroscopy. The reaction rate constants derived from fluorescence-based analysis were comparable to those calculated from HPLC analysis. Due to the simplicity and the time-scale feature of steady state fluorescence spectroscopy, we speculate that this could be applied to high throughput screening of inhibitors of DncV, or other dinucleotide cyclases. As demonstrated in previous publication, the hydrolysis process could also be monitored with fluorescence CDN analogs. Considering the excellent isomorphicity and distinctive photophysical properties of our emissive CDNs, they could be great surrogates for other enzymes or receptors involved in CDN signaling and facilitating the investigation of these proteins or riboswitches with fluorescence-based techniques.

5.5 Acknowledgements

Chapter 3, 4 and 5, in full, are currently being prepared for submission for publication for the material. Li, Y.; Fin, A; Ludford, P. T.; Rovira, A. R.; Tor, Y., Monitoring the formation and degradation of c-di-GMP analogs using fluorescence. The thesis author was the primary author of this material.

5.6 Experimental

For the characterization of the photophysical properties of emissive CDNs dissolved in water, absorption and emission spectra were taken under the same conditions as in previous publication.

For kinetics analysis of CDN synthesis, 500 μM of GTP or GTP analogs were incubated at 37 °C with 2.3 μM of DncV in a buffer containing 0.1 M NaCl, 40 mM Tris pH 7.5 and 10 mM $MgCl_2$. 7 μL aliquots of reaction were taken out at designated time points, and added to quenching solution containing 120 μL of water and 1μL of alkaline phosphatase CIAP (Promega) and incubated at 37 °C for another 5 minutes. The mixtures were then transferred to cuvette, and the emission spectra were taken at 37 °C, with excitation wavelength 380nm, and slits width 3nm.

5.7 References

1. Zhou, J.; Zheng, Y.; Roembke, B. T.; Robinson, Sarah M.; Opoku-Temeng, C.; Sayre, D. A.; Sintim, H. O., Fluorescent analogs of cyclic and linear dinucleotides as phosphodiesterase and oligoribonuclease activity probes. *RSC Adv.* **2017,** *7* (9), 5421-5426.

2. Gentner, M.; Allan, M. G.; Zaehringer, F.; Schirmer, T.; Grzesiek, S., Oligomer formation of the bacterial second messenger c-di-GMP: reaction rates and equilibrium constants indicate a monomeric state at physiological concentrations. *J Am Chem Soc* **2012,** *134* (2), 1019-29.

3. Sholokh, M.; Improta, R.; Mori, M.; Sharma, R.; Kenfack, C.; Shin, D.; Voltz, K.; Stote, R. H.; Zaporozhets, O. A.; Botta, M.; Tor, Y.; Mély, Y., Tautomers of a Fluorescent G Surrogate and Their Distinct Photophysics Provide Additional Information Channels. *Angewandte Chemie International Edition* **2016,** *55* (28), 7974-7978.

4. Genty, B.; Briantais, J.-M.; Baker, N. R., The relationship between the quantum yield of photosynthetic electron transport and quenching of chlorophyll fluorescence. *Biochimica et Biophysica Acta (BBA) - General Subjects* **1989,** *990* (1), 87-92.

5. Jean, J. M.; Hall, K. B., 2-Aminopurine fluorescence quenching and lifetimes: Role of base stacking. *Proceedings of the National Academy of Sciences* **2001,** *98* (1), 37-41.

6. Kelley, S. O.; Barton, J. K., Electron Transfer Between Bases in Double Helical DNA. *Science* **1999,** *283* (5400), 375-381.

6 Innate immune response triggered by fluorescent CDN analogs

6.1 Introduction

Along the discovery of 2',3'-cGAMP, a mammalian CDN produced by cGAS upon sensing cytoplasmic dsDNA, it has been illustrated that CDNs act as agonists of the innate immune response of mammalian cells through the STING pathway, which has made CDNs and the CDN-triggered pathways popular targets for immunotherapeutic purposes. [1-5] In order to analyze the isofunctionality of the emissive CDN analogs, we investigated their potency in triggering innate immune responses in mammalian cells by analyzing the activation of transcription factor IRF3 and the induction of IFN-β.

6.2 Results

To investigate the potency of the synthetic c-di-GMP analogues as activators of the IFN response in eukaryotic cells, RAW 264.7 cells were transfected with various concentrations of c-di-GMP, c-di-^{tz}GMP, c-di-thGMP, c-GthGMP and c-G^{tz}GMP. The phosphorylation of IRF3 to pIRF3 was analyzed by immunoblotting and IFN-β mRNA production by RT-qPCR.

CDNs were transfected into RAW 264.7 cells with digitonin as described in previous studies.[6-7] Cells were lysed with NP-40 buffer 2 hours after transfection, and total protein was collected for immunoblotting against phosphorylated IRF3 and β-actin. No pIRF3 was observed for untreated cells (UT) and digitonin permeabilized cells (DG) (**Figure 6.1a**). Low concentrations of c-di-GMP and c-di-^{tz}GMP (1 μM) did not trigger

obvious IRF3 phosphorylation, but pIRF3 was detected when cells were transfected with higher concentration of either CDNs (**Figure 6.1a**). No obvious dose-response was observed for c-di-GMP and c-di-^{tz}GMP at concentration higher than 5 μM. On the other hand, c-di-thGMP (1–10 μM) did not trigger observable IRF3 activation but both c-GthGMP and c-G^{tz}GMP triggered IFR3 phosphorylation more potently than c-di-GMP and the other homodimeric c-di-GMP analogues.

Since the synthetic c-di-GMP analogues were able to activate IRF3, we analyzed their potency for inducing IFN-β mRNA production using RT-qPCR. RAW 264.7 cells were transfected with 1, 5 and 10 μM of CDNs as described above and incubated for 2, 4 and 6 hours. Total RNA was isolated and used for RT-qPCR as described in the Methods section. As shown in **Figure 6.1b** and **6.1c**, c-di-GMP induced most IFN-β mRNA production 4 hours post transfection, while for c-di-^{tz}GMP, c-GthGMP, and c-G^{tz}GMP, the highest response was observed after 2 hours. The same trend was observed for all three concentrations of CDNs tested (**Figure 6.1b**, **Figure 6.2a–b**). The IFN response to c-di-thGMP was minimal, but c-GthGMP showed the highest potency in inducing IFN-β mRNA production (**Figure 6.1b–d**, **Figure 6.2a–d**) among all the CDNs tested. After 2h of incubation, 5 μM of c-GthGMP induced 10-fold higher IFN-β mRNA production than c-di-GMP, the native messenger.

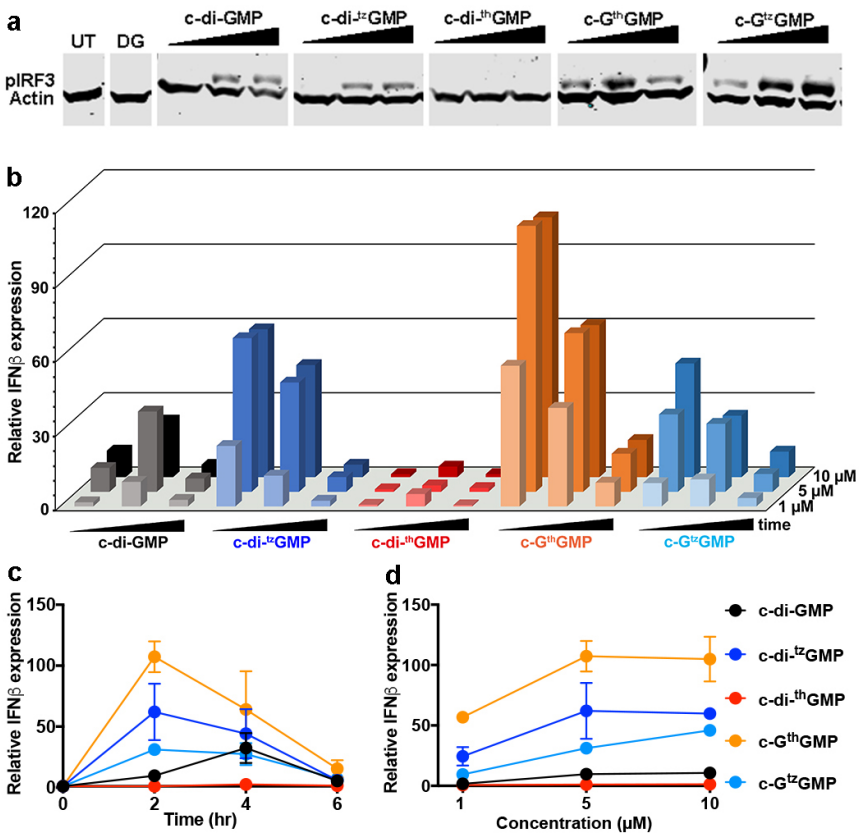

Figure 6.1 Innate immune response triggered by c-di-GMP and its analogues. (a) IRF3 phosphorylation induced by c-di-GMP analogues. 1, 5 and 10 μM of each CDN was used to transfect RAW 264.7 cells. Cells were lysed with NP-40 lysis buffer 2 hours post transfection, 20 μg of total protein was loaded on SDS-polyacrylamide gel. Proteins were transferred to PVDF membrane after gel electrophoresis, and immunoblotted against pIRF3 and β-actin. (b) IFN production induced by c-di-GMP and its analogues. RAW 264.7 cells were transfected with 1, 5, 10 μM of c-di-GMP, c-di-^{tz}GMP, c-GthGMP, c-di-GthGMP and c-G^{tz}GMP respectively, and incubated for 2, 4, 6 hours respectively before lysed by TRIzol™. RNA purification and RT-qPCR were conducted following the protocol described in the Methods section. (c) IFN response after 2, 4, 6 hours of incubation with 5 μM of CDNs. (d) IFN response to 1 μM, 5 μM and 10 μM of CDNs after 2h of incubation. Assays were done in duplicates. Error bars indicate SD.

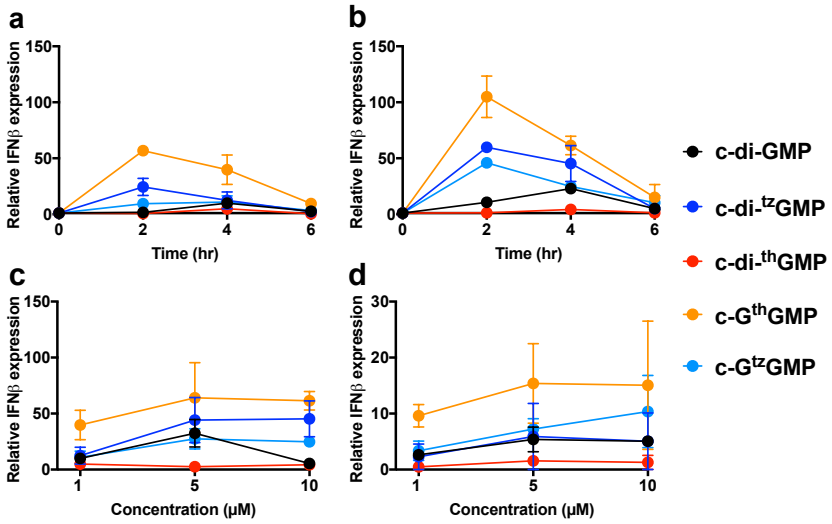

Figure 6.2 IFN production induced by c-di-GMP and its analogues. RAW 264.7 cells were transfected with 1, 5, 10 μM of c-di-GMP, c-di-^{tz}GMP, c-GthGMP, c-di-GthGMP and c-G^{tz}GMP respectively, and incubated for 2, 4, 6 hours respectively before lysed by TRIzol reagent. RNA purification and RT-qPCR were conducted following the protocol in Method section. (a), (b), IFN response after 2, 4, 6 hours of incubation with 1, 10 μM of CDNs, respectively. (c), (d), IFN response to 1, 5, 10 μM of CDNs after 4, 6 hours of incubation. Assays were done in duplicates. Error bars indicate SD.

6.3 Discussion

The ability of bacterial CDNs, including c-di-GMP, c-di-AMP and c-GAMP, to trigger the innate immune response in eukaryotic cells is likely one of the most significant function of these small nucleotides.[1, 8] STING, the ER-localized cellular receptor, is responsible for sensing exogenous CDNs produced by bacterial infection, and endogenous CDN produced by the host cGAS in response to sensing cytosolic dsDNA.[5, 9-11] STING undergoes conformational changes upon activation by CDNs, which recruits TBK1 to activate transcription factors IRF3, and leads to the production of type I interferons and other cytokines.[1, 10, 12-13] It has been demonstrated that the activation of the STING pathway in a tumor microenvironment can greatly facilitate

tumor regression, which has triggered interests in such small molecules and their analogues as modulators in cancer immunotherapy.[2, 14-18]

IRF3's activation can be recognized by its phosphorylation. Since the physiological concentration of c-di-GMP has been estimated to be in the sub- to low-micromolar range, [19-21] 1, 5 and 10 μM of CDNs were used to study their dose-response. The different c-di-GMP analogues activate the STING pathway with different potencies, as judged by IRF3 phosphorylation levels (**Figure 6.1a**). To more quantitatively analyze the activation of the STING pathway, CDN-induced, IFN-β production was measured by RT-qPCR in a time and dose dependent manners. As apparent from **Figure 6.1**, the ability to induce IFN-β production drops in the order: c-GthGMP > c-di-^{tz}GMP > c-G^{tz}GMP > c-di-GMP > c-di-thGMP, although it is apparent the cellular processes show complex concentration/time dependency. The effect of CDN concentrations above 5 μM seems to plateau (except for c-G^{tz}GMP). Importantly, however, their time dependency appears to peak, albeit at different times for different CDN analogues, with the synthetic analogs c-di-^{tz}GMP, c-G^{tz}GMP and c-GthGMP inducing earlier IFN-β response compared to the native c-di-GMP (**Figure 6.1c**, **Figure 6.2a–b**).

Among the synthetic CDNs tested, the two analogues containing thG, the least isomorphic G surrogate that lacks N7, display dramatically different potency in activating the STING pathway, with c-di-thGMP being essentially ineffective, while c-GthGMP exerts the strongest effect on IFN-β induction. Multiple factors can contribute to these effects, as the observed intensity and duration of the cellular signaling response reflect both the affinity of the ligand to STING, as well as its resistance to intracellular degradation processes. It is therefore not surprising that c-di-thGMP does not serve as a

potent STING agonist, since it is the least isomorphic CDN analogues, with two altered purine surrogates. Retaining one native G residue, however, as in c-GthGMP, compensates for such structural perturbations, while likely increasing the resistance to PDE digestion. The net result is a fast and persistent innate immune response, which may be beneficial in certain circumstances.

6.4 Conclusions

According to the published structures of CDN analogues, modifying the phosphate and sugar moieties of the CDNs has been a common strategy in order to get more potent STING agonists. The disclosed enzymatic pathway provides a rapid entry into such territory and our results indeed illustrate that modifying the nucleobases, rather than the phosphate or sugar moieties, could led to more potent STING agonists. Particularly intriguing is the high potency of the mixed analogs c-GthGMP and c-G^{tz}GMP, where a native guanosine residue is accompanied by an unnatural synthetic one. These analogs maintain STING recognition, but their cellular degradation is likely hampered, resulting in extended and potent immune response. These observations put forth new approaches for the design, preparation and implementation of new CDN analogues with altered recognition features and tuned potency and duration of the triggered cellular immune response.

6.5 Acknowledgements

Chapter 6, in full, is currently being prepared for submission for publication for the material. Li, Y.; Fin, A; Ludford, P. T.; Rovira, A. R.; Tor, Y., Synthesis and Cellular Activity of Systematically Modified Cyclic Dinucleotides. The thesis author was the primary author of this material.

6.6 Experimental

Immunoblotting

RAW 264.7 cells were plated on 24-well plates (5×10^5 cells per well) and incubate at 37 °C for 48 h. Cells were then transfected with 1–10 μM of CDN in a permeabilization buffer containing 10 μg/mL digitonin, 50 mM HEPES, pH 7, 100 mM KCl, 3 mM $MgCl_2$, 85 mM sucrose, 1 mM ATP, 0.1 mM DTT, 0.2% BSA for 30 mins at 37 °C, then incubated with regular growth medium for 2h. Cells were lysed with NP-40 lysis buffer containing protease inhibitor cocktail (Roche), PhosSTOP (Roche) and PMSF, and total protein was collected and quantified by BCA assay. Protein extracts were resolved by SDS-PAGE with 7.5% gel and transferred to PVDF membrane. Proteins were detected with the following primary antibodies: rabbit anti-pIRF3 monoclonal antibody (Cell Signaling Technology), mouse anti-β actin monoclonal antibody (Sigma-Aldrich).

RT-qPCR

RAW 264.7 cells were plated on 48-well plates (2.5×10^5 cells per well) and transfected with CDN using the same method as above after 48 hours of incubation at 37 °C. Cells were then incubate with regular growth medium for designated time, and total RNA was isolated with TRIzol™ reagent and purified with RNeasy mini kit (Qiagen) following the manufacturer's protocol. Following elution, RNA yields were evaluated using a Nanodrop spectrophotometer (Nanodrop technologies). RNA samples were converted to cDNA with SuperScript III First-Strand Synthesis kit (Invitrogen) with random hexamers following the manufacturer's protocol. Quantitative PCR (SYBR Green) analysis was performed in duplicates on an Applied Biosystems 7300

Real-time PCR system (Invitrogen). Transcription level of IFN-β gene (fwd primer: CAG CTC CAA GAA AGG ACG AAC, rev primer: GGC AGT GTA ACT CTT CTG CAT) of each sample was normalized to housekeeping gene TBP (forward primer: GAA GCT GCG GTA CAA TTC CAG, reverse primer: CCC CTT GTA CCC TTC ACC AAT) using the delta-delta CT method.

6.7 References

1. Danilchanka, O.; Mekalanos, J. J., Cyclic dinucleotides and the innate immune response. *Cell* **2013,** *154* (5), 962-70.

2. Corrales, L.; Glickman, L. H.; McWhirter, S. M.; Kanne, D. B.; Sivick, K. E.; Katibah, G. E.; Woo, S. R.; Lemmens, E.; Banda, T.; Leong, J. J.; Metchette, K.; Dubensky, T. W., Jr.; Gajewski, T. F., Direct Activation of STING in the Tumor Microenvironment Leads to Potent and Systemic Tumor Regression and Immunity. *Cell Rep* **2015,** *11* (7), 1018-30.

3. Diner, E. J.; Burdette, D. L.; Wilson, S. C.; Monroe, K. M.; Kellenberger, C. A.; Hyodo, M.; Hayakawa, Y.; Hammond, M. C.; Vance, R. E., The innate immune DNA sensor cGAS produces a noncanonical cyclic dinucleotide that activates human STING. *Cell Rep* **2013,** *3* (5), 1355-61.

4. Dubensky, J., T. W. ; Kanne, D. B.; Leong, M. L., Rationale, progress and development of vaccines utilizing STING-activating cyclic dinucleotide adjuvants. *Ther Adv Vaccines* **2013,** *1* (4), 131–143.

5. Barber, G. N., STING: infection, inflammation and cancer. *Nat Rev Immunol* **2015,** *15* (12), 760-70.

6. Girardin, S. E.; Boneca, I. G.; Carneiro, L. A. M.; Antignac, A.; Jéhanno, M.; Viala, J.; Tedin, K.; Taha, M.; Labigne, A.; Zäthringer, U.; Coyle, A. J.; DiStefano, P. S.; Bertin, J.; Sansonetti, P. J.; Philpott, D. J., Nod1 Detects a Unique Muropeptide from Gram-Negative Bacterial Peptidoglycan. *Science* **2003,** *300* (5625), 1584–1587.

7. Wu, J.; Sun, L.; Chen, X.; Du, F.; Shi, H.; Chen, C.; Chen, Z. J., Cyclic GMP-AMP is an endogenous second messenger in innate immune signaling by cytosolic DNA. *Science* **2013,** *339* (6121), 826-30.

8. McWhirter, S. M.; Barbalat, R.; Monroe, K. M.; Fontana, M. F.; Hyodo, M.; Joncker, N. T.; Ishii, K. J.; Akira, S.; Colonna, M.; Chen, Z. J.; Fitzgerald, K. A.; Hayakawa, Y.; Vance, R. E., A host type I interferon response is induced by cytosolic sensing of the bacterial second messenger cyclic-di-GMP. *J Exp Med* **2009,** *206* (9), 1899-911.

9. Ishikawa, H.; Ma, Z.; Barber, G. N., STING regulates intracellular DNA-mediated, type I interferon-dependent innate immunity. *Nature* **2009,** *461* (7265), 788-92.

10. Tanaka, Y.; Chen, Z. J., STING Specifies IRF3 Phosphorylation by TBK1 in the Cytosolic DNA Signaling Pathway. *Sci. Signal.* **2012,** *5*, ra20.

11. Kranzusch, P. J.; Wilson, S. C.; Lee, A. S.; Berger, J. M.; Doudna, J. A.; Vance, R. E., Ancient Origin of cGAS-STING Reveals Mechanism of Universal 2',3' cGAMP Signaling. *Mol Cell* **2015,** *59* (6), 891-903.

12. Shang, G.; Zhu, D.; Li, N.; Zhang, J.; Zhu, C.; Lu, D.; Liu, C.; Yu, Q.; Zhao, Y.; Xu, S.; Gu, L., Crystal structures of STING protein reveal basis for recognition of cyclic di-GMP. *Nat Struct Mol Biol* **2012,** *19* (7), 725-7.

13. Dobbs, N.; Burnaevskiy, N.; Chen, D.; Gonugunta, V. K.; Alto, N. M.; Yan, N., STING Activation by Translocation from the ER Is Associated with Infection and Autoinflammatory Disease. *Cell Host Microbe* **2015,** *18* (2), 157-68.

14. Fu, J.; Kanne, D. B.; Leong, M.; Glickman, L. H.; McWhirter, S. M.; Lemmens, E.; Mechette, K.; Leong, J. J.; Lauer, P.; Liu, W.; Sivick, K. E.; Zeng, Q.; Soares, K. C.; Zheng, L.; Portnoy, D. A.; Woodward, J. J.; Pardoll, D. M.; Dubensky Jr., T. W.; Kim, Y., STING agonist formulated cancer vaccines can cure established tumors resistant to PD-1 blockade. *Sci. Transl. Med.* **2015,** *7* (283), 283ra52.

15. Ahn, J.; Konno, H.; Barber, G. N., Diverse roles of STING-dependent signaling on the development of cancer. *Oncogene* **2015,** *34* (41), 5302-8.

16. Baird, J. R.; Friedman, D.; Cottam, B.; Dubensky, T. W., Jr.; Kanne, D. B.; Bambina, S.; Bahjat, K.; Crittenden, M. R.; Gough, M. J., Radiotherapy Combined with Novel STING-Targeting Oligonucleotides Results in Regression of Established Tumors. *Cancer Res* **2016,** *76* (1), 50-61.

17. Curran, E.; Chen, X.; Corrales, L.; Kline, D. E.; Dubensky, T. W., Jr.; Duttagupta, P.; Kortylewski, M.; Kline, J., STING Pathway Activation Stimulates Potent Immunity against Acute Myeloid Leukemia. *Cell Rep* **2016,** *15* (11), 2357-66.

18. Wilson, D. R.; Sen, R.; Sunshine, J. C.; Pardoll, D. M.; Green, J. J.; Kim, Y. J., Biodegradable STING agonist nanoparticles for enhanced cancer immunotherapy. *Nanomedicine* **2018,** *14* (2), 237-246.

19. Simm, R.; Morr, M.; Kader, A.; Nimtz, M.; Romling, U., GGDEF and EAL domains inversely regulate cyclic di-GMP levels and transition from sessility to motility. *Mol Microbiol* **2004,** *53* (4), 1123-34.

20. Weinhouse, H.; Sapir, S.; Amikam, D.; Shilo, Y.; Volman, G.; Ohana, P.; Benziman, M., c-di-GMP-binding protein, a new factor regulating cellulose synthesis in Acetobacter xylinum. *FEBS Letters* **1997,** *416* (2), 207-211.

21. Romling, U.; Galperin, M. Y.; Gomelsky, M., Cyclic di-GMP: the first 25 years of a universal bacterial second messenger. *Microbiol Mol Biol Rev* **2013,** *77* (1), 1-52.